

**An Investigation of the Effects of Temperature and Frequency
on Asphalt Pavement Strain Using an Accelerated Testing System**

by

Jonathan Scott Gould

a Thesis

Submitted to the Faculty

of the

WORCESTER POLYTECHNIC INSTITUTE

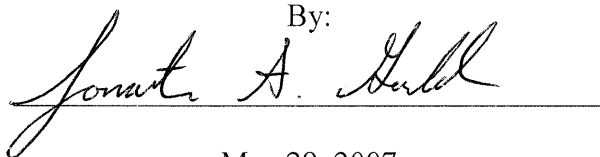
In partial fulfillment of the requirements for the

Degree of Master of Science

in

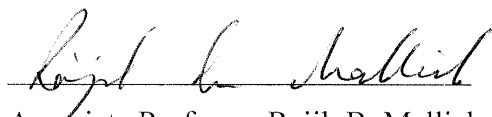
Civil Engineering

By:

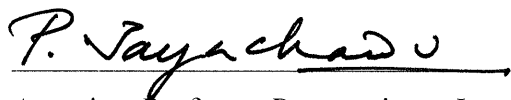


May 29, 2007

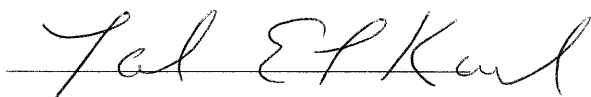
APPROVED:



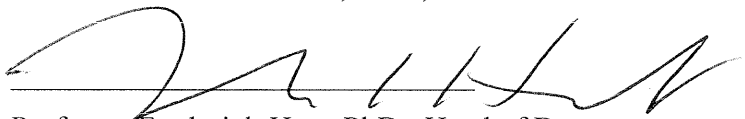
Associate Professor Rajib B. Mallick, PhD., PE, Major Advisor



Associate Professor Paramasivam Jayachandran, PhD., Committee Member



Professor Tahar ElKorchi, PhD., Committee Member



Professor Frederick Hart, PhD., Head of Department

Abstract

The determination of strain is an important step when using a mechanistic-empirical structural design, such as the AASHTO 2002 Design Guide. This thesis investigated the use of accelerated pavement testing system on Hot Mix Asphalt pavements to determine actual transverse and longitudinal strains under loads of varying frequency at different temperatures. A Model Mobile Load Simulator (MMLS3) was used in this study.

Laboratory compacted pavement slabs were instrumented with thermocouples for monitoring the pavement's temperature, and with strain gauges in transverse and longitudinal directions at the bottom surface to measure strain. The slabs were subjected to loading by the MMLS3, running at different speeds. The pavement slab and accelerated loading equipment were enclosed in an environmental chamber to control temperatures during testing. Strains were also determined from layered elastic analysis after determining modulus values by two different methods – Resilient modulus testing and Witczak's dynamic modulus equation. Comparisons of pavement strains calculated through the use of layered elastic design software and actual strains obtained during loading were made.

The test results have shown a significant difference between strain values obtained using an instrumented pavement slab and those obtained with the use of standard resilient modulus values or dynamic modulus values determined by using a typical layered elastic design model. To avoid the discrepancies, two approaches are proposed – The first is modeling strain with accelerated pavement testing and the second one is using a correction factor.

Acknowledgements

I would like to extend much appreciation and gratitude to my advisor Dr. Rajib B. Mallick for giving me the opportunity to work with the state-of-the-art testing facilities of the pavement research laboratory in the department of Civil and Environmental Engineering at Worcester Polytechnic Institute. He gave me the opportunity to work in many externally funded projects, increasing my knowledge of pavement engineering considerably. Without the advice and guidance of my thesis committee this study would not have been possible.

Throughout my graduate program I had the privilege to work with Professor Frederick Hugo of University of Stellenbosch, South Africa. I also thank Johan Muller for helping us to solve many technical problems we faced while running the MMLS3.

I don't want to forget my colleagues, Sean O'Brian, Ethan Ray, Don Pellegrino, Arthur Bealand and Yamini Nanagiri whose unlimited help can't go without mentioning.

Special thanks also go to my friend Sudip Bhattacharjee for providing guidance into understanding the complexities of pavement systems and in collaboration on findings in his doctoral dissertation which related to my thesis work.

Most importantly, an extra special thanks goes to my wife Nancy and my Family, for giving me continuous encouragement and support, which has allowed the completion of my thesis to become reality versus a distant idealism.

Table of Contents

Abstract.....	ii
Acknowledgements.....	iii
Table of Contents.....	iv
List of Figures.....	vi
List of Tables.....	viii
1 Introduction.....	1
2 Literature Review.....	2
2.1 Pavement Design Guides.....	2
2.2 Prediction of Strain in Pavement.....	8
2.3 Properties of Hot Mix Asphalt.....	10
2.4 Introduction to Accelerated Loading.....	14
2.5 Model Mobile Load Simulator (MMLS3).....	15
2.6 Conclusions from Literature Review.....	17
3 Equipment.....	17
3.1 Dynamic Cone Penetrometer (DCP).....	17
3.2 Soil Stiffness Gauge (SSG).....	19
3.3 Pavement Quality Indicator (PQI).....	21
3.4 Universal Testing Machine (UTM).....	21
3.5 Model Mobile Load Simulator MK3 (MMLS3) Testing System.....	24
3.5.1 Mold and Vibratory Compactor.....	24
3.5.2 MMLS3.....	25
3.5.3 Environmental Chamber and HVAC System.....	26
3.6 Instrumentation and Data Acquisition System (DAS).....	27
4 Materials.....	28
4.1 Sand Base.....	28
4.2 Steel Plate.....	30
4.3 D80 Neoprene Rubber.....	30
4.4 RS-1 Emulsion Tack Coat.....	30
4.5 Hot Mix Asphalt.....	31
4.6 Asphalt Binder.....	32
5 Test and Analysis Plan.....	34
5.1 Pavement System.....	35
5.2 Pavement Slab.....	35
5.3 Loading System.....	35
5.4 Data Acquisition.....	35
5.5 Data Analysis.....	36

6 Development of Pavement Slab, Structure & Test Protocol.....	38
6.1 Pavement System.....	38
6.2 Pavement Slab.....	38
6.2.1 Slab Compaction.....	39
6.2.2 Slab Cutting and Preparation	41
6.2.3 Slab Instrumentation.....	43
6.3 Testing.....	44
7 Results and Analysis.....	47
7.1 Actual MMLS3 Resilient Strain Results.....	47
7.2 BISAR Layered Elastic Analysis Results.....	53
7.2.1 5-Pulse Resilient Modulus (E).....	54
7.2.2 Witczak's Modified Dynamic Modulus Equation (E^*).....	56
7.3 Effect of Difference in Strains on the Fatigue Life in Pavements	60
7.4 Alternative Approach for Determining Strain	63
8 Conclusions.....	67
9 Recommendations.....	69
10 References.....	70
Appendix A – Data Tables.....	76
A.1 MMLS3 Strain Gauge Results.....	76
A.2 BISAR (E) Model Results.....	80

List of Figures

Figure 2.1 – Boussinesq's Equation Diagram	6
Figure 2.2 – Layered Elastic Inputs	7
Figure 3.1 – Dynamic Cone Penetrometer [26]	19
Figure 3.2 – Humboldt GeoGauge™, Soils Stiffness Gauge (SSG)	20
Figure 3.3 – Pavement Quality Indicator Schematic (PQI) [30]	21
Figure 3.4 – Universal Testing Machine, 5-Pulse Resilient Modulus Testing	22
Figure 3.5 – Resilient Modulus Testing Jig	23
Figure 3.6 – 5-Pulse Resilient Modulus Test	23
Figure 3.7 – Mold and Compaction System	25
Figure 3.8 – Longitudinal Cross Section of the MMLS3	26
Figure 3.9 – Vredestein Tire Schematic	26
Figure 4.1 – Pavement System Cross Section	28
Figure 4.2 – Graph and equation for temperature vs. viscosity for asphalt binder	32
Figure 5.1 – Overview of Testing Plan	34
Figure 5.2 – Example of Transverse and Longitudinal Strains, respectively.	36
Figure 5.3 – Overview of Analysis Plan	37
Figure 6.1 – Radiant Heat lamps hung above the mold during compaction (typical)	40
Figure 6.2 – Compaction of a pavement slab	41
Figure 6.3 – Cutting, spreading, and movement of pavement slabs	42
Figure 6.4 – Sandwiching pavement slab for transport, instrumentation, and storage	42
Figure 6.5 – Slab instrumentation	44
Figure 6.6 – Lowering MMLS3 into testing position and leveling (typical)	45
Figure 7.1 – 2.08 Hz Temperature vs. Actual MMLS3 Resilient Strain	47
Figure 7.2 – 1.56 Hz Temperature vs. Actual MMLS3 Resilient Strain	48
Figure 7.3 – 1.05 Hz Temperature vs. Actual MMLS3 Resilient Strain	49
Figure 7.4 – 0.51 Hz Temperature vs. Actual MMLS3 Resilient Strain	50
Figure 7.5 – Actual MMLS3 Strain – Temp. Curves of Transverse Strain vs. Freq.	52
Figure 7.6 – Actual MMLS3 Strain – Temp. Curves of Longitudinal Strain vs. Freq.	52
Figure 7.7 – HMA Resilient Modulus (E) vs Temperature	54
Figure 7.8 – BISAR model inputs and outputs	55
Figure 7.9 – BISAR (E, 10Hz) Strain & MMLS3 Actual Strain (10Hz) vs. Temp.	56
Figure 7.10 – Temp. Curves of BISAR (E*) Strain vs. Frequency	58
Figure 7.11 – Temp. Curves of BISAR (E*) & MMLS3 Actual, Strain vs. Frequency ...	59
Figure 7.12 – BISAR (E, E*) Strain & Extrapolated MMLS3 Actual Strain (10Hz) vs. Temperature	60
Figure 7.13 – Loads to Failure Comparison at 10 degrees Celsius	61
Figure 7.14 – Loads to Failure Comparison at 20 degrees Celsius	62
Figure 7.15 – Loads to Failure Comparison at 30 degrees Celsius	62
Figure 7.16 – Strain Correction Model for E and E* strains at 10 degrees Celsius	64
Figure 7.17 – Strain Correction Model for E and E* strains at 20 degrees Celsius	64
Figure 7.18 – Strain Correction Model for E and E* strains at 30 degrees Celsius	65

Figure A.2.1 – BISAR MODEL, 10 Degrees Celsius	80
Figure A.2.2 – BISAR MODEL, 15 Degrees Celsius	81
Figure A.2.3 – BISAR MODEL, 20 Degrees Celsius	81
Figure A.2.4 – BISAR MODEL, 25 Degrees Celsius	82
Figure A.2.5 – BISAR MODEL, 30 Degrees Celsius	82

List of Tables

Table 4.1 – Sand Stiffness by GeoGauge™	29
Table 4.2 – Dynamic Cone Penetrometer Results	29
Table 4.3 – PG 64-28 Binder Properties provided by Hudson Laboratories	32
Table 4.4 – Typical A and VTS Properties of PG Graded Binders	33
Table 7.1 – Transverse & Longitudinal Ratios for Actual MMLS3 Resilient Strain	50
Table 7.2 – Actual MMLS3 Strain extrapolated from 2.08 to 10.0 Hz	53
Table 7.3 – BISAR Strain using E values attained during 5-Pulse Resilient Modulus Testing.....	55
Table 7.4 – BISAR Strain using E* values attained using Witczak’s Equation.....	57
Table 7.5 – Predicting MMLS3 Actual Strains	63
Table 7.6 – Correction Factors for the Indirect Test Method or Witczak’s Dynamic Modulus Method.....	65
Table A.1.1 – MMLS3 Strain Gauge Results, 2.52 m/s	76
Table A.1.2 – MMLS3 Strain Gauge Results, 1.97 m/s	77
Table A.1.3 – MMLS3 Strain Gauge Results, 1.32 m/s	78
Table A.1.4 – MMLS3 Strain Gauge Results, 0.54 m/s	79

1 Introduction

Laboratory determined fatigue life of Hot Mix Asphalt (HMA) depends on several factors, such as mix properties, magnitude of loading, mode of loading (stress controlled or strain controlled), specimen dimensions and temperature. Many studies have been conducted on the determination of fatigue life of HMA pavement, but few have made use of a unidirectional scale model accelerated loading system to realistically simulate pavement strain based on various temperatures and loading frequencies. Although there have been some studies performed with small wheel tracking devices, which attempted to simulate realistic small scale pavement loading, most of them used a less than realistic bi-directional mode of loading. In this study, a model HMA pavement slab was constructed in a laboratory setting and tested under repeated wheel loading using the Model Mobile Load Simulator 3 (MMLS3). The most important aspect of the MMLS3 is that it uses a scaled model both in dimension and loading.

This study will present an in-depth literature review on the development of the AASHTO pavement design guides, predicting strain in pavements, hot mix asphalt properties, and a look at accelerated pavement testing. A description of the equipment and materials used, testing protocols, the results and analysis, along with conclusions and recommendations for future research will also be presented. The primary objective of this study was to evaluate actual the effects of frequency and temperature on the resilient strain of a pavement slab using a 1/3 scale Mobile Model Loading System and to draw a comparison to calculated values of strain.

2 Literature Review

A literature review was performed on the history and future of pavement design guides and how their use of a mechanistic-empirical design process will utilize a pavements strain to develop a design. It also includes a prediction of strain in pavements through the use of layer elastic design procedures, and an investigation into HMA modulus; what it is, how it's calculated, and its ability to determine a pavements effectiveness of carrying a load. Lastly, it will take a closer look into the use of accelerated loading devices for testing. Specifically the use of the MMLS3 as a means to better replicate actual conditions and in doing so, provide actual distresses through a scaled pavement system.

2.1 Pavement Design Guides

In a study conducted by the Federal Highway Administration (FHWA) between 1995 and 1997 it was concluded that nearly 80 percent of all states used one of the 1972, 1986, or 1993 design guides.[1] These guides were all empirically based on performance equations using data obtained from the 1950's American Association of State Highway and Transportation Officials (AASHTO) Road Test program. Currently the most widely used design guide is the 1993 AASHTO design.

One of the major deficiencies with current design methods is they are based on outdated pavement distress models. For instance, the 1993 design guide provides designers the ability to design a pavement system and determine if it is sufficient. However, this is based on pavement failure models subjected to 1960 traffic levels. Today's traffic volumes are four times greater, with trucking percentages 285 percent higher. In fact today's trucking numbers account for nearly 5 percent of the total traffic volume (in vehicle-miles) seen on the nations roadways as opposed to 3.2% in the 1970's. [1] Although it may not be seem like a large change, trucking traffic affects pavements to a much greater degree than does car traffic

When completing the 1986 design guide it was noted that a more practical approach to designing pavements would be to incorporate a mechanistic approach. Due to equipment

and computational limitations at that time it was not pursued; however, all of the aspects mentioned then are addressed in the 2002 version. They include: unique loading conditions (tire configurations, loading pressures, etc.), stabilized materials, procedures to evaluate premature distresses, asphalt aging, seasonal climatic effects (freeze-thaw), and improved drainage modeling.

There are many limitations that 1993 design guide does not and is not able to consider when designing a new pavement, with a major one being the inability of implementing rehabilitation techniques. The following table is a comprehensive list developed by the AASHTO Joint Task Force on Pavements (JTTF) back in 1996 and included in the introduction of the *AASHTO 2002 Guide for Design of Pavement Structures* [1]:

- Truck loading deficiencies: Heavy truck traffic has increased by 10 to 20 percent. Original Road Test data collected in the 1950's included less than 1 million equivalent single axle load (ESAL) applications and damages were extrapolated using regression analysis. This simply is not a practical approach considering a typical pavement today surpasses that 1 million ESAL load in its first year of serviceability.
- Rehabilitation deficiencies: Rehabilitation procedures were not considered when developing the previous versions of the AASHTO design guides. With the economic saving provided in a rehabilitation project versus a reconstruction project, it is critical that a new design guide account for this.
- Climate effects: AASHTO's Road Tests results included distresses observed at the location the testing was performed. A better approach would be to include climatic conditions for the specific areas the new pavement systems are being constructed or rehabilitated. This is done by including climatic data from over 800 testing locations throughout the country.
- Subgrade deficiencies: Only one type of subgrade was used in the Road Test; however, many types exist across the country. A way to incorporate their

specific properties is necessary to predict performance of the designed pavement system.

- Surface material deficiencies: Again only one type of HMA surface mix was used in the AASHTO Road Test. Today there are numerous different types of hot mix asphalt mixes being produced with varying asphalt grades, aggregate types, air void restrictions, even design methods i.e. Marshall and Superpave Mix Designs. It is obvious that a characterization of these mixes must be done using specific mixture properties.
- Base material deficiencies: There are also many different types of base material being used today as opposed to only two bound/unbound base materials used in original tests.
- Construction and drainage deficiencies: At the time of the Roads Test no drainage was used. It has become standard practice to incorporate a well draining base into today's designs, especially our state highways.
- Truck characterization deficiencies: Many vehicles have varying wheel configurations and suspension variations along with differing tire pressures which have increased from 80 psi in the 1950's to upwards of 120 psi in today's fleet.
- Design life deficiencies: The original Road Test was conducted over a period of two years. The results did not investigate the effect of long term climate cycles of material aging. Many roads are designed for 20 to 40 years, therefore a more repetitive, cyclic approach should be used to model long term effects.
- Also incorporated into the new design guide would be validation of reliability and performance deficiencies, which were either not considered or not validated in earlier versions of the design guides.

It is evident based upon the list of deficiencies developed by the JTFP that when developing a new design guide there was a need to incorporate not only an empirical approach but also a mechanistic one; thus, the development of the mechanistic-empirical designs.

The *AASHTO 2002 Guide for Design of Pavement Structures* using a mechanistic-empirical (M-E) method is the newest approach to designing pavement systems taking into consideration state-of-the-art material characterization properties. It is currently being reviewed by several State DOT's and in a few instances, such as Indiana DOT, it has already begun implementation. The design guide represents a significant change in the way pavements are designed.

The M-E design procedure provides the designer the ability to evaluate the effect of various materials against pavement performance. From an engineering point of view, there is much to be desired about the mechanistic approach to pavement design. The term 'mechanistic' refers to the application of principles of engineering mechanics, which provides a rational design process.[1] Yoder and Witczak [2] stated that for a design process to be rational that three elements be included fully: 1) the theory used to predict the assumed failure or distress parameter, 2) the evaluation of material properties be applicable to the selected theory, and 3) the determination of the relationship between the magnitude and the parameter in question to the performance level desired. The mechanistic approach to the M-E design procedure is most utilized when determining mix properties.

There was a gradual build-up when developing today's current layered elastic design method which utilizes primarily engineering mechanics relating to stress and strain in the pavement layers. The analysis of stress, strain, and deflections in ideal masses were primarily derived from Boussinesq equations which stated that "the vertical stress at any depth below the Earth's surface due to a point load at the surface is dependent upon the radial distance and depth from the point load." A diagram and equation of Boussinesq's theory is show in Figure 2.1.

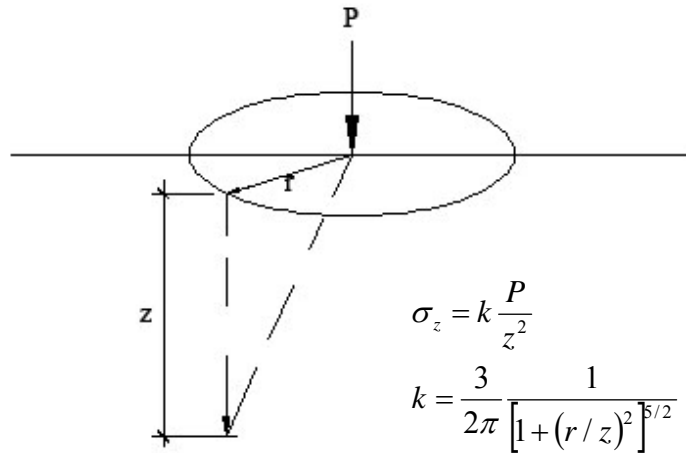


Figure 2.1 – Boussinesq's Equation Diagram

Most pavements are comprised of multiple layers whose purpose is to distribute the surface load over a greater base area. Further work was done by Burmister [3,4,5] which provided an approach that could support actual multi-layer pavement systems (2-layer) being constructed. Layered elastic models assume that each pavement structural layer is homogeneous, isotropic, and linearly elastic and hold several assumptions. They included: 1) a surface layer assumed to be infinite in the X-Y directions but having a finite depth Z, 2) an underlying layer infinite in all directions, X-Y-Z, and 3) a full bond between layers [2].

Further research was completed by Fox and Acum [6] and later expanded upon by Jones [7] and Peattie [8] which could provide normal and radial stresses at the intersection of the plate axis and the layer interfaces.[2] Due to the symmetry in stress analysis, many types of strain were also able to be computed. This includes the vertical and horizontal stresses and strains for the bottom of layers 1 and 2 as well as the top of layer 3. The stress and strain values at these critical locations in a pavement system allow for the development of multi-layered elastic designs.

There are several properties that need to be determined in order to find the stress and strains at specific locations throughout the pavement system. This step has prevented layered elastic design from being utilized sooner. Just in the past decade have test

methods been developed which allow researchers a time and cost effective approach of determining the necessary material properties used in this mechanistic approach. Two of these properties, shown in Figure 2.2, are elastic modulus values, which is discussed in Section 2.3, and Poisson's ratio.

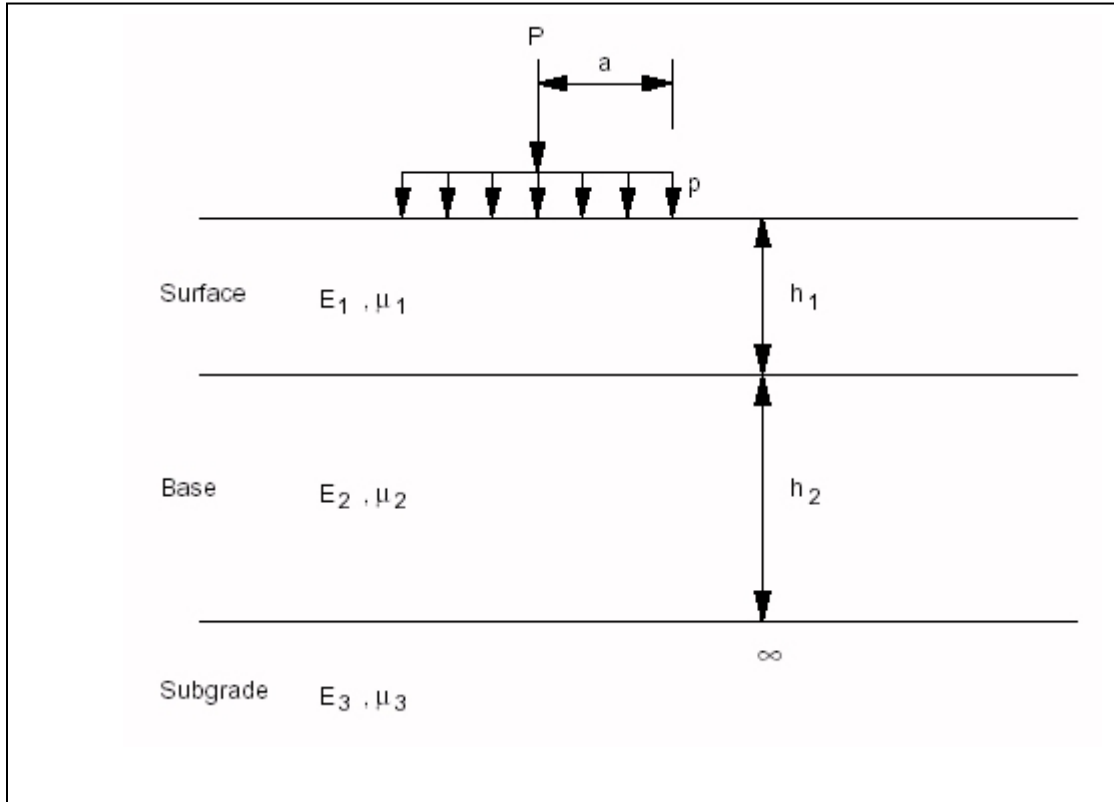


Figure 2.2 – Layered Elastic Inputs

There are currently many ways to determine the elastic modulus of materials, including: laboratory test like the Indirect Tension Test, in-situ testing by use of a Falling Weight Deflectometer, or computational methods such as Witczak's dynamic modulus equation, to name a few. There are also many computer programs such as Shell's BISAR program, which have the ability to analyze these multi-layered systems with minimal computational effort. BISAR facilitates the mechanistic modeling of the pavement structure and calculates the stresses and strains caused by vehicle loading at specified locations within the pavement system. The strains developed under initial loading can

then be used in the *AASHTO 2002 Guide for Design of Pavement Structures* to develop a pavement design.

A second approach, and one which will be emphasized in this study, is to bypass the layered elastic theory with its multiple assumptions and to directly determine the actual strain developed at the bottom of a HMA surface layer. This can be done through accelerated load testing and provides an actual strain value which can be used in the 2002 Design Guide procedure.

Due to the ability of the mechanistic procedures ability to better account for climate, aging, present day materials, and present day vehicle loads, variations in pavement performance versus pavement life can be reduced. The ultimate result will hopefully provide a reduction in life cycle costs, due to an improved design process which does not over or under design pavement systems.

2.2 Prediction of Strain in Pavement

Strain is expressed as the total elongation divided by the original length of the specimen. Strain can occur in one of two forms; either elastic strain or plastic deformation. Elastic strain is a reversible deformation which dissipates once a stress is removed from the material. Plastic deformation is an irreversible deformation that occurs when the material is pushed past its elastic limit. Prior to reaching an elastic limit a material can return back to its original shape. After passing its elastic limit, permanent deformation will occur [9]. Strain magnitude is also a function of time and a materials viscosity.

One of the main objectives of this study was to use a readily available and relatively uncomplicated program to produce an initial prediction that could later be compared to a measured laboratory response. It is important to note that linear layered elastic models are the current practice for both pavement analysis and design, and are therefore an appropriate model to evaluate strain in HMA pavements.

As mentioned earlier, one of the most widely used layered elastic programs in pavement engineering is BISAR. It is an acronym for Bituminous Structures Analysis in

Roads and was developed by Shell International Petroleum Company in 1978. BISAR is a program to find stresses and strains in asphalt pavements. It assumes that the pavement structure is infinite in the X and Y directions. The Z direction is the depth and is dependent on the input. The pavement layers are assumed to be linear elastic. The required input for BISAR includes the number of layers in the structural system, modulus of elasticity and Poisson's ratio for each of those layers, thickness of each layer, number of loads being applied to the system, the horizontal and vertical components of these loads, the position and radius of the loading, number of points where the displacement, stress and strain are to be determined, and the location of the analysis points [10]. The program facilitates the mechanistic modeling of a pavement structure and calculates the stresses and strains caused by vehicle loading.

BISAR is a straightforward and easy to use program. The first step is to run the program file BISARIN.EXE which creates an input file for the Layered Elastic Program 'BISAR'. Once running BISARIN you are prompted to create a file name and a title. The program then asks the number of problems to be run (1 in this study). The number of layers in the pavement system is subsequently entered along with the type of system, whether it is flexible, rigid, or composite (a flexible system was used in this study). The elastic modulus, Poisson's ratio, layer thickness, and bond level, with 0 for complete adhesion and 1000 for frictionless slip (a bond level of zero was used in this study) were then entered for each layer.

Load information is then requested, including number of loading areas, vertical load, radius of loading area, and the X and Y coordinates of loading. The X and Y coordinates take into consideration offset loading (for the purposes of this study, the offset coordinates were assumed to be zero). One evaluation position was desired at the bottom of the first layer and was to achieve values just above the bottom of the first layer a Z value of one hundredth less than the surface layer thickness was input.

The program then terminates and it is time to run the input file in BISAR.EXE. Once BISAR.EXE is run, it prompts for the name of an input file (this is the filename entered in BISARIN.EXE). You then enter an output filename, and the program runs the

scenario. Results can be viewed by opening the output file in Microsoft® Word or Notepad applications.

2.3 Properties of Hot Mix Asphalt

Hot mix asphalt is a mixture of asphalt, coarse and fine aggregates, and filler dust. When mixed to a specific design specification it produces an asphalt concrete pavement [11]. Asphalt is the black liquid which coats the stone particles and provides adhesion between aggregates. The temperature of the asphalt plays a critical role in the mix's ability to carry load. Cold asphalt responds elastically to loading while hot asphalt responds viscously to loading.

A purely elastic material is one in which all the energy stored in the sample during loading is returned when the load is removed. As a result, the stress and strain curves for elastic materials move completely in phase. A complete opposite to an elastic material is a purely viscous material. This type of material does not return any of the energy stored during loading. All the energy is lost once the load is removed. These materials have no stiffness component, only damping. All others that do not fall into one of the above classifications are known as viscoelastic materials. Typical temperature ranges allow asphalt pavements to display both properties simultaneously. Some of the energy stored in a viscoelastic system is recovered upon removal of the load, and the remainder is dissipated. One of the unique characteristics of viscoelastic materials is that their properties are influenced by many parameters. They can include: frequency, temperature, time effects (such as creep and relaxation), aging, and several other irreversible effects. However, the most important of these effects include temperature and frequency [12].

It is commonly known that the material properties of asphalt mixtures are affected significantly when subjected to temperature variations. For example, a typical asphalt mixture having a resilient (elastic) modulus of 4.5 GPa at 4°C will most likely have the resilient modulus of around 1.5 GPa at 40°C. Huang states that “any good constitutive model for asphalt mixtures should include the change of material behavior with temperature.” In addition to temperature dependency, HMA mixtures exhibit loading rate dependency and plasticity. Rate dependency is reflected on the creep, stress

relaxation, as well as the phase angle between stress and strain during cyclic loading. The plastic behavior component of asphalt mixtures results in the permanent deformation of the asphalt pavements [13].

A material's elastic modulus is actually an estimate of its modulus of elasticity (E). While the modulus of elasticity is stress divided by strain for a slowly applied load, it is known as resilient modulus for repeatedly applied loads, similar to those experienced by pavements [14].

There are two standard methods of determining the modulus of HMA. The first and more simplistic of the two utilizes diametric resilient modulus testing, following ASTM D4123 *Standard Test Method for Indirect Tension Test for Resilient Modulus of Bituminous Mixtures*. This test applies a repeated load of fixed magnitude and cycle duration to a cylindrical test specimen. A typical HMA test specimen is used by turning it on its side so that it can be loaded in its diametric plane. The specimen's resilient modulus can be calculated using the horizontal deformation and an assumed Poisson ratio.

The second method developed by Witczak is based on the dynamic modulus test, which measures a specimen's stress-strain relationship under a continuous sinusoidal loading. For linear viscoelastic materials, this relationship is defined by a complex number called the “complex modulus” (E^*) [15]. The dynamic modulus test is considered reliable for new, un-aged dense-graded asphalt concrete mixes with gravel or crushed stone aggregates [16]. The complex modulus test measures the response of the material to cyclic loading at different frequencies. As we have discussed, asphalt concrete is a viscoelastic material, meaning that its response to a particular load depends on the magnitude of the load, the rate of application, and the duration of the load. Therefore, it is important to evaluate how the material responds to different frequencies or rates of loading, which corresponds to the different traffic speeds pavement could experience in the field. The dynamic modulus of any mix may be estimated using Equation 2.1 which has been developed from many of tests utilizing various HMA mixes.

Equation 2.1 – Witczak’s Dynamic Modulus Equation [17]

$$\begin{aligned} \text{Log}E^* = & -0.261 + (0.008225 * P_{200}) - (0.00000101 * P_{200}^2) + \\ & (0.00196 * P_4) - (0.03157 * V_a) - \left[0.415 * \left(\frac{V_{beff}}{V_{beff} + V_a} \right) \right] + \\ & \left[\frac{1.87 + (0.002808 * P_4) + (0.0000404 * P_{3/8}) - (0.0001786 * P_{3/8}^2) + (0.0164 * P_{3/4})}{1 + e^{(-0.716 * \log(f) - 0.7425 * \log(\eta))}} \right] \end{aligned}$$

Where:

- E = Dynamic modulus, 10^5 psi
- η = Asphalt viscosity, 10^6 poise (at estimated temperature degree)
- f = Frequency of loading, Hz.
- V_a = Percent air voids by volume
- V_{beff} = Percent effective asphalt content by volume
- $P_{3/4}$ = Percent retained on the 3/4 inch sieve, by total cumulative aggregate weight
- $P_{3/8}$ = Percent retained on the 3/8 inch sieve, by total cumulative aggregate weight
- P_4 = Percent retained on the No. 4 sieve, by total cumulative aggregate weight
- P_{200} = Percent passing the No. 200 sieve, by total cumulative aggregate weight

Many of the variables in Witczak's equation are mix related and are readily available from the HMA pavement's mix design or from conventional testing procedures for in-place mixes. Two of the variables, including asphalt viscosity and frequency of loading, need to be further determined using the Equation 2.3 and Equation 2.4.

As mentioned earlier, asphalt's viscosity is extremely important due to its temperature dependency. To determine the viscosity at testing temperature we need to know shear modulus (G^*) and the asphalt's phase angle (δ) at each test temperature. Equation 2.2 uses the G^* and the δ to determine the binder's viscosity. These values are determined by measuring the binders shear modulus in an un-aged state and also in an accelerated aged condition using a Rolling Thin Film Oven (RTFO).

Equation 2.2 – Binder viscosity using Shear Modulus and Phase Angle

$$\eta = \left(\frac{G^*}{10} \right) * \left(\frac{1}{\sin \delta} \right)^{4.8628}$$

Where:

- η = Asphalt viscosity, 10^6 poise (at estimated temperature degree)
- G^* = Asphalt complex shear modulus, Pa
- δ = Asphalt phase angle, degrees

The values, when input into Equation 2.2, provide a viscosity for a given temperature. Thus, for several temperature values we determined a corresponding viscosity value.

The variables A and VTS show in Equation 2.3 – HMA Viscosity are then found by linear regression of Equation 2.2 after log-log transformation of the viscosity (in centipoise) data and log transformation of the temperature ($^{\circ}$ Rankine) data seen in Figure 4.2. Once the A and VTS variables are determined for a specific asphalt the viscosity can be found for any temperature.

Equation 2.3 – HMA Viscosity

$$\log(\log \eta) = A + (VTS * \log(T_R))$$

Where:

- η = Asphalt viscosity, 10^6 poise (at estimated temperature degree)
- T_R = Temperature which viscosity was estimated in Rankine
- VTS = Viscosity-Temperature Susceptibility
- A = Intercept

The second parameter needed when determining the complex modulus of an HMA mixture is the frequency of loading, which is determined using Equation 2.4. The frequency is equal to one over the time of loading.

Equation 2.4 – Frequency of loading

$$f = \frac{1}{T}$$

Where:

f = Frequency of loading, Hz.

T = Time of Loading, m/s

2.4 Introduction to Accelerated Loading

Over the past decade, accelerated pavement testing has evolved into one of the primary methods of testing pavement performance in the industry. This increase can be attributed to the savings associated with reduced costs and time needed to conduct a study. Van-de-Ven in a report entitled “Scaled Down APT Considerations for Viscoelastic Materials” [18], conveyed that there may be a need to perform preliminary testing prior to full-scale testing to monitor the effect of change of different variables.

While there is no debate as to the necessity of large scale field projects such as WesTrack [19] and LINTRACK [20], the cost and time needed for such an endeavor is beyond the means of most researchers and their agencies. It is with this in mind that several types of accelerated testing facilities have developed throughout the world. These facilities can be categorized into two main types: full-scale pavement test facilities and small-scale pavement test facilities. Each of these facilities offer a unique and applicable approach to understanding the complex behaviors associated with a pavement mix. Full-scale testing provides a study with real-world construction practices, while a laboratory produced mixture allows for highly controlled testing variables by means of precise material characterization. Small-scale testing presents a unique ability to combine the best of both.

Full-scale pavement test facilities can use Heavy Vehicle Simulators which apply a load and tire pressure equivalent to the real-world loading experienced by the pavement. These fully instrumented test sections are generally created in such a manner as to provide different mix types or mix variables. Pavement performance can be analyzed through the continuous acquisition of instruments, such as strain gauges, thermocouples, and pressure sensors. Typical construction practices used in the creation of these test segments allow for the accelerated testing results to be directly compared to the in-service pavement performance. These facilities can be found throughout the world, from

WesTrack in Nevada maintained by the Federal Highway Administration (FHWA) to LINTRACK at the Technical University of Delft in the Netherlands. Other significant facilities can be found at the Texas A&M University and at the National Center for Asphalt Technology (NCAT) located in Auburn, Alabama.

Small-scale accelerated pavement testing devices have been developed for use on laboratory prepared specimens to provide for relative comparisons. The size and costs associated with these devices have allowed them to become common place in research laboratories worldwide. The controlled environment of this testing equipment allows research to be conducted in a meticulous manner, while paying particular attention to detail. However, the limitations due to equipment size, unrealistic loads, tire pressures, and pavement substructure mean that actual pavement performance may be difficult to ascertain. Examples of these are beam fatigue tests, indirect tensile fatigue tests, rut and fatigue testing using the Asphalt Pavement Analyzer (APA), and countless more.

One of the newly developing technologies uses a small-scale pavement testing device, which utilizes a scaled model pavement structure in a controlled laboratory environment. It also incorporates a unidirectional loading pattern and programmable tire wander mimicking actual trafficking situations. The benefit of this system is its ability to provide an overall scaled approach to the testing. This means that the test variables, including the pavement structure, the pavement slab or sample, applied load, and tire pressures are all in proportion allowing for laboratory results to be compared to real-world pavement performance.

2.5 Model Mobile Load Simulator (MMLS3)

The second generation of the MMLS3 device allowed the testing equipment to be purchased and used by significantly more researchers. The MMLS3 was designed as a smaller version of the original, and uses 1:3 scale pavement geometries and loading criterion. It is being used successfully in the field when compared to conventional Heavy Vehicle Simulators (HVS) to monitor rutting and fatigue potential of mixes. Studies conducted include one by Hugo et al [21] titled A Case Study of Model APT in the Field, which investigated the Fatigue and rutting performance of a full-scaled pavement section

near Jacksboro, Texas. Another was performed by Epps et al [22] on the Performance Prediction with the MMLS3 at WesTrack to predict rutting in actual pavements. Studies have even been done under wet loading conditions as reported by Smit et al [23] and Walubita et al [24]. It not only can be used in the field by placing it directly on the pavement but it can be used in the laboratory on a scaled model pavement structure.

The test set up used for loading with the MMLS3 represents an actual pavement constructed to one-third scale and tested under realistic contact stresses. The pavement structure can include subgrade, subbase, and HMA paving layers, all of which are of 1:3 scale and are compacted using a hand driven steel drum vibratory roller. The layers are prepared in a manner similar to conventional roadway construction, being sure to obtain adequate density in each lift.

The MMLS3 has 8 bogies, 1 axle every other bogie and 1 wheel per axle. It uses four rubber-treaded tires with a width of 80 mm. They can be inflated to a maximum pressure of 800 kPa (116 psi) and can provide loads of 1.9 to 2.7 kN (427 to 607 lbf) [25]. The applied loads are maintained during testing by self-adjusting springs in the axle system and the tire pressure can be controlled by inflating or deflating the tires. The nominal wheel load application rate is 7200 per hour which translates to a nominal speed of 2.5 m/s (5.5 mph) [25]. The frequency can easily be controlled through the use of a dial in the main control unit. The dimensions of the device are 2400 x 600 x 1150 mm (8 x 2 x 3.5 ft) and it weighs approximately 800 kg (1750 lbs) [25]. An environmental chamber can be placed over the mold and testing device which allows pavement temperature to be controlled through vents placed on both sides of the pavement surface. One vent blows air across the pavement while the other acts as a return. A time controlled butterfly valve alternates the direction of flow across the pavement slab. A spray system can also be incorporated to allow for testing of moist pavements.

More recent advances of the MMLS3 accelerated testing system include an insert which was constructed to allow for modified 150mm (6 inch) diameter gyratory samples to be tested. The insert fits directly inside the mold allowing the MMLS3 to sit above

and provide unidirectional loading to the samples. Additionally, the set up allows for the mold to be filled with hot or cold water, fully submerging the samples.

2.6 Conclusions from Literature Review

After reviewing the literature, it can be realized that there have been a wide range of situations where the accelerated pavement testing has been performed. It can be concluded that in almost all of the testing conducted using the accelerated testing machines, very few have been performed which evaluate the effects of frequency and temperature using a 1:3 scale Mobile Model Loading System (MMLS3) on the resilient strain of a pavement slab. This intermediate step between full-scale testing machines and existing small-scale testing machines will provide a necessary advance in the ability to better predict the performance of HMA pavements when subjected to various traffic and weather conditions. This is critical when using the new 2002 design guide's M-E approach, which considers a pavement's initial strain when designing a suitable pavement structure.

3 Equipment

Testing equipment used in determining the material properties that make up the pavement system include the dynamic cone penetrometer (DCP), the soil stiffness gauge (SSG), the universal testing machine (UTM), the mobile model load simulator (MMLS3), and the instrumentation and data acquisition system (DAS).

3.1 Dynamic Cone Penetrometer (DCP)

The Dynamic Cone Penetrometer or DCP was based on the Scala penetrometer developed in 1956 by Scala for assessing in-situ California Bearing Ratio (CBR) of cohesive soils. The DCP is currently used to measure the in-situ CBR and elastic modulus of materials [26]. It has seen extensive use throughout the world including South Africa, the United Kingdom, the United States, and Australia. This is primarily due to its simple to use and rugged design. It is also an economical alternative to other

methods and provides results of soil strength and indirectly the modulus of the subgrade and pavement structures.

The DCP is used for measuring the material resistance to penetration in terms of millimeters per blow while the cone of the device is being driven into the pavement structure or the subgrade [26]. ASTM D6951¹, describes the DCP as consisting of an 8-kg hammer that drops from a height of 575 mm driving a 60-degree cone tip with base diameter of 20 mm vertically into the pavement structure or the sub grade. An illustration of the DCP can be seen in Figure 3.1. The DCP penetration index (DPI) is recorded as the slope of the relationship between number of blows and depth of penetration (in millimeters per blow) at a given linear depth segment. DCP data has been correlated with various pavement design parameters, including; CBR, shear strength, elastic modulus, back-calculated elastic modulus from the falling weight deflectometer (FWD) tests, and others [26]. Equation 3.1 – DPI Correlation to CBR developed by the US Army Corp of Engineers is used by the US Army Corp of Engineers and has been adopted by several state agencies as a means to correlate DPI to CBR values.

Equation 3.1 – DPI Correlation to CBR developed by the US Army Corp of Engineers

$$\log(CBR) = 2.46 + -1.12 * \log(DPI)$$

¹ ASTM D6951, “Standard Test Method for Use of the Dynamic Cone Penetrometer in Shallow Pavement Applications”, ASTM International

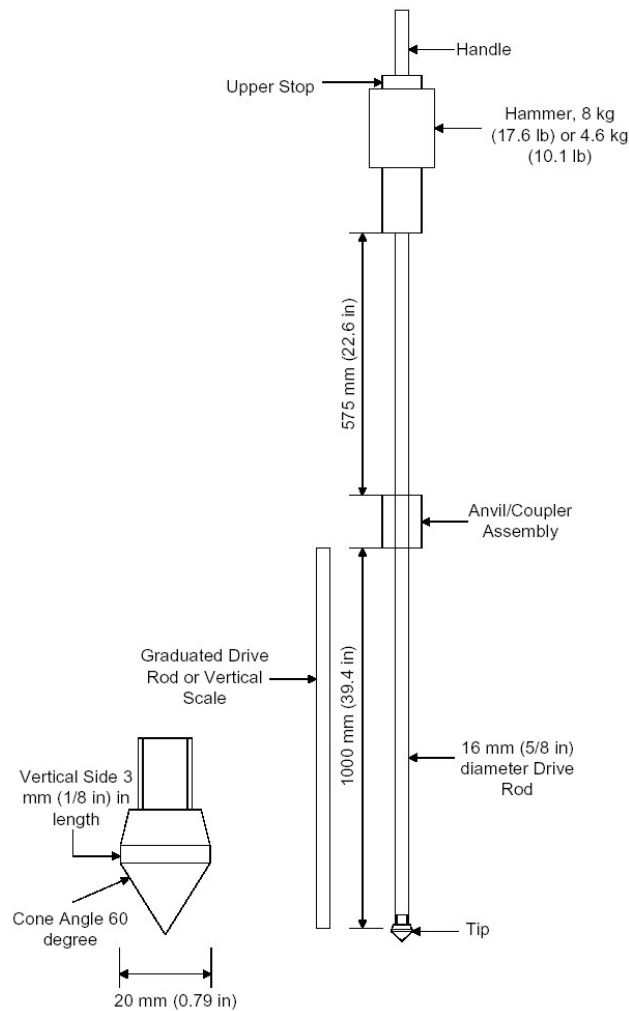


Figure 3.1 – Dynamic Cone Penetrometer [26]

3.2 Soil Stiffness Gauge (SSG)

The soil stiffness gauge (SSG) is an instrument for measuring the direct stiffness of soils. The device was developed out of a strategic collaboration between several private firms, the US Army, and funding being provided by the Federal Highway Administration [27]. After successful demonstrations were performed, Humboldt Manufacturing was approached to commercialize the gauge. It is now marketed by Kessler Soil Engineering Products as the Humboldt GeoGauge™ seen in Figure 3.2. The benefits of the SSG are that it is a lightweight, portable device for testing soil stiffness and is faster, cheaper, safer, and more accurate than the current standard methods. The

device is currently being evaluated by the American Association of State and Highway Officials (AASHTO) and the American Society for Testing and Materials (ASTM).

The SSG measures near-surface stiffness through the use of small dynamic forces applied to the soil at 25 steady state frequencies between 100 and 196 Hz. Based upon the force and displacement-time history, stiffness is calculated as the average force per unit displacement over the measured frequencies [26]. The GeoGauge™ measures and displays the layer's structural stiffness and the material's Young's modulus from the surface to a depth of 230 to 310 mm [28]. The data can be easily downloaded to a computer where the results can be recorded and analyzed. The GeoGauge meets ASTM D675829 requirements and takes less than a minute to run each test. Elastic modulus can be determined using Equation 3.2.

Equation 3.2 – Young's Modulus Equation using the GeoGauge™ [26, Equation 2.2]

$$E = \frac{K(1-\nu^2)}{1.77R} MPa$$

Where:

- K = GeoGauge™ Stiffness
- ν = Poisson's Ratio of Sand (0.40 assumed)
- R = Radius of outer ring (57.15mm)



Figure 3.2 – Humboldt GeoGauge™, Soils Stiffness Gauge (SSG)

3.3 Pavement Quality Indicator (PQI)

The pavement quality indicator (PQI) is designed and built to provide quick and accurate readings of density, temperature and moisture content on hot mix asphalt pavements. The PQI is a non-nuclear device which takes density readings in a matter of seconds. Its primary use is intended for newly laid asphalt pavements with thicknesses of approximately 25 to 150 mm (1 to 6 inch). The density of asphalt pavement is directly proportional to the measured dielectric constant of the material. TransTech's Pavement Quality Indicator™ uses electrical waves to measure the dielectric constant using an innovative, toroidal electrical sensing field established by the sensing plate as seen in Figure 3.3 [30]. The electronics in the PQI convert the field signals into material density readings and display the results on the screen. Once the device had been calibrated direct density readings can be consistently obtained.

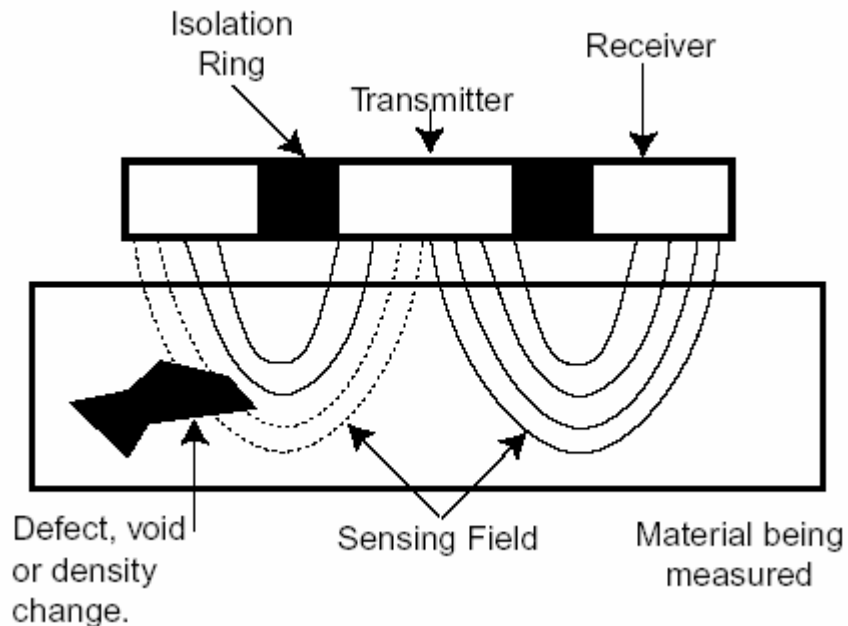
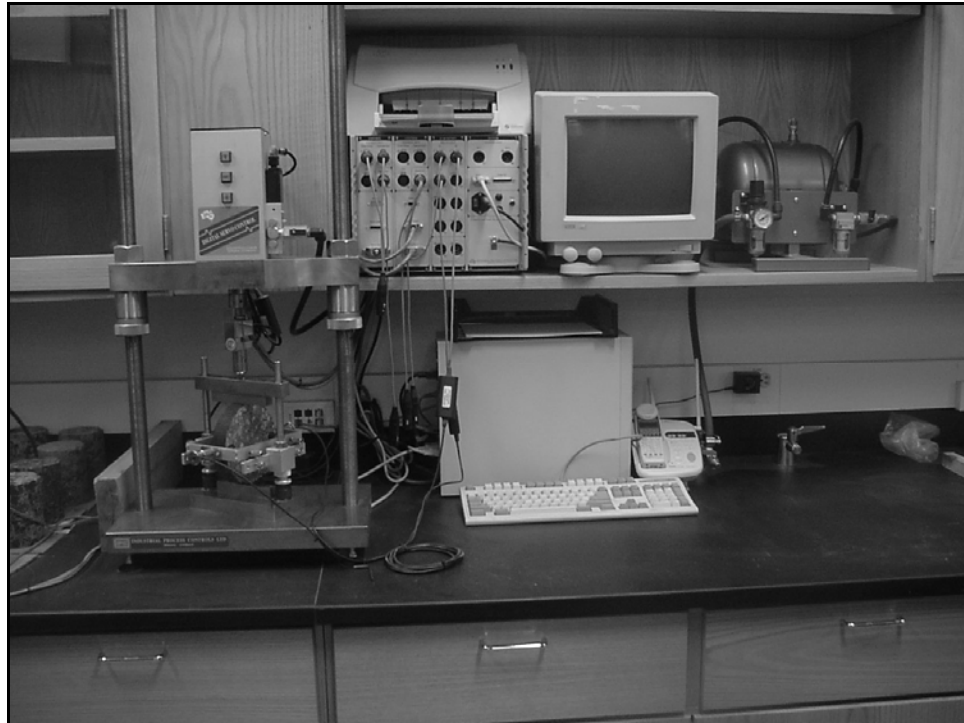


Figure 3.3 – Pavement Quality Indicator Schematic (PQI) [30]

3.4 Universal Testing Machine (UTM)

Testing for resilient modulus (MR) values was done using the Universal Testing Machine (UTM), developed by Industrial Processes Incorporated (IPC), Australia. The

equipment, shown Figure 3.4, is comprised of a software controlled 14P Pneumatic Servo controlled loading system, capable of applying loads up to 40 kN (8,992 lbf) [31]. It was enclosed in an environmental chamber allowing it to run samples at various temperatures ranging from -20 to 70°C (-4 to 158°F). Testing is done in accordance with ASTM D4123².



Note: Seen without the environmental chamber.

Figure 3.4 – Universal Testing Machine, 5-Pulse Resilient Modulus Testing

For the purpose of this study, 100mm (4 inch) diameter samples, of approximately 63mm (2.5 inch) thick and approximately 95% of the Theoretical Maximum Density (TMD), were tested in the five pulse indirect tensile testing jig, seen in Figure 3.5. This allows for a load to be applied vertically through the sample and lateral linear variable differential transducers (LVDT) measure the lateral deflection of the samples.

² ASTM D4123, “Standard Test Method for Indirect Tension Test for Resilient Modulus of Bituminous Mixtures”, ASTM International

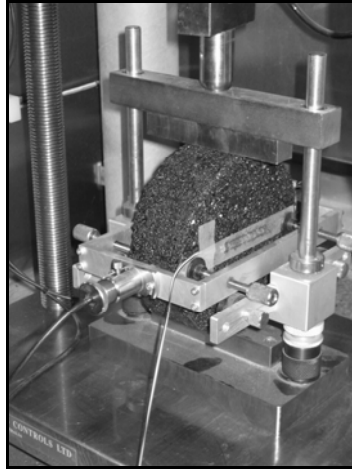


Figure 3.5 – Resilient Modulus Testing Jig

They were tested at a temperature of approximately 25°C (77°F) while a load of 400 N (90 lbf) was applied to the sample for 5 condition pulses followed by 5 testing pulses using a frequency of 10 Hz (Figure 3.6). T_L and T_R represents the loading duration and rest time respectively. T is the period of loading, whiled F_0 is the magnitude.

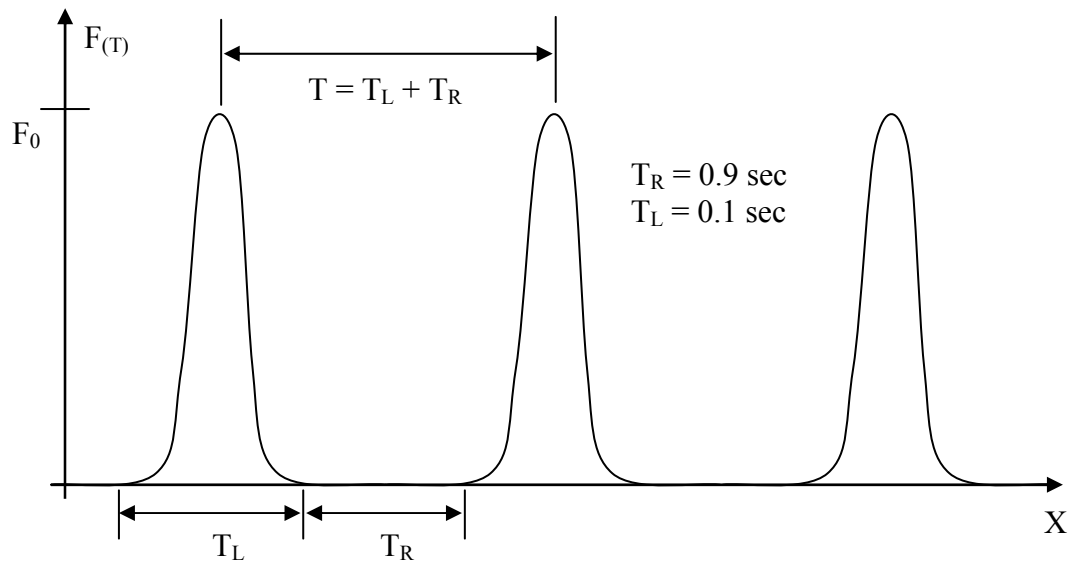


Figure 3.6 – 5-Pulse Resilient Modulus Test

Using a Poisson's ratio of .35, assumed to be typical for HMA pavements, along with the sample's diameter and thickness, a resilient modulus value is calculated by recording

repeated load and total deformation throughout testing. For calculation the resilient modulus is defined as: The magnitude of the dynamic load multiplied by Poisson's ratio plus a constant of .2734 divided by the total deformation times the specimen's thickness.

Equation 3.3 is provided in ASTM D4123 titled the "Standard Test Method for Indirect Tension Test for Resilient Modulus of Bituminous Mixtures".

Equation 3.3 – Resilient Modulus

$$M_R = \frac{P(\mu + 0.2734)}{\Delta h * t}$$

The procedure is hands-free, meaning once the sample information has been entered into the computer software and the LVDT's are zeroed, the test runs to completion without the assistance of an operator and the test results are displayed on the screen. The results can be printed and saved in ASCII format, making it convenient to access and analyze the information.

3.5 Model Mobile Load Simulator MK3 (MMLS3) Testing System

The MMLS3 system is comprised of three parts: 1) the mold to provide confinement of the pavement system and vibratory steel drum compactor for compaction of the pavement slab and pavement structure, 2) the unidirectional loading equipment used to apply the wheel loads to the pavement system, and 3) an environmental chamber used to enclose the pavement system and loading equipment and heated or cooled, as indicated by the testing protocol.

3.5.1 Mold and Vibratory Compactor

The mold assembly and vibratory compacting steel drum set up is comprised of two stackable 150mm (6") high by 3m (9') long and 1m (3') wide molds which provide confinement for the material being compacted from the subgrade to the pavement surface. Figure 3.7 illustrates the means by which a typical pavement slab is compacted.

A 16mm (5/8”) steel plate has been laid on top of 214mm (8.42”) of compacted subbase which is used as part of the pavement system during testing of the hot mix asphalt slab.



Figure 3.7 – Mold and Compaction System

3.5.2 MMLS3

Figure 3.8 illustrates the MMLS3 as seen from the side. It is comprised of four, 300 mm (12”) rubber pneumatic tires, Vredestein V-76 4.0 6-ply (Figure 3.9), which can be inflated to 690 kPa (100 psi) applying a load of 1.9 kN (427 lbf) or 2.7 kN (607 lbf). [25]. The load on each of the four wheels is controlled by adjusting the tension in the spring attached between the wheel and bogie and is maintained by adjusting the height of the machine above the pavement using four crank handles. The system also has the ability to apply lateral wander, mimicking the movement of vehicles on a typical pavement system; however, wander was not investigated in this study.

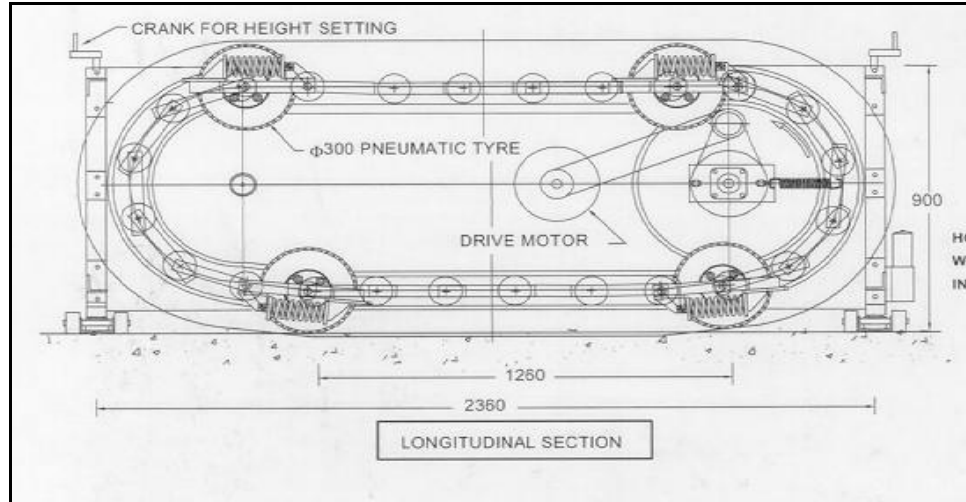


Figure 3.8 – Longitudinal Cross Section of the MMLS3

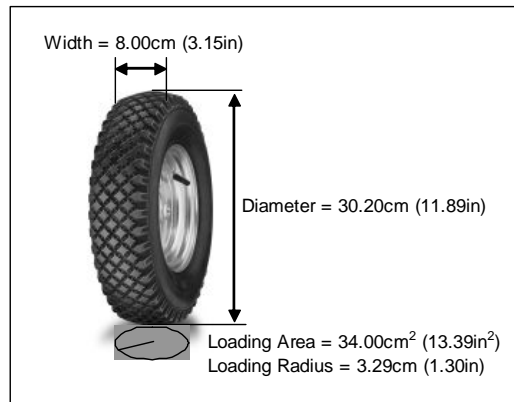


Figure 3.9 – Vredestein Tire Schematic

3.5.3 Environmental Chamber and HVAC System

The heating, ventilation, and air conditioning system provides hot or cold air to the pavement system through 150mm (6 inch) insulated flexible heating ducts to two diffusers placed on each side of the pavement slab. This set up allows for one diffuser to blow hot or cold air across the pavement surface, where the second diffuser is in suction acting as a cold/hot air return, balancing the system. The diffusers reverse roles approximately every four minutes, ensuring balanced temperatures across the pavement slab. The unit is capable of maintaining temperatures ranging from 5°C (41°F) to upwards of 60°C (140°F).

3.6 Instrumentation and Data Acquisition System (DAS)

To record strain at the bottom of the pavement layer, Omega Engineering model number SGD-50/120-LY40 [32], 120-ohm foil strain gauges were selected and checked against predicted strains from cores tested in the indirect tensile mode. The gauges were calibrated using an aluminum beam of known properties and load. Signals from strain gauges were checked by running the MMLS3 at different speeds and the effects of noise were checked by acquiring data with and without running the MMLS3 and comparing the results. Type J thermocouples, Omega Engineering model number 5TC-TT-24 [33], with Teflon insulation were used to monitor the temperature at the base of the pavement. A National Instruments® (NI) data acquisition system [34] running on Labview® software [35] was selected for data acquisition and connected to a computer for data storage and analysis.

Figure 3.10 provides a graphical representation of the process in which data was collected. The data from the monitoring gauges was directed into sub modules where the wires were fastened. The sub modules were connected to modules specific to the type of gauges being used, either thermocouples or strain gauges. Those modules were then inserted into the data controller box which was wired to a computer where the Labview® software controlled the data collection. Microsoft® Excel was used as the primary post processing tool.

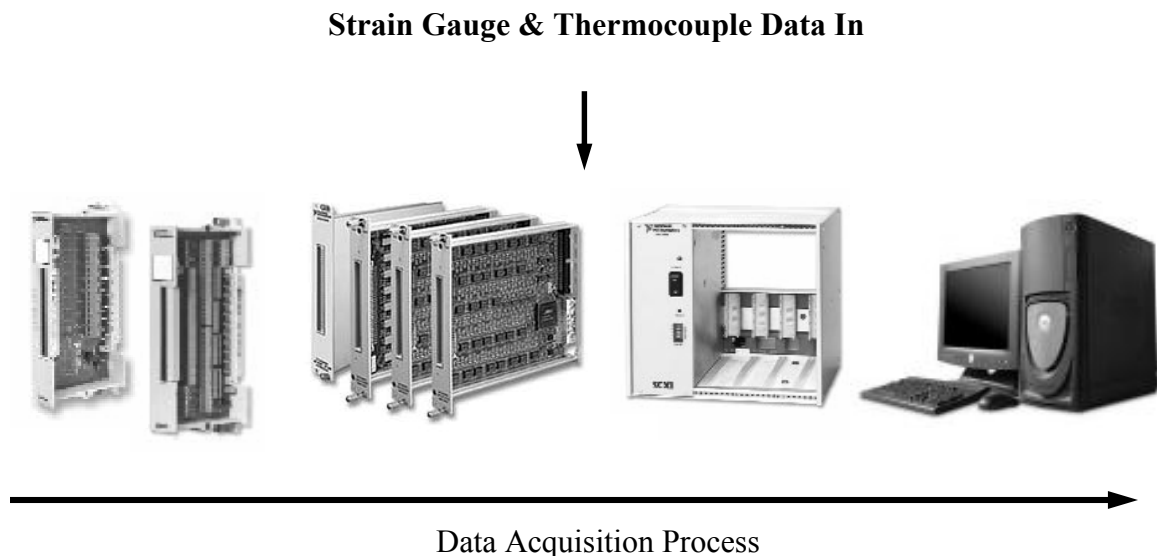


Figure 3.10 – Data Acquisition Process

4 Materials

A typical test section consisted of the pavement layer above three layers of 25mm (1”) thick D80 neoprene rubber sheets followed by a 16mm (5/8”) thick steel plate and a 214mm (8.5”) thick layer of sand. The materials and thicknesses of the pavement system were chosen, keeping in mind the scaled testing model, illustrated in Chapter 0. The pavement was subjected to a load of 2.7kN (607lbf) with a contact radius of 3.29cm (1.3”) and an average tire pressure of 655kPa (95psi). Figure 4.1 provides a cross section view of the pavement system used in this study.

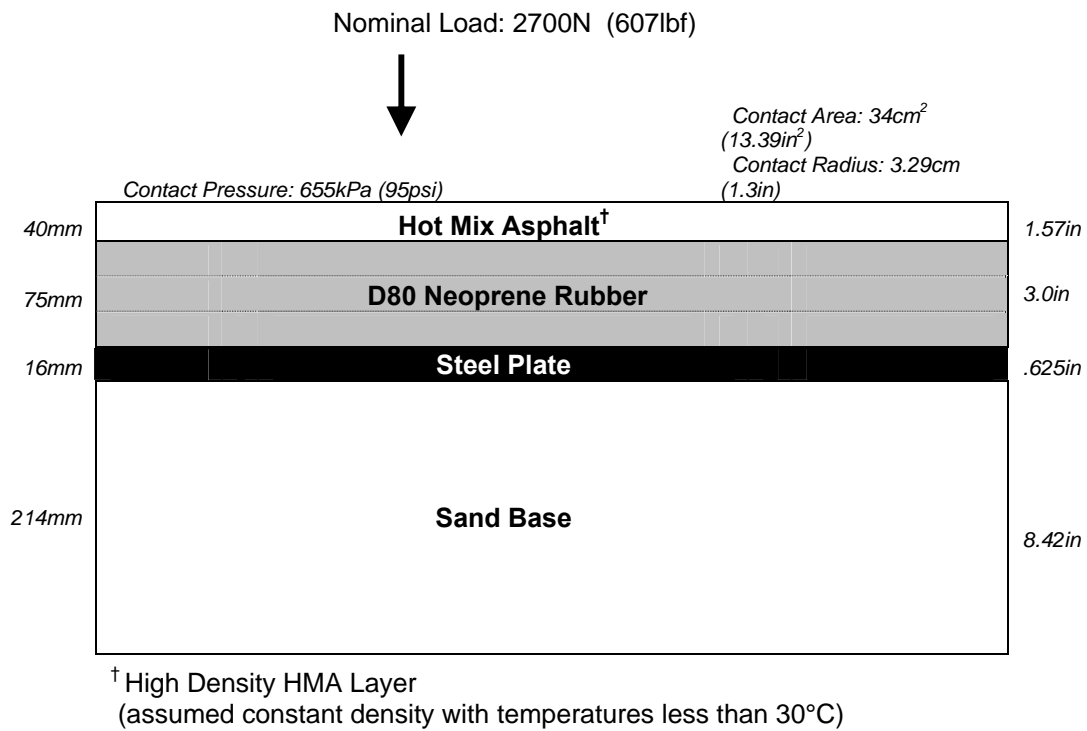


Figure 4.1 – Pavement System Cross Section

4.1 Sand Base

Washed natural sand was chosen as the base material for the pavement system and water was added until the material reached optimum moisture content, based on moisture density relationship testing as specified in AASHTO T180³ specification. The

³ AASHTO T180, “Moisture-Density Relations of Soils Using 4.54kg(10lb.) Rammer and a 457mm(18in.) Drop”

sand was compacted using a vibratory roller atop 16mm (5/8”) and 25mm (1”) Neoprene rubber sheet to minimize the noise. The sand was rolled until an average modulus of 35.1MPa (5,091psi) was indicated by use of the GeoGauge™. The results can be found in Table 4.1 calculated using Equation 3.2.

Table 4.1 – Sand Stiffness by GeoGauge™

Measured Stiffness, K (MN/m)	Young's Modulus, E (MPa)
5.35	42.2
4.36	34.4
4.24	33.4
4.17	32.9
4.21	33.2
4.66	36.7
4.35	34.3
4.26	33.6
Average	35.1

The stiffness of the sand base was also checked using a DCP yielding a stiffness of 35.7MPa. Dynamic Penetration Index (DPI) results are shown in Table 4.2 and converted to California Bearing Ration (CBR) values using Equation 4.1 and Equation 4.2. The two CBR values were converted to Young’s Modulus (E) values and averaged in Equation 4.3.

Table 4.2 – Dynamic Cone Penetrometer Results

Position	Number of blows	DCP readings (cm)	Midrange depth of readings (cm)	Dynamic Penetration Index (cm/blow)
1	0	0.0		
	1	4.0	2.0	4.0
	2	6.5	5.3	2.5
	3	8.8	7.7	2.3
2	0	0.0		
	1	10.3	5.2	5.2
	2	15.1	12.7	7.5
3	0	0.0		
	1	4.9	2.5	2.5
	2	12.0	8.5	6.0

$DPI_{AVG} = 42.8\text{mm}$

Equation 4.1 – DPI to CBR calculation base on USAE Waterways Experimentation Station [36]

$$CBR_a = \frac{292}{DPI^{1.12}} = 4.35 \qquad E_a = 17.6 * CBR_a^{0.64} = 45.0 \text{MPa}$$

Equation 4.2 – DPI to CBR as reported in “The Structural Design of Bituminous Roadways” [37]

$$CBR_b = \frac{1}{(0.017019 * DPI)^2} = 1.88 \qquad E_b = 17.6 * CBR_b^{0.64} = 26.4 \text{MPa}$$

Equation 4.3 – Average Young’s Modulus determined from DCP testing.

$$E_{AVG} = \frac{(E_a + E_b)}{2} = 35.7 \text{MPa}$$

4.2 Steel Plate

A 16mm (5/8”) steel plate was incorporated into the pavement substructure to stiffen up the subbase during testing and compaction. The steel plate was a single piece of A36 cold rolled steel with a modulus of 20,000 MPa (29,007,550psi) and Poisson’s ratio of 0.26.

4.3 D80 Neoprene Rubber

Three layers of 80 durometer Neoprene rubber with dimensions of 25mm thick by 2,742mm long and 915mm were used as the layer just below the asphalt pavement. The Neoprene layers were tacked with RS-1 asphalt emulsion to ensure a fully bonded, no slip structure. Fifty millimeter gaps were left on both ends of the D80 Neoprene which were filled with sand. Direct compression testing of the rubber revealed a modulus of 43.75 MPa (6,345psi) and an assumed Poisson’s ratio of 0.45 was used.

4.4 RS-1 Emulsion Tack Coat

The RS-1 emulsion tack coat was an anionic asphalt emulsions which is rapid setting and used in sand seal and tack coating applications [38]. Emulsion consists of

three basic ingredients: paving asphalt, water, and emulsifying agent. Rapid set emulsions have a maximum of 35% water and thus should not be diluted [38]. Conventionally tack coat is used to ensure a good bond between the existing pavement surface and the new HMA overlay. It is also commonly placed between each lift of HMA as well as on all vertical surfaces that the new pavement will be placed against.

The tack coat was applied as recommended by the manufacturer and allowed to set until it turned from brown to black indicating that the moisture had evaporated and it was at its full strength. Tack coats were applied between all of the pavement structure layers, with the exception of the subbase and steel plate.

4.5 Hot Mix Asphalt

Hot mix asphalt is the uppermost layer of the pavement system and the surface being loaded by the MMLS3. The HMA was a standard Maine Department of Transportation 9.5mm (3/8”) mix with aggregates obtained from Lane Construction’s Belfast quarry. The following table displays the specifications of aggregates used in making the HMA slabs:

Table 4.3 – Aggregate Properties & Gradation

Aggregate Property	Value	Sieve Size		%
		(inch)	(mm)	Passing
Nominal Maximum Aggregate Size	9.5mm	0.500	12.5	100
Coarse Aggregate Angularity	98.6/98.2	0.375	9.5	95
Fine Aggregate Angularity	47	4	4.75	60
Sand Equivalent Test	73	8	2.36	47
Washington Degradation (ME Dot)	75	16	1.18	33
Combined Aggregate Bulk Specific Gravity	2.687	30	0.6	20
		50	0.3	12
		100	0.15	8
		200	0.075	5

4.6 Asphalt Binder

The asphalt binder used in testing was obtained from Hudson Laboratories, Inc. Providence, RI. The penetration grading (PG) of the asphalt was 64 -28 and percent binder used in the pavement slab was 5.9 percent by mass. By using the viscosity-temperature susceptibility (VTS) model, the temperature susceptibility of the binder can be characterized using two parameters - VTS and A (intercept). Values were provided by Hudson Laboratories where the regression parameter 'A' was equal to 10.312 and the 'VTS' was -3.44. Typical viscosity-temperature relationship parameters, which are incorporated in the *AASHTO 2002 Guide for Design of Pavement Structures* [1], are shown in Table 4.4.

Table 4.3 – PG 64-28 Binder Properties provided by Hudson Laboratories

From test data of 64-28 asphalt binder by CITGO:					
Temp (°C)	G* (Pa)	delta (δ)	Viscosity (CP)	Log (Rnk)	Log(Log(η))
52	5678	81.39	599.97	2.7674	0.4438
58	2593	83.45	267.69	2.7753	0.3852
64	1249	85.19	127.06	2.7831	0.3230
70	629	86.62	63.47	2.7908	0.2559
76	332	87.50	33.33	2.7983	0.1827

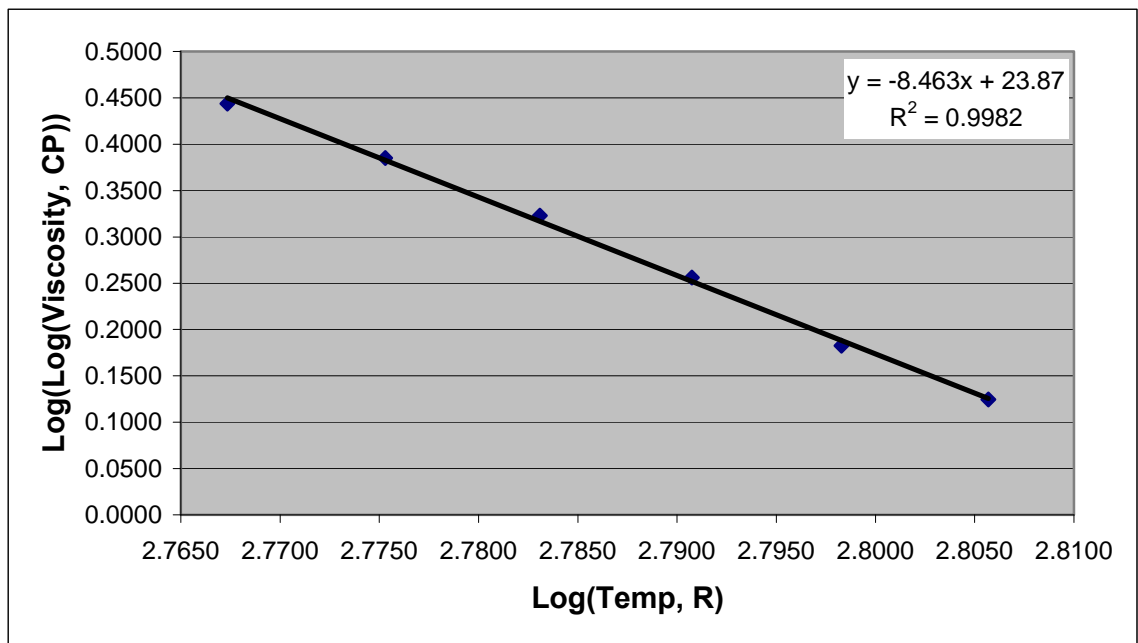


Figure 4.2 – Graph and equation for temperature vs. viscosity for asphalt binder

Table 4.4 – Typical A and VTS Properties of PG Graded Binders

High Temp Grade	Low Temperature Grade														
	-10		-16		-22		-28		-34		-40		-46		
	VTS	A	VTS	A	VTS	A	VTS	A	VTS	A	VTS	A	VTS	A	
46										-3.901	11.504	-3.393	10.101	-2.905	8.755
52	-4.570	13.386	-4.541	13.305	-4.342	12.755	-4.012	11.840	-3.602	10.707	-3.164	9.496	-2.736	8.310	
58	-4.172	12.316	-4.147	12.248	-3.981	11.787	-3.701	11.010	-3.350	10.035	-2.968	8.976			
64	-3.842	11.432	-3.822	11.375	-3.680	10.980	-3.440	10.312	-3.134	9.461	-2.798	8.524			
70	-3.566	10.690	-3.548	10.641	-3.426	10.299	-3.217	9.715	-2.948	8.965	-2.648	8.129			
76	-3.331	10.059	-3.315	10.015	-3.208	9.715	-3.024	9.200	-2.785	8.532					
82	-3.128	9.514	-3.114	9.475	-3.019	9.209	-2.856	8.750	-2.642	8.151					

5 Test and Analysis Plan

The testing plan consisted of five distinct steps. The primary step was to acquire a data acquisition system, data collection program, and computer which could collect and store the data files. The second step in the process was to set up a pavement system which would appropriately model a typical pavement system at 1/3 scale. Third, a pavement was mixed and compacted creating a HMA test slab. The test slab was then instrumented with thermocouples and strain gauges. Once the pavement system, slab, and data acquisition system were in place the MMLS3 was run at varying frequencies and temperatures. The fifth step was to analyze the strain data and develop conclusions and recommendations based on the results of testing. Figure 5.1 is a graphical representation of the testing plan and sequence.

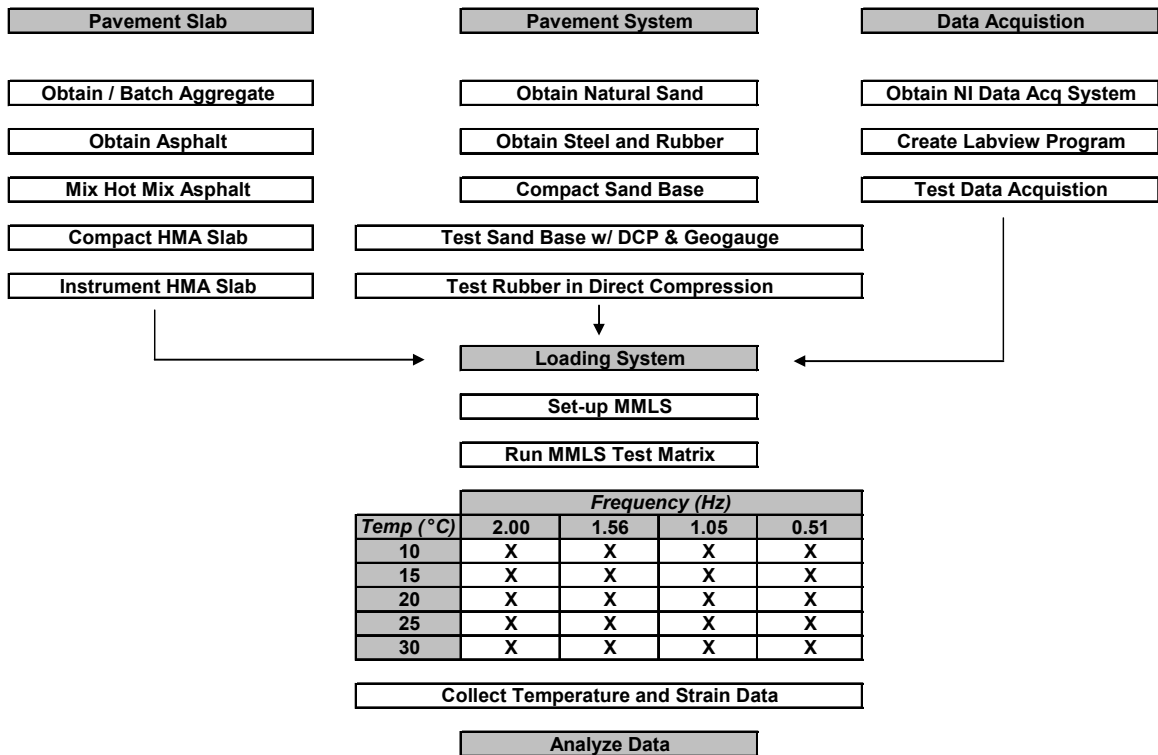


Figure 5.1 – Overview of Testing Plan

5.1 Pavement System

To accurately model the strain in the pavement slab under 1:3 scale loading provided by the MMLS3, the pavement system must also be 1:3 scale. An appropriately scaled pavement was designed in a prior project conducted at Worcester Polytechnic Institute (WPI) in which Fatigue Characterization under Accelerated Loading was studied [39]. In the WPI study the development of a model pavement and testing protocol using the MMLS3 was studied in depth and was used in this study. The steps of the process applicable to the current study will be presented in detail in Chapter 6 - Development of Pavement Slab, Structure & Test Protocol.

5.2 Pavement Slab

The pavement slab, from batching through compaction, was created in the Pavement Research Laboratory at WPI. The aggregate was obtained through the assistance of the Maine Department of Transportation (MeDOT) and Lane Construction's Belfast, Maine quarry. Liquid asphalt was received from Providence's Hudson Laboratories. The slab was compacted using a vibratory roller and compacted to approximately 95-96% voids and a thickness of 1.57 inches.

5.3 Loading System

The loading system comprised of the model mobile loading system. The MMLS3 was run at four different frequencies (approximately 0.5, 1.0, 1.5, and 2.0 Hz) over a range of temperatures (10, 15, 20, 25, 30°C or 50, 59, 68, 77, 86°F). A load of 2.7 kN (606 lbf) was applied using an average tire pressure of 655 kPa (95 psi).

5.4 Data Acquisition

Perhaps the most important aspect of the test plan was the data acquisition system which was used to monitor the temperature and strain produced during the loading of the pavement. The rate of acquisition needed to be such that a plot of strain versus time illustrated the results properly, including the minimum and maximum strain. To ensure the strain gauge readings were accurate and the acquisition system was functioning

properly, they were tested on a standard aluminum beam. The data was acquired using National Instruments hardware and LabView 7.1 software. Temperature and Strain was measured at a rate of 100 scans per second over a range of 10 seconds, resulting in 10,000 points of data for each strain gauge and thermocouple. Data was collected at 5 minute intervals for the duration of testing.

5.5 Data Analysis

With thousands of scans per file and hundreds of files per test, there was a need to analyze the data quickly and accurately. Microsoft Excel was chosen and a macro was developed which could provide analysis of the pavements resilient strain in both the transverse and longitudinal directions. A formula of Max minus Min was used for the transverse strains while Max minus Mode was used for the longitudinal strains. It was determined that this equation could provide sufficiently accurate results. A graphical representation can be seen in Figure 5.2.

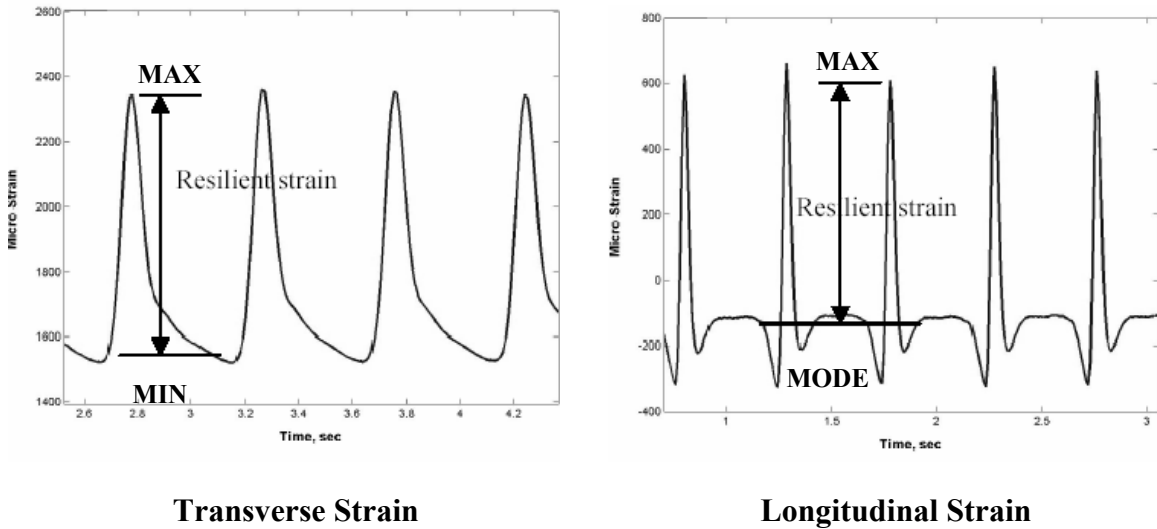


Figure 5.2 – Example of Transverse and Longitudinal Strains, respectively.

These results will be referred to as actual MMLS3 or measured strain throughout this paper. BISAR was used to calculate theoretical strains at the base of the pavement layer using specific layer properties. Furthermore, Witzack's equation was used to supply HMA modulus values to BISAR at varying temperature-frequency combinations and the results were compared to actual MMLS3 strains. A schematic of the analysis plan can be seen below in Figure 5.3 – Overview of Analysis Plan.

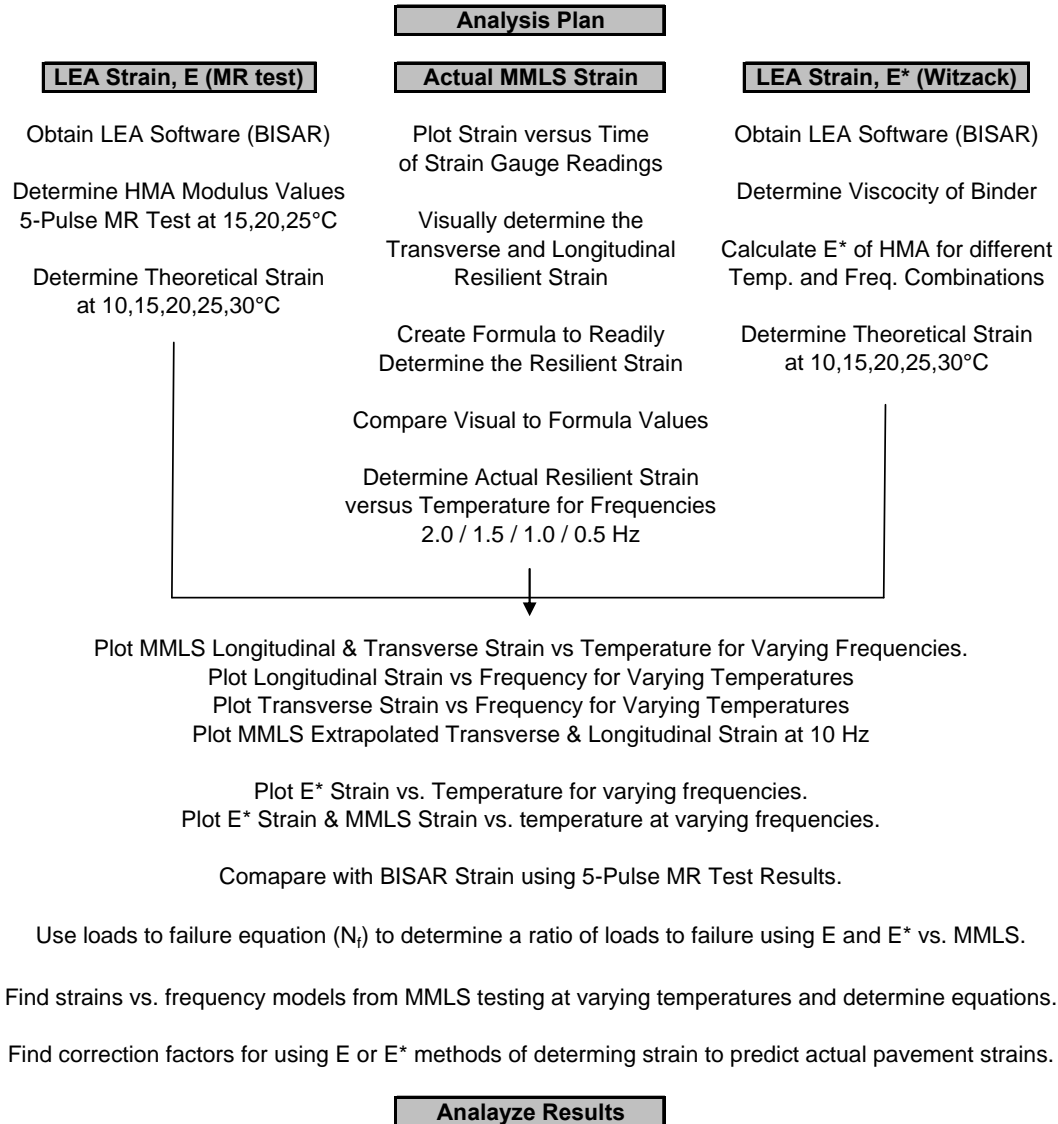


Figure 5.3 – Overview of Analysis Plan

6 Development of Pavement Slab, Structure & Test Protocol

As discussed in Chapter 0, the pavement system and slab development was based upon a previous study in which the materials were selected and chosen based upon their impact in a 1:3 scaled testing situation. The following sections will describe the process of constructing the pavement system and pavement slab, in the order in which they occurred.

6.1 Pavement System

The pavement system started with a thick, low modulus layer of washed natural concrete sand from a local landscaping supplier and was brought to optimum moisture content. Once optimum moisture was achieved, the 8+ inches was compacted by vibratory compaction using the roller provided with the MMLS3 system. Further compaction was achieved by placing a 5/16 inch steel plate and 1 inch D80 neoprene rubber sheet to limit noise. This allowed additional compaction to take place without the shoving of material under the load of the roller. The steel plate and rubber sheet was subsequently removed and the layer was flattened using a typical screed while the thickness was monitored. Additional passes of the roller, in static mode, were made and the layer was then tested for stiffness using the DCP and GeoGauge™. The steel plate was then re-lowered into the MMLS3 mold and a coating of RS-1 emulsion was applied. Three layers of D80 neoprene rubber were lowered and tacked in a similar manner. This provided the basic model pavement system in which the slab would later be placed. Young's modulus and Poisson ratios were calculated for the sand and rubber and assumed for typical A-36 steel. A structural representation was shown in Figure 4.1.

6.2 Pavement Slab

Creation of a laboratory specimen, while relatively straightforward, takes on a different meaning when creating a 37.5mm (1.5 inch) thick, 91cm (3 foot) wide and 273 cm (9 foot) long slab in the confines of a lab using standard laboratory equipment. Initially it must be determined whether there is sufficient oven space for drying and heating the aggregates and binder to mixing and compaction temperatures. Once

adequate oven space can be secured, the second issue is to have enough man power on hand to mix and compact the slab in the limited time frame. Mixing should take no more than one half hour in order to sufficiently maintain the aging time period specified by ASTM D6925. The third aspect to a laboratory compaction of such a large scale is having the equipment to compact the slab effectively.

The pavement slab was constructed in WPI's Pavement Research Laboratory. The aggregate was classified as Belfast 9.5mm mix and comprised 20% Tertiary sand, 40% Stockton sand, and 40% half inch ledge. The aggregate was oven dried at 110 degrees Celsius until a constant weight was achieved. The aggregate was then weighed out into 8kg samples according to the gradation shown in Table 4.4 and subsequently heated to mixing temperature. The asphalt binder had a penetration grade (PG) of 64-28. The mixing temperature of the asphalt was 155°C (311°F) and had a compaction temperature of 145°C (293°F). The heated 8kg's of aggregate were placed on a scale and asphalt binder was added to achieve an asphalt content of 5.9% by weight and subsequently mixed using a 5-gallon bucket mixer. Once adequately mixed, the hot mixed asphalt was returned to the 155°C oven for an average of two hours of aging. The amount of mix required for lay down was determined using volumetric calculations, which would provide the target density of 94 to 96 percent of theoretical maximum density in the space provided.

6.2.1 Slab Compaction

Compaction of the slab was done on top of the pavement system using wooden forms to confine the mix while being compacted. Prior to compaction, a 1/8 inch wooden tile board [40] was placed on top of the Neoprene rubber to create a buffer for cutting the asphalt slab into quarters. A sheet of asphalt roofing paper was placed on top of the board to prevent adhesion between the mix and the board. A series of six radiant heat lights [41], seen in Figure 6.1, were hung 375mm above the compaction form to uniformly heat the system prior to placing the mix, as well as to contain the mixes heat during the compaction process.



Figure 6.1 – Radiant Heat lamps hung above the mold during compaction (typical)

Compaction, which can be seen in Figure 6.2, began by placing the asphalt mix into the forms and leveling with a rake while being careful to limit segregation. Lab personnel with experience in the construction of slabs were employed in the process. The vibratory roller was continuously sprayed with water during compaction to limit peeling of the thin lift being created. The pressure of the roller was controlled through a hand crank which used threaded rods on both ends of the roller to apply a downward pressure. This was controlled through experience and by watching the thin slab for any shoving during compaction. A non-nuclear device called a pavement quality indicator (PQI) was also used in between roller passes to help determine when the target density was met. The PQI had been calibrated on previous slabs of similar make-up. The compaction consisted of continuous compaction until the mix cooled to a temperature of 85°C (185°F) and at a pressure which didn't allow shoving of the mix. A final series of passes was then made in static mode.



Figure 6.2 – Compaction of a pavement slab

6.2.2 Slab Cutting and Preparation

Following compaction, the slab was allowed to cool overnight to room temperature and the wooden forms were removed. Lines were then drawn onto the slab using silver paint markers to indicate where the slab was to be cut. Dry ice was placed on plastic over the cutting lines and the slab was locally cooled to 0 to 5 degrees Celsius. The low temperatures provided by the dry ice throughout the process prevented stress-induced damage prior to testing by increasing the stiffness of the material. The slab was quartered using a diamond blade on a skill saw using a fine mist sprayer to limit dust and provide cooling to the blade. A wet-dry vacuum was also used to control the amount of water build up on and around the slab segments. The entire slab quarters were cooled using dry ice and then carefully spread using a steel wedge (Figure 6.3), slid onto $\frac{3}{4}$ inch plywood, sandwiched between another piece of plywood (Figure 6.4) and flipped. The asphalt roofing paper was subsequently peeled off and the slabs were labeled using paint marker.



Figure 6.3 – Cutting, spreading, and movement of pavement slabs



Figure 6.4 – Sandwiching pavement slab for transport, instrumentation, and storage

6.2.3 Slab Instrumentation

Instrumentation of the pavement slab began by creating grooves in the bottom of the pavement to house the strain gauges, thermocouples, and associated wiring. This was achieved by placing the slabs, while still on the plywood to provide support, onto a bench top where a radial arm saw could be used. Four diamond blades were placed on the machine to cut ½ inch grooves for the strain gauges, while two were used for cutting the wire grooves, and a single blade for the thermocouple wires. The slabs were then vacuumed in preparation for instrumentation.

The first step prior to placing the strain gauges was to use a flat head screwdriver or a ½ inch chisel to smooth raised bumps formed due to four blades being used during cutting. The second step was to place a smooth, hard barrier between the aggregate particles in the mix and the strain gauge. This was achieved by spreading a thin layer of 2-part epoxy in the grooves, preventing individual particles from breaking the thin wires of the strain gauge. After a drying period of 10 minutes a second layer of two part epoxy was spread and the strain gauge placed into the sticky layer and allowed to dry. The third step was to solder the strain gauge wires to the leads of the strain gauge itself, as seen in Figure 6.5. This was followed by applying a third application of two part epoxy in and around the connection points to prevent the wires from shorting and to inhibit the failure of the connections under loading. The final step was to fill the remaining void above the strain gauge with a material of similar behavior; Liquid asphalt of the same grade as the mix was used to provide protection and support in the system.



Figure 6.5 – Slab instrumentation

In order for the testing to work properly, the strain gauges were checked to ensure proper connections. This was done by using a voltmeter and checking the resistance between wire 1 and 2, 2 and 3, and 3 and 1. One of the checks should result in a resistance of zero ohms because they are connected together to one lead on the strain gauge. The other two checks should display a resistance of approximately 120 ohms due to strain gauge being of a 120 ohm nature. Thermocouples were only visually checked and a total of four were used in the pavement slab to monitor the overall temperature of the pavement during testing.

6.3 Testing

Final set up began by spreading RS-1 emulsion on the area of the Neoprene rubber which was to be covered by the pavement slab quarter. Once the emulsion was set the cooled slab was carefully flipped and placed on the rubber, leaving the strain gauges and thermocouples on the bottom of the slab. The wires were then attached to the National Instruments data acquisition system and when the pavement returned to room temperature, the gauges were calibrated. The test slab was held in place on four sides by

using quickset premix concrete. This was done to confine the test slab and minimize any shear movement. The Quickset concrete took approximately two to three hours to cure sufficiently. The profilometer, a device that measures the contour of the pavement surface, was used prior to loading to determine surface profiles. Profiles were determined to estimate rutting which can be volumetrically related to change in density.

The MMLS3, environmental chamber, and HVAC system were then made ready to apply loading to the pavement under a variety of different frequencies and temperatures. The tire load was checked to ensure the load was accurate and the machine was lowered into position being careful to keep all the wheels off the pavement surface. The machine was then leveled and lowered until a proper gap was achieved in the tire loading system. This allowed the load to remain constant under limited rutting.



Figure 6.6 – Lowering MMLS3 into testing position and leveling (typical)

The environmental chamber was set up to provide an insulated area for the HVAC to cool down. Once the air temperature reached an average of 20 degrees Celsius, the tire pressure was set to 655 kPa (95 psi) and the system was allowed to cool to its minimum

test temperature of 10°C (50°F). The strain gauges were calibrated and zeroed using a National Instruments® program called Measurement and Automation. This electronic calibration proved far simpler and more accurate than the previous attempts of manual zeroing using a different data acquisition system. Testing began with higher frequencies continuing to the lowest frequency to minimize the amount of rutting and permanent strain induced to the pavement slab.

7 Results and Analysis

This chapter will provide an interpretation and analysis of the data acquired during testing of the pavement slabs at varying temperatures and frequencies. Further comparisons will be made between actual MMLS3 results and those obtained by using Shell's BISAR Layered Elastic Analysis program using Indirect Tension Tests (E) and Witczak's Equation (E*).

7.1 Actual MMLS3 Resilient Strain Results

The following four graphs illustrate the effect of increasing temperature and frequencies on the micro strain ($\mu\epsilon$) experienced at the bottom of the pavement slab. Actual data can be found in Table A.1.1 through Table A.1.4 of Appendix A – Data Tables.

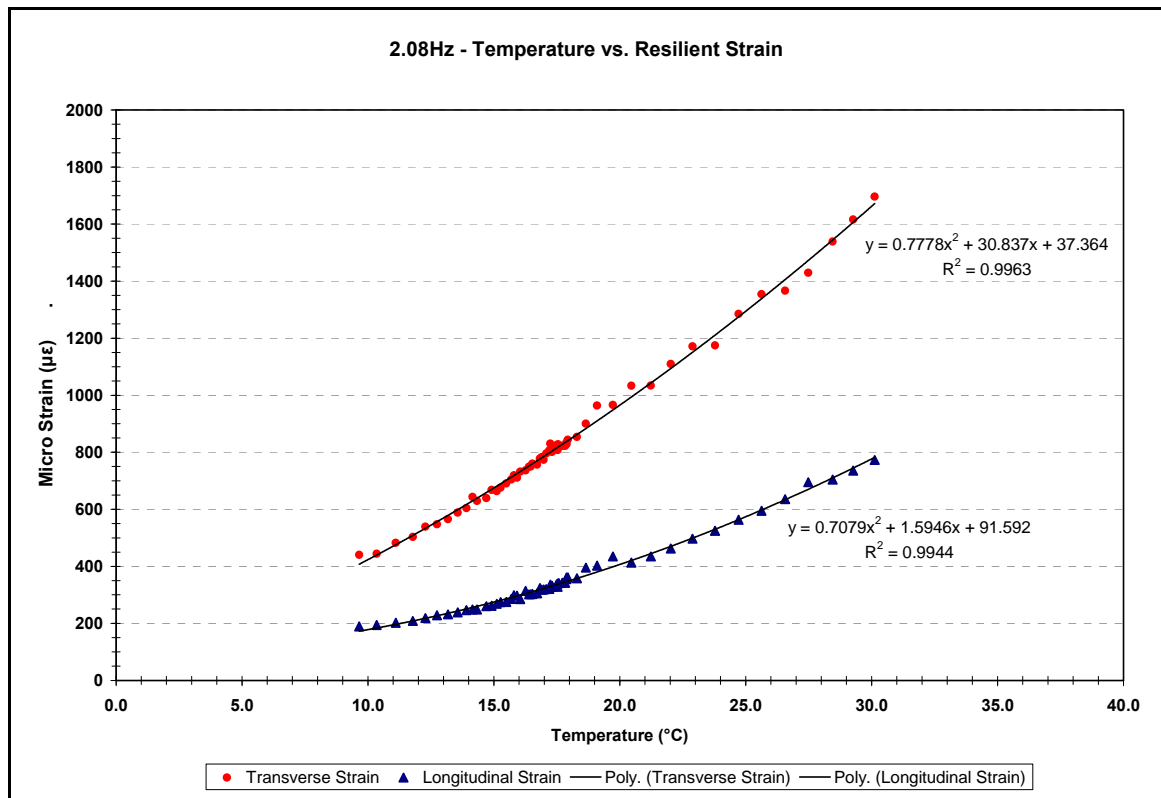


Figure 7.1 – 2.08 Hz Temperature vs. Actual MMLS3 Resilient Strain

The first impression of Figure 7.1 demonstrates that the transverse strain is affected more than the longitudinal strain as the temperature increases. Note that the longitudinal strain is initially 43 percent that of the transverse and increases to only 46 percent throughout the testing; a change of 3 percent. This indicates that both forms of strain at a higher frequency of 2.08 Hz exhibit similar strain increases.

As the frequency of loading decreases (approximately 0.5 Hz per test scenario) strain values increase as does the ratio between the transverse and longitudinal strain both at initial temperatures and most noticeably at final temperatures. For example, in Figure 7.2 (1.56 Hz), the initial transverse strain is exactly twice that of the longitudinal, but by a temperature of 30 °C, the longitudinal strain is closer to seventy percent that of the transverse; a change of 20 percent.

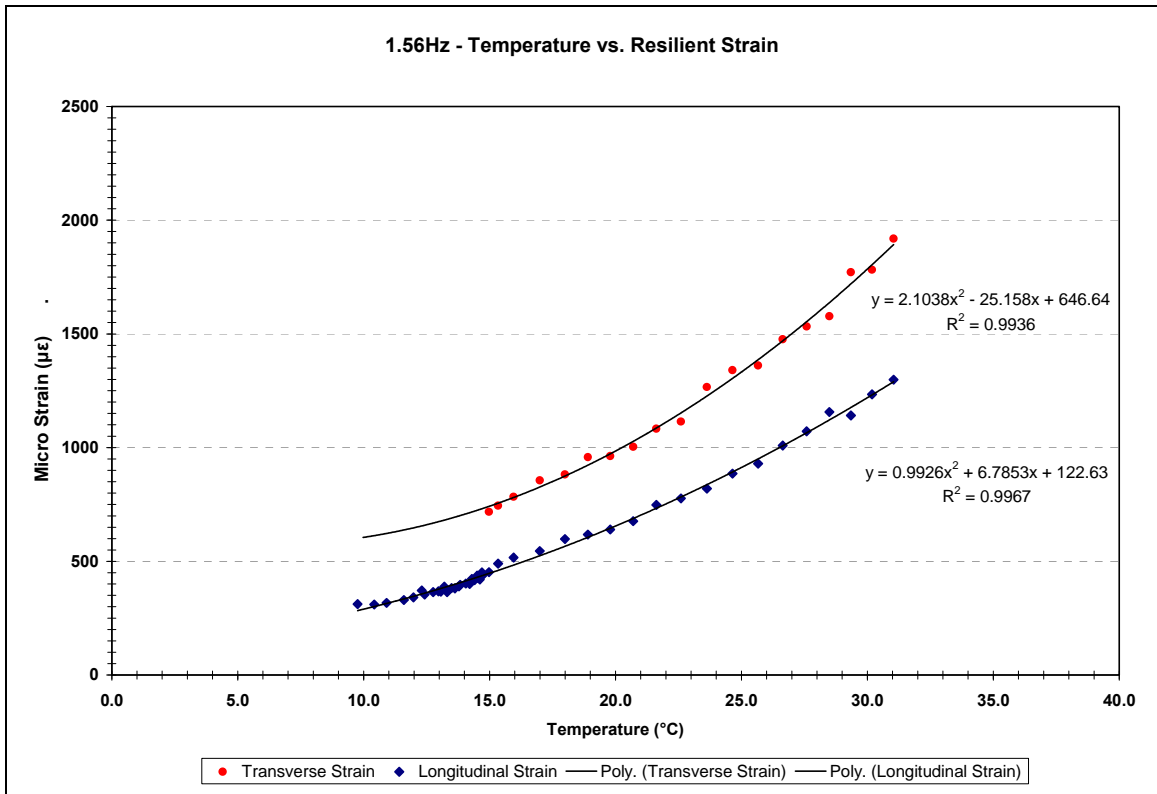


Figure 7.2 – 1.56 Hz Temperature vs. Actual MMLS3 Resilient Strain

It starts to become more evident that as we decrease the loading frequency, the strains increase in value and in particular the longitudinal strain increases at a far greater

rate. With a loading frequency of 1.05 Hz, seen in Figure 7.3, the initial ratio between transverse and longitudinal strain is 59 percent while at a temperature of 30 °C it is 90 percent; a change of 30 percent. It is also worth noting that a reduction of the loading frequency by ½ has led to a strain increase at 10 °C in transverse strain of 166% and 230% in longitudinal strain.

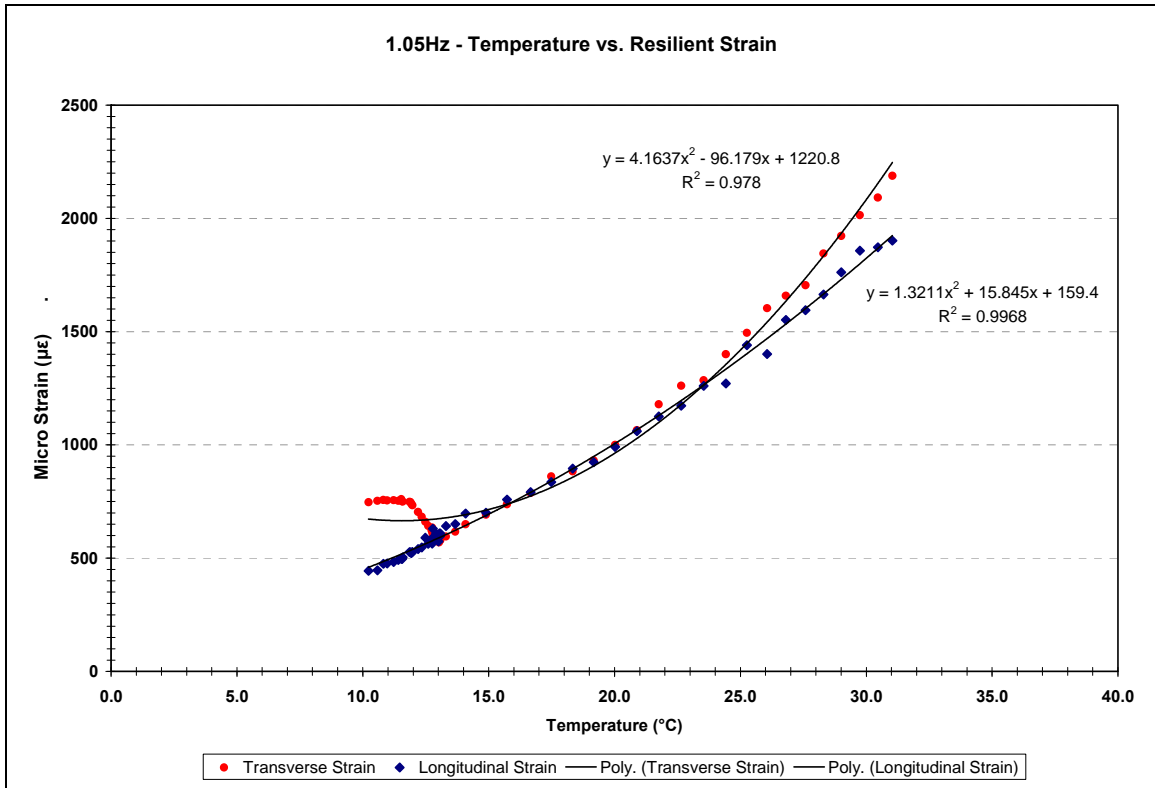


Figure 7.3 – 1.05 Hz Temperature vs. Actual MMLS3 Resilient Strain

In Figure 7.3, based upon the trends in this study, it seems that the longitudinal and transverse strains should be almost the same at lower temperatures. After 15 °C, the increase in strains exhibits more expected characteristics. When comparing the test results for the 0.51 frequency test, seen in Figure 7.4, it is apparent that the initial strain value is greater than the previous scenario.

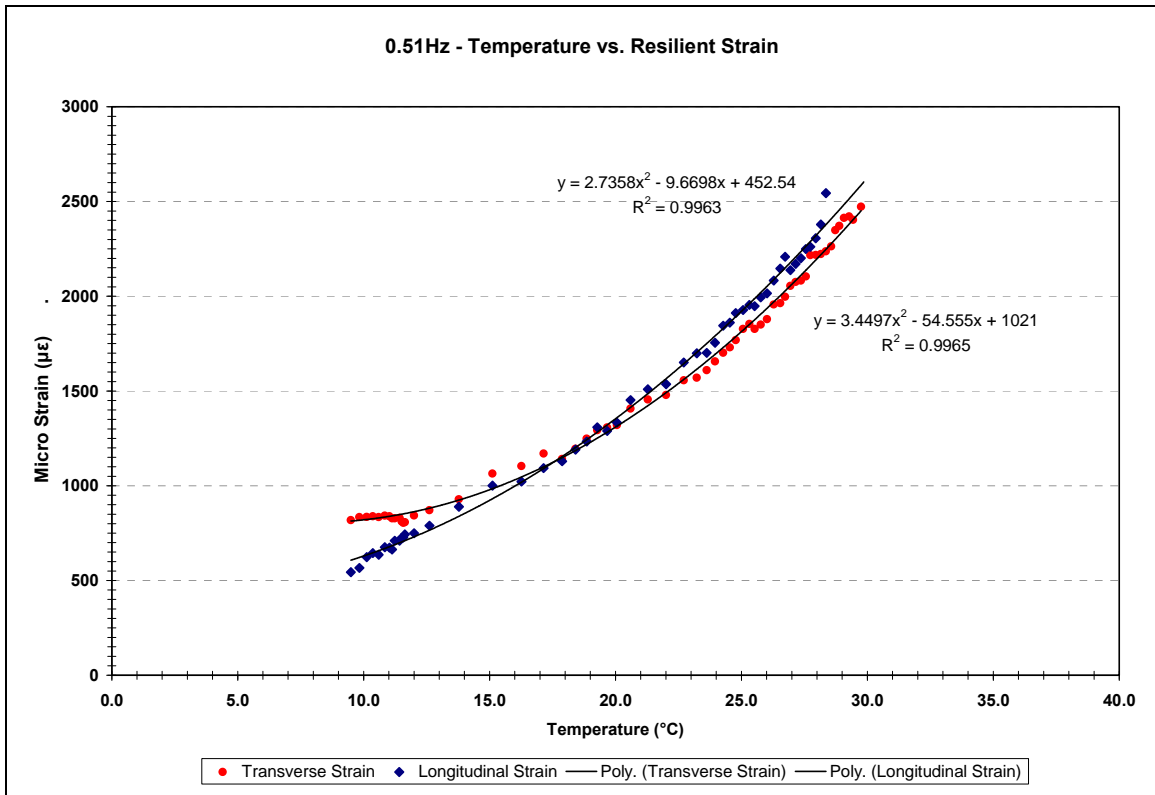


Figure 7.4 – 0.51 Hz Temperature vs. Actual MMLS3 Resilient Strain

One observation shown in Table 7.1 is that the initial difference in transverse strain from a frequency of 2.08 Hz to 0.51 Hz at 10 °C was 189% and nearly 298% for the longitudinal strain. Likewise, at a temperature of 30 °C for the same frequency scenarios, the transverse strain increased a similar 142%, while the longitudinal increased to over 500%. (Initially the transverse strain increased at a faster rate but as temperatures increased as the longitudinal strain illustrated similar strain increases).

The overall conclusions based upon actual MMLS3 strains are that as temperature increases, strain increases; the strains are further increased by a decrease in the loading frequency. Also, the longitudinal strain, though initially less than the transverse, increases at a greater rate than the transverse strain; eventually, allowing the longitudinal strain to become the limiting factor in a pavements ability to carry load.

Table 7.1 – Transverse & Longitudinal Ratios for Actual MMLS3 Resilient Strain

Frequency Hertz	Temperature Degrees C	Transverse Strain ($\mu\epsilon$)	Longitudinal Strain ($\mu\epsilon$)	Trans.(2.08) / Transverse	Long.(2.08) / Longitudinal	Transverse / Longitudinal
2.08	9.7	441	190	-	-	43%
1.56	9.8	618	312	140%	164%	50%
1.06	9.7	734	435	166%	229%	59%
0.51	9.7	835	566	189%	298%	68%
2.08	30.1	1696	773	-	-	46%
1.56	30.2	1782	1234	105%	160%	69%
1.06	30.5	2092	1873	123%	242%	90%
0.51	29.4	2403	3917	142%	507%	163%

Due to the frequency limitations of the MMLS3 (a maximum of 2.08 Hertz,) resilient strain values were extrapolated up to a frequency of 10 hertz for all five temperatures and both transverse and longitudinal strain. This step was necessary to compare the laboratory tests to both real world applications, as well as to compare the results to existing resilient strain models.

It was necessary to choose a trend line to extrapolate the data out to 10 Hz, which had both a high correlation to the actual data while at the same time holding true to the idea that the strain realistically should never reach zero. This was accomplished through the use of a power curve, with most R^2 values greater than .90 and all greater than .75. The closer the R^2 value is to one, the greater the ability of that model to predict a trend. A value of R^2 equal to one would imply that the trend line provides a perfect prediction.

Due to the fact that the power trend line provided a high quality prediction for most of the test scenarios, it was used even though it deteriorated slightly when applied to temperatures below 15 °C. Figure 7.5 and Figure 7.6 illustrate the extrapolation and the extrapolated data is provided in Table 7.2.

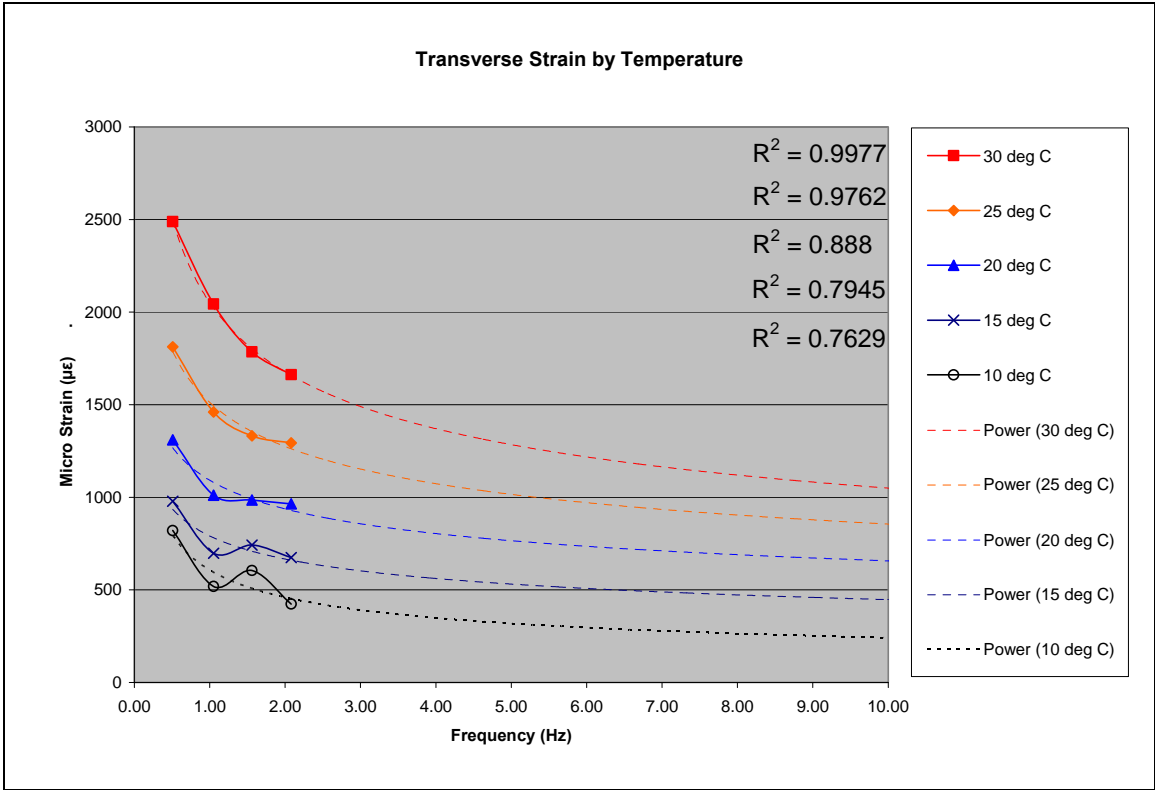


Figure 7.5 – Actual MMLS3 Strain - Temperature Curves of Transverse Strain vs. Frequency

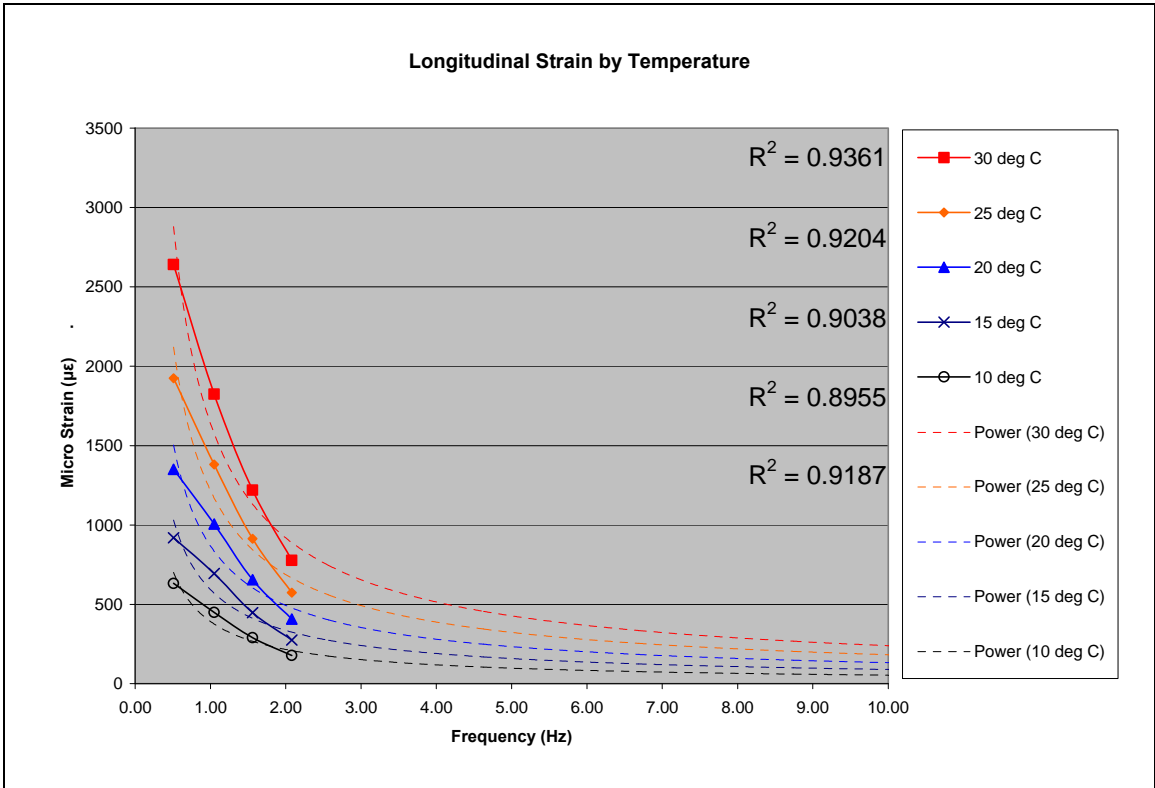


Figure 7.6 – Actual MMLS3 Strain - Temperature Curves of Longitudinal Strain vs. Frequency

When comparing the extrapolated strain values, it is worth noting that at a frequency of 0.51 Hz (which are actual results), the values for both transverse and longitudinal strains are nearly equivalent. We noted earlier that the longitudinal strain was actually becoming greater than the transverse strain for the most extreme scenario. As the frequency increases, there is a corresponding decrease in the severity of strain. The transverse strain diminishes at a fairly mild rate and at a frequency of 10 Hertz is nearly five times that of the longitudinal strain, which reduced quite rapidly to very low values.

Table 7.2 – Actual MMLS3 Strain extrapolated from 2.08 to 10.0 Hz

Frequency (Hz)	Transverse Strain ($\mu\epsilon$)					Longitudinal Strain ($\mu\epsilon$)				
	Temperature ($^{\circ}\text{C}$)									
	10	15	20	25	30	10	15	20	25	30
10.00	<i>232</i>	<i>436</i>	<i>643</i>	<i>837</i>	<i>1025</i>	50	84	125	171	224
9.00	<i>243</i>	<i>448</i>	<i>659</i>	<i>860</i>	<i>1058</i>	55	92	136	187	246
8.00	<i>255</i>	<i>462</i>	<i>677</i>	<i>887</i>	<i>1096</i>	61	102	150	207	272
7.00	<i>269</i>	<i>478</i>	<i>698</i>	<i>917</i>	<i>1141</i>	69	114	168	232	305
6.00	<i>287</i>	<i>498</i>	<i>723</i>	<i>954</i>	<i>1194</i>	79	130	191	264	348
5.00	<i>310</i>	<i>522</i>	<i>754</i>	<i>1000</i>	<i>1262</i>	93	151	223	308	407
4.00	<i>340</i>	<i>552</i>	<i>793</i>	<i>1058</i>	<i>1349</i>	113	182	269	372	493
3.00	<i>383</i>	<i>595</i>	<i>847</i>	<i>1139</i>	<i>1470</i>	146	232	342	475	631
2.08	424	675	965	1294	1662	178	275	407	574	777
1.56	605	743	985	1333	1785	290	448	655	913	1220
1.05	519	698	1012	1461	2044	449	694	1005	1382	1823
0.51	820	979	1310	1813	2489	632	920	1351	1924	2640

Note: Italic, non-bold values are extrapolated from Figure 7.5 and Figure 7.6 trend lines.

The general impression from this extrapolation is that longitudinal and transverse strains, while at given speeds and temperatures may behave similarly, can react differently at other variations of frequency and temperature.

7.2 BISAR Layered Elastic Analysis Results

Analysis using the BISAR program was conducted using two common methods of obtaining resilient modulus values. The first uses a standard test method specified by ASTM D4153; the second is a computed through the use of Witczak’s Equation with input parameters based upon the mixtures aggregate and binder properties.

7.2.1 5-Pulse Resilient Modulus (E)

Standard resilient modulus (E) values were obtained through 5-Pulse Resilient Modulus tests conducted on 100mm (4 inch) diameter samples which were obtained from the perimeter of the pavement slab which had not undergone MMLS3 loading. Because the HMA layer properties are dependent on temperature, the modulus was determined by using an indirect tensile machine at three mid-range temperature values and extrapolated to include the two extremes.

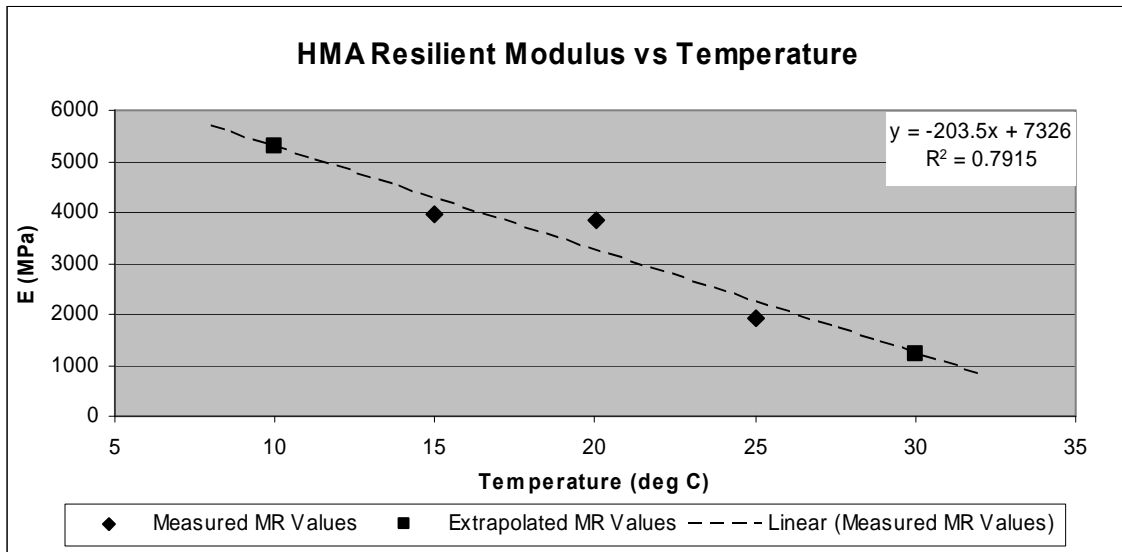


Figure 7.7 – HMA Resilient Modulus (E) vs Temperature

BISAR MODEL						
Temperature (°C)	10		DATE: 4/ 9/2005 TIME: 11: 9: 3. 6			
SYSTEM NUMBER 1						
Layer Number	Calculation Method (0-1000)	Young's Modulus (E)	Poisson's Ration (ν)	Layer Thickness (in)		
1	Smooth	767395	0.35	1.57		
2	Smooth	6345	0.45	3.00		
3	Smooth	29007550	0.63	0.63		
4		5091	0.40			
0=Smooth (complete adhesion), 1000=(frictionless slip)						
Load Number	Normal Load	Shear Stress	Radius of Loaded Area	Load-Position		Shear Direction
	(lbf)	(σ)	(in)	X	Y	
				(lb-in)	(lb-in)	
1	607	0.00	1.3	0.00	0.00	0.00
Position Number:	1			X-Coordinate (in):	0.00	
Layer Number:	1			Y-Coordinate (in):	0.00	
				Z-Coordinate (in):	1.56	
TOTAL STRESSES, STRAINS AND DISPLACEMENTS						
	Horizontal in X	Horizontal in Y	Vertical in Z	Shear YZ	Shear XZ	Shear XY
Stress (σ)	2.440E+02	2.440E+02	-8.720E+00	0.000E+00	0.000E+00	0.000E+00
Strain (ϵ)	2.100E-04	2.100E-04	-2.340E-04	0.000E+00	0.000E+00	0.000E+00
Displacement (in)	0.000E+00	0.000E+00	6.040E-03			

Figure 7.8 – BISAR model inputs and outputs

The resilient modulus values, based upon ASTM D4123, were input into BISAR along with pavement layer properties, loading properties, loading frequency, and temperatures as shown in Figure 7.8. The results were then plotted and an exponential trend line was fit to the data using the same theory as the MMLS3 testing; the strain in the pavement can not reach zero. The results can be found in Table 7.3 – BISAR Strain using E values attained during 5-Pulse Resilient Modulus Testing.

Table 7.3 – BISAR Strain using E values attained during 5-Pulse Resilient Modulus Testing.

	Temperature (°C)				
	10	15	20	25	30
E, 10Hz Actual	210	264	269	457	645
E, 10Hz (Exponential)	193	256	338	447	591

Note: The exponential trend line values were used in the following graphs and calculations.

It is clear from Figure 7.9 that these values are significantly higher than the extrapolated longitudinal strain and yet significantly lower than the extrapolated transverse strain seen during actual laboratory testing using the MMLS3.

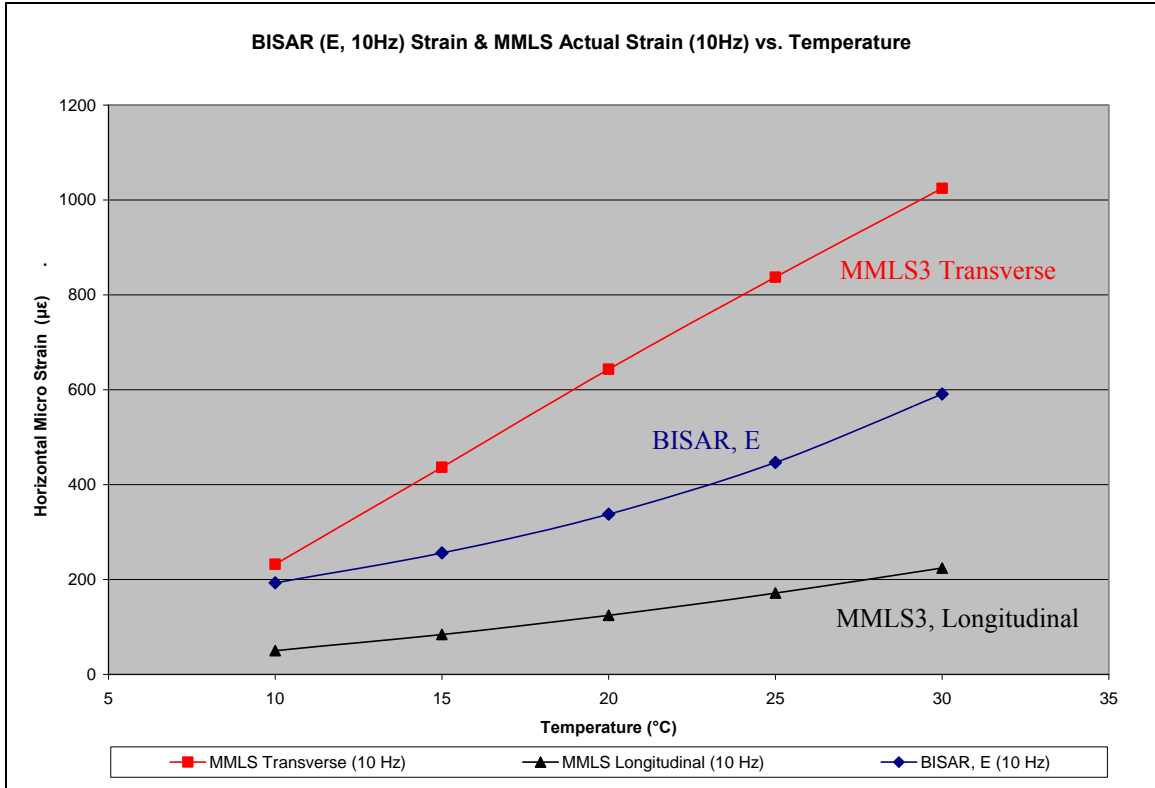


Figure 7.9 – BISAR (E, 10Hz) Strain & MMLS3 Actual Strain (10Hz) vs. Temperature

7.2.2 Witczak’s Modified Dynamic Modulus Equation (E^*)

A second commonly used approach to determining horizontal strain in pavements is to incorporate Witczak’s modified dynamic modulus equation known as E^* . We defined E^* in Equation 2.1, and described the need for two important variables: the frequency and the asphalt’s viscosity at testing temperature.

Once the viscosity was determined for each temperature it could be combined with the frequency of loading and mix properties to develop Witczak’s E^* value. The E^* value was later entered into BISAR for each temperature and frequency combination and the results were recorded in Table 7.4 and plotted in Figure 7.10 – Temperature Curves of

BISAR (E*) Strain vs. Frequency. Individual program files can be found in Appendix A.2.

Table 7.4 – BISAR Strain using E* values attained using Witczak’s Equation.

Temp (°C)	Temp (°R)	Freq (Hz)	Viscosity (10 ⁶ poise)	Log (E*) (10 ⁶ psi)	E* (Mpa)	E* (psi)	Strain (με)
10	509.67	0.51	12.0962	0.8219	4576	663760	292
10	509.67	1.05	12.0962	0.9201	5737	832144	248
10	509.67	1.56	12.0962	0.9705	6444	934629	226
10	509.67	2.08	12.0962	1.0055	6985	1013067	213
10	509.67	10.0	12.0962	1.1703	10207	1480458	158
15	518.67	0.51	0.6793	0.3726	1626	235889	646
15	518.67	1.05	0.6793	0.4822	2093	303589	537
15	518.67	1.56	0.6793	0.5430	2408	349229	483
15	518.67	2.08	0.6793	0.5872	2666	386636	448
15	518.67	10.0	0.6793	0.8205	4561	661561	297
20	527.67	0.51	0.0590	0.0331	744	107960	1120
20	527.67	1.05	0.0590	0.1201	909	131876	975
20	527.67	1.56	0.0590	0.1714	1023	148432	899
20	527.67	2.08	0.0590	0.2102	1119	162315	845
20	527.67	10.0	0.0590	0.4394	1897	275094	577
25	536.67	0.51	0.0074	-0.1703	466	67574	1500
25	536.67	1.05	0.0074	-0.1115	534	77378	1380
25	536.67	1.56	0.0074	-0.0753	580	84099	1310
25	536.67	2.08	0.0074	-0.0472	619	89716	1260
25	536.67	10.0	0.0074	0.1325	936	135710	956
30	545.67	0.51	0.0013	-0.2828	360	52158	1740
30	545.67	1.05	0.0013	-0.2445	393	56965	1660
30	545.67	1.56	0.0013	-0.2204	415	60212	1610
30	545.67	2.08	0.0013	-0.2014	434	62902	1560
30	545.67	10.0	0.0013	-0.0736	582	84437	1310

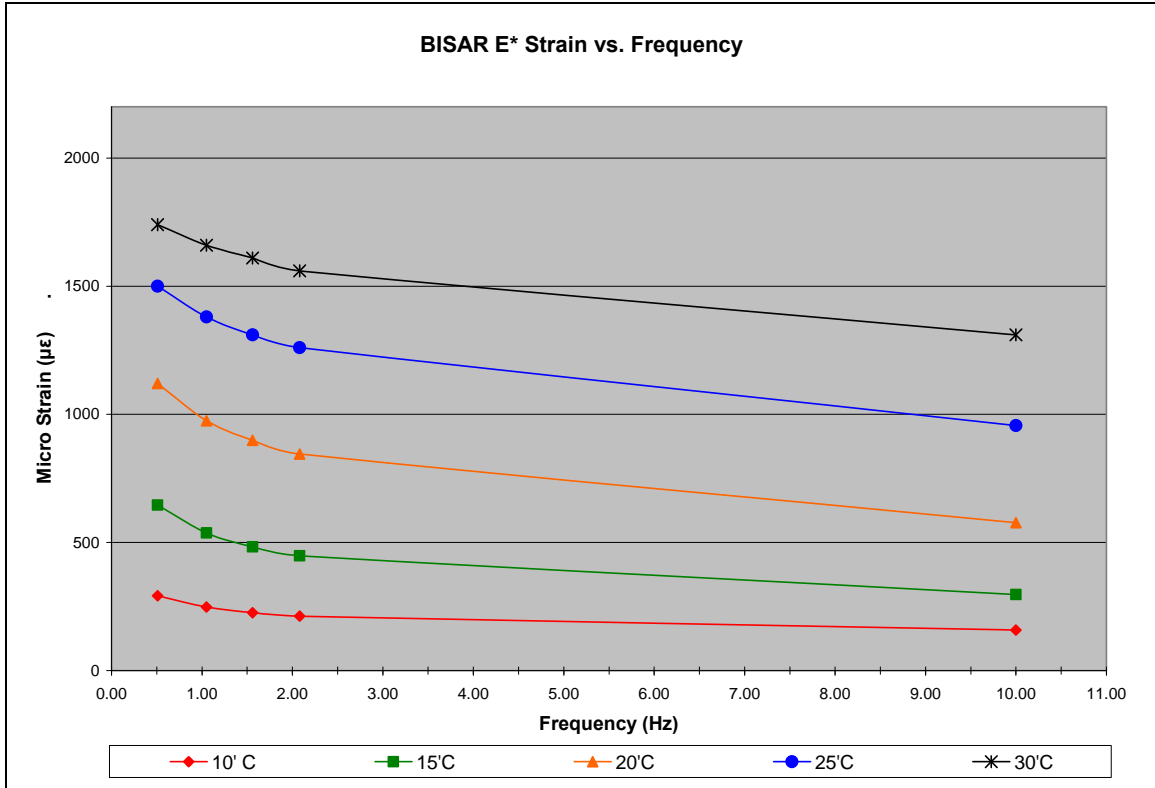


Figure 7.10 – Temperature Curves of BISAR (E*) Strain vs. Frequency

Figure 7.11 shows a comparison of BISAR E* strains vs. MMLS3 strains. Even with a modified dynamic modulus value (Witczak's E*), it is evident that there is a significant difference between the layered elastic design computed values, which only distinguish strain in the horizontal and vertical directions, and the MMLS3 which obtained strains in both a longitudinal and transverse direction. Furthermore, longitudinal strains were substantially different at varying temperature/frequency combinations than the transverse strains were; this is illustrated in Figure 7.11. MMLS3 transverse strains are plotted as dashed lines while longitudinal strains are thin and solid. Transposed over these are BISAR E* results, displayed as thick solid lines. The BISAR E* results appear to underestimate both transverse and longitudinal strain values at frequencies under 1.0 to 1.5 Hz. The BISAR models overestimate longitudinal strains greater than 1.5 Hz, however this may be acceptable due to the fact the longitudinal strain is often less than transverse strains, except under specific high temperature, low frequency situations. In most circumstances, the transverse strains appear to have the

more extreme values. The BISAR models, even using the E* method, both under and overestimate the strain for frequencies greater than 2.0 Hz depending on the testing temperature.

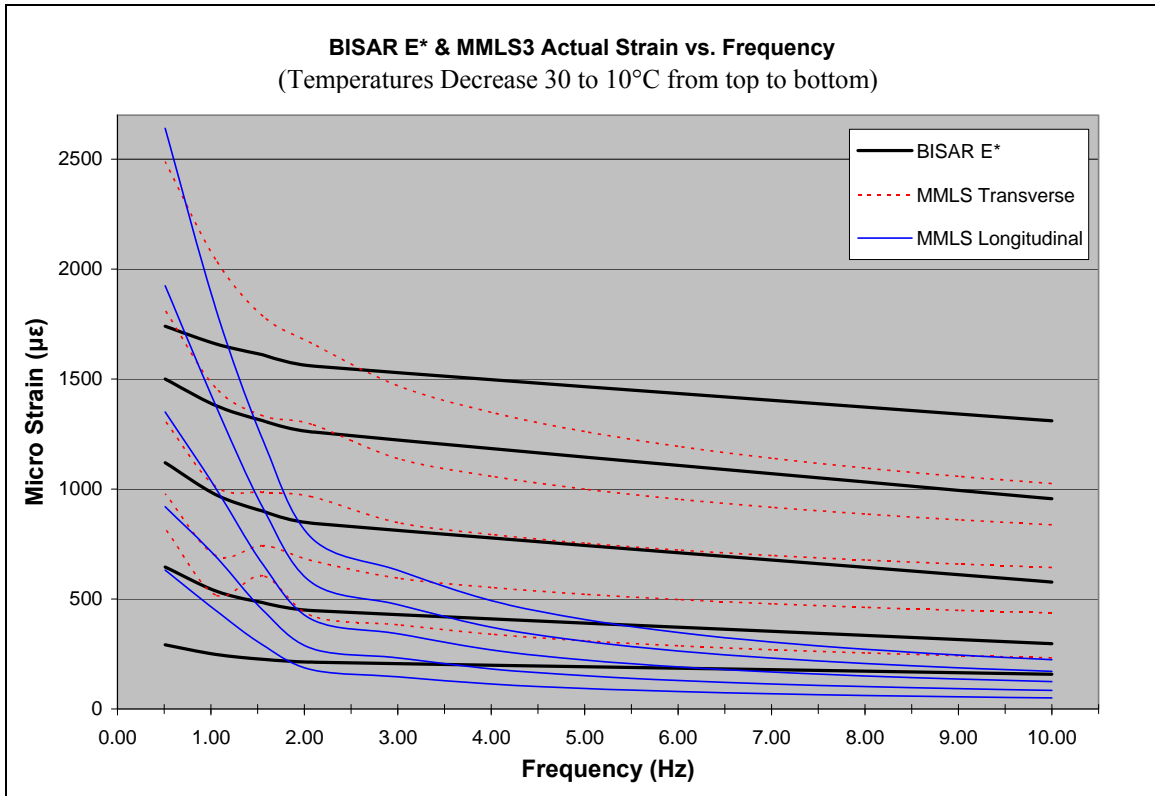


Figure 7.11 – Temperature Curves of BISAR (E*) & MMLS3 Actual, Strain vs. Frequency

As shown in the plot above, it is very difficult to examine all three methods of determining strain and compare them over several temperature/frequency scenarios. Therefore, Figure 7.12 compares all three methods, including transverse and longitudinal strains of the MMLS3 testing, across several temperature bands for a frequency of 10 Hz.

Figure 7.12 shows how the BISAR results utilizing the E values obtained through the 5-Pulse Resilient Modulus test underestimated the actual transverse strains observed in the MMLS3 testing. When applying Witczak’s modified E* values there is a slight improvement in the ability to predict the greater of the two strains observed in the pavement; However, at temperatures greater than 25 °C it appears to overestimate the

strain. In fact, when extrapolated out to 45 °C or 114 degrees Fahrenheit, BISAR predicts a strain nearly 80 percent greater than actual results appear to indicate, leading to the question: Are we over designing our pavements?

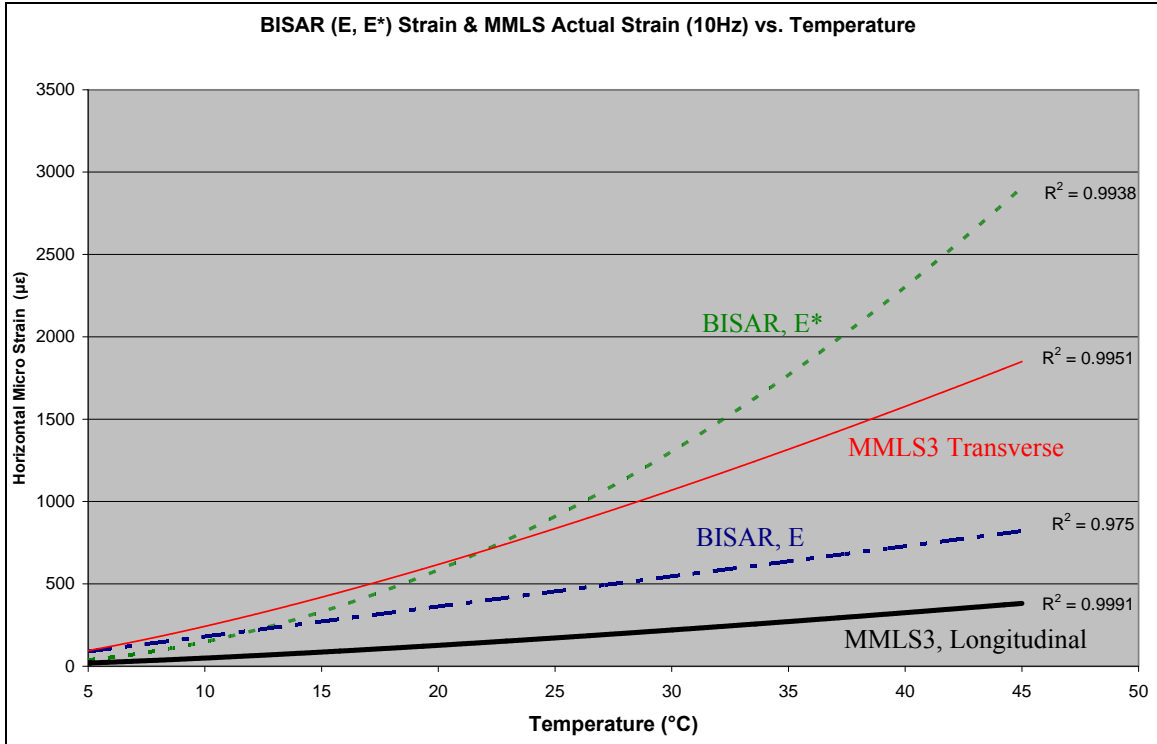


Figure 7.12 – BISAR (E, E*) Strain & Extrapolated MMLS3 Actual Strain (10Hz) vs. Temperature

7.3 Effect of Difference in Strains on the Fatigue Life in Pavements

The fatigue life of asphalt pavements is generally expressed as an equation that relates the number of loads to failure to the initial tensile strain at the bottom of the surface layer of HMA. One generally accepted equation is shown in Equation 7.1 [42].

Equation 7.1 – Loads to Failure

$$N_f = 8.0 * 10^{13} * \epsilon^{-3.561}$$

Where:

N_f = Loads to failure

ε = Initial strain

Using this equation the effect of difference in strains, as calculated and as obtained from MMLS3 testing, were evaluated. Figure 7.13 through Figure 7.15 illustrate the fatigue life as calculated from BISAR E and BISAR E* methods compared to the fatigue life calculated from actual MMLS3 strains obtained during testing. Each plot shows a ratio of the calculated N_f from E or E* methods and calculated N_f from MMLS3 strain over a range of frequencies for a specific temperature.

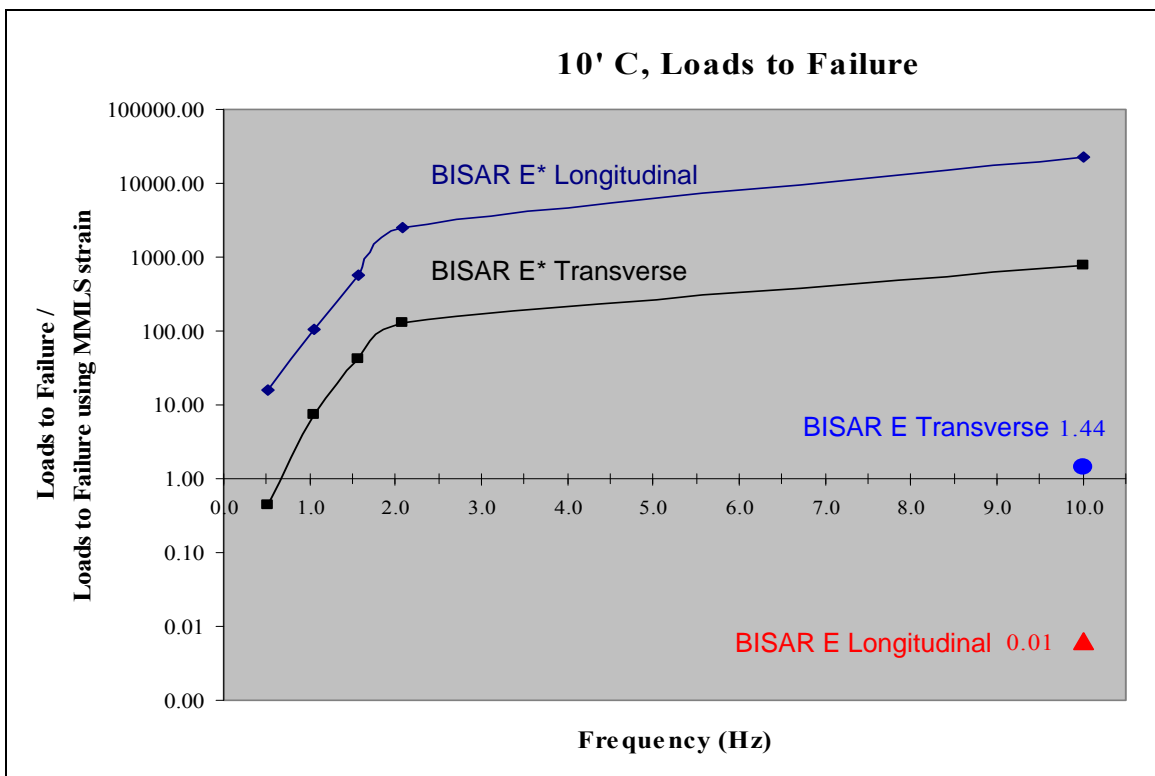


Figure 7.13 – Loads to Failure Comparison at 10 degrees Celsius

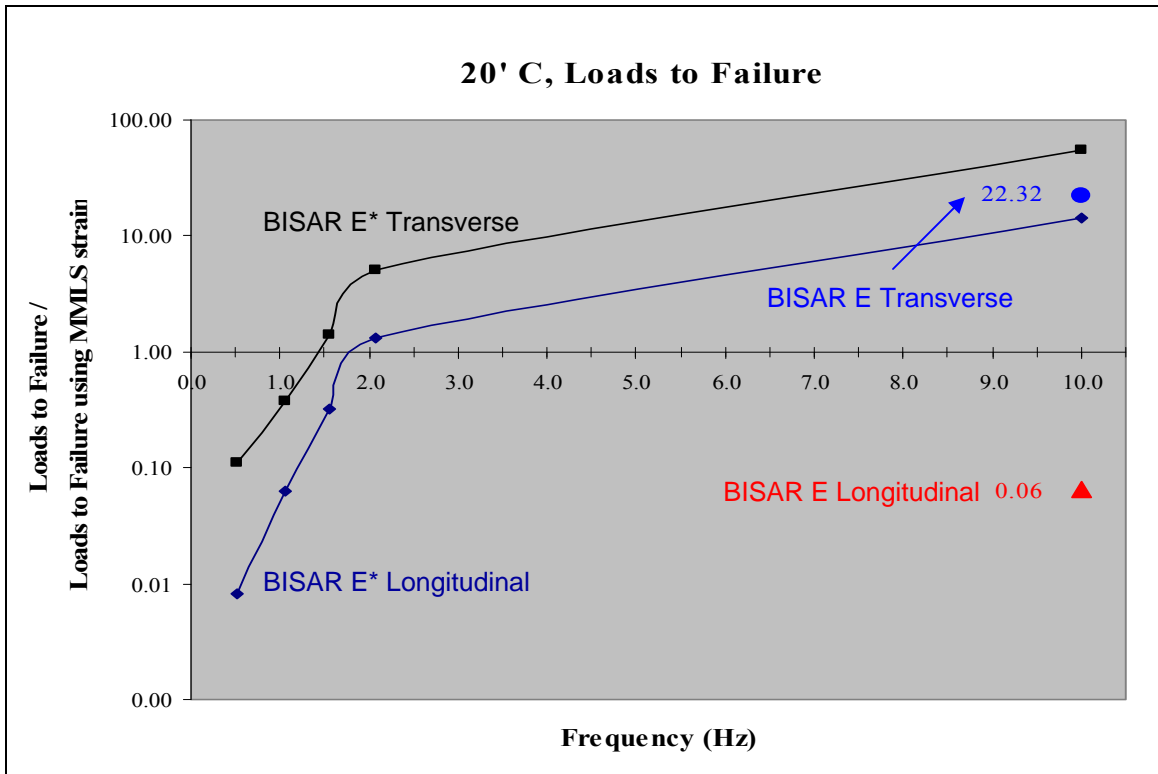


Figure 7.14 – Loads to Failure Comparison at 20 degrees Celsius

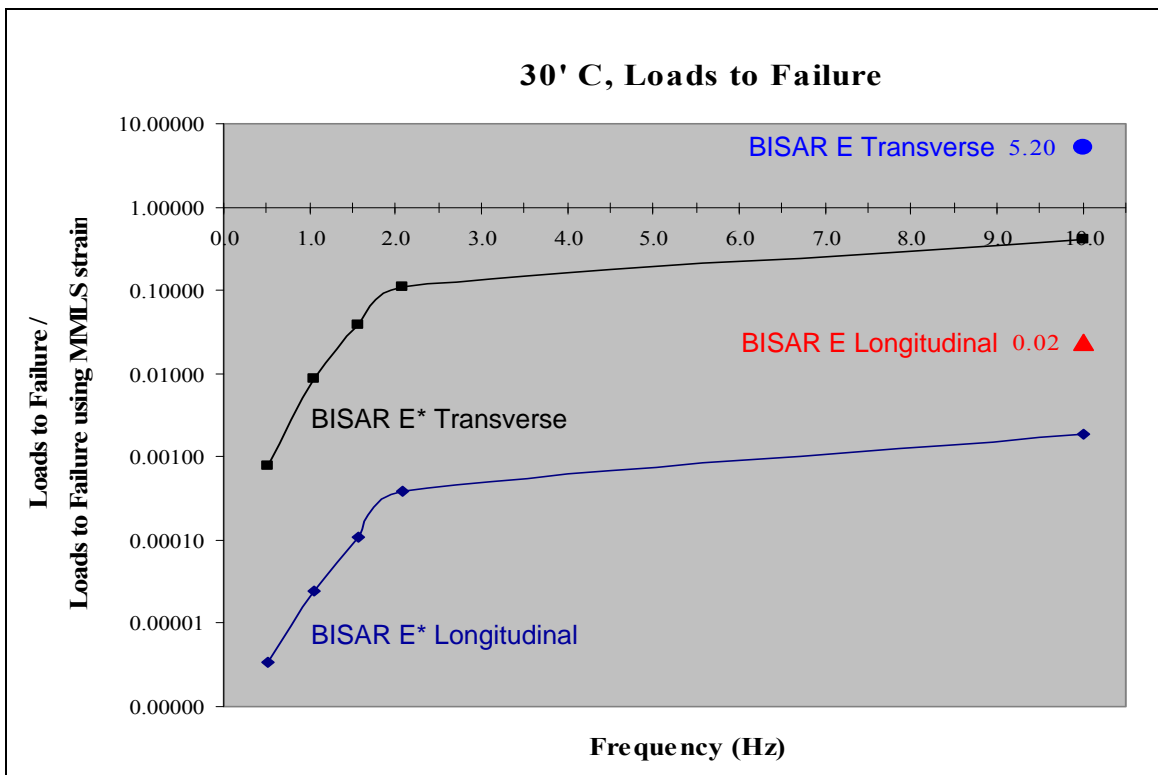


Figure 7.15 – Loads to Failure Comparison at 30 degrees Celsius

Note that load to failure calculations from BISAR E and BISAR E* are significantly different than loads to failure calculated from actual MMLS3 strains. Additionally, the ratio of N_f calculated from E and E* and N_f calculated from MMLS3 strains depends on frequency, temperature, as well as which strain, either longitudinal or transverse, is used for the ratio. These observations point out the importance of using an alternate approach for accurate predictions of strains in asphalt pavements.

7.4 Alternative Approach for Determining Strain

Two approaches are suggested: 1) Modeling of frequency vs. strain for different temperatures (since it is easier to change the frequency while maintaining constant temperatures) and using the model for predicting strain at any temperature or frequency. 2) Calculating strains from E* or E and then predicting the actual strain using a correction factor that is specific to the design frequency and temperature.

For the first approach the following regression equations (Table 7.5) have been derived from tests conducted with the MMLS3 at .5, 1, 1.6, 2 Hz. and 10, 15, 20, 25, 30°C, as illustrated in Figure 7.5 and Figure 7.6.

Table 7.5 – Predicting MMLS3 Actual Strains

Predicting MMLS3 Actual Strain		
Temp	Prediction Equation	
°C	Longitudinal Strain	Transverse Strain
10	$391.91*f - 0.8621$	$607.31*f - 0.3997$
20	$868.11*f - 0.8159$	$1092.3*f - 0.2207$
30	$1640*f - 0.8359$	$2052.1*f - 0.291$

Note: f = frequency (Hz)

For the second approach correction factors were developed from strains calculated from E, E*, and MMLS3 testing. These correction factors are shown below in Table 7.6. and illustrated in Figure 7.16 through Figure 7.18.

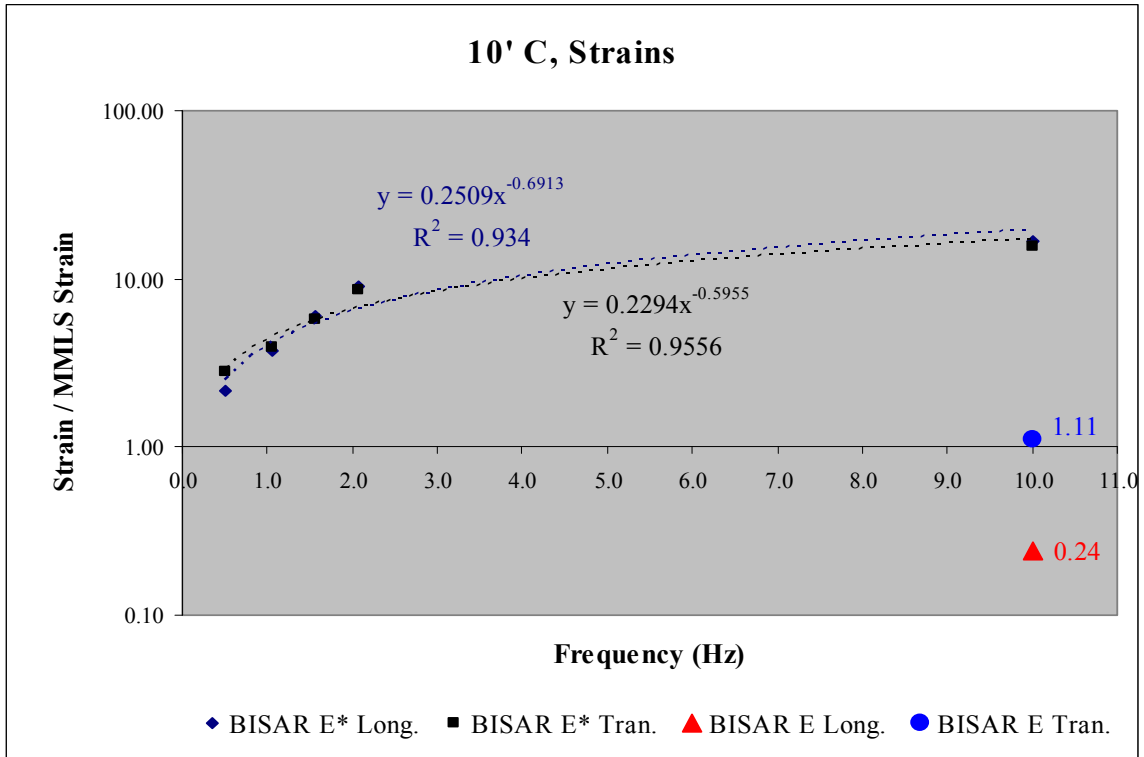


Figure 7.16 – Strain Correction Model for E and E* strains at 10 degrees Celsius

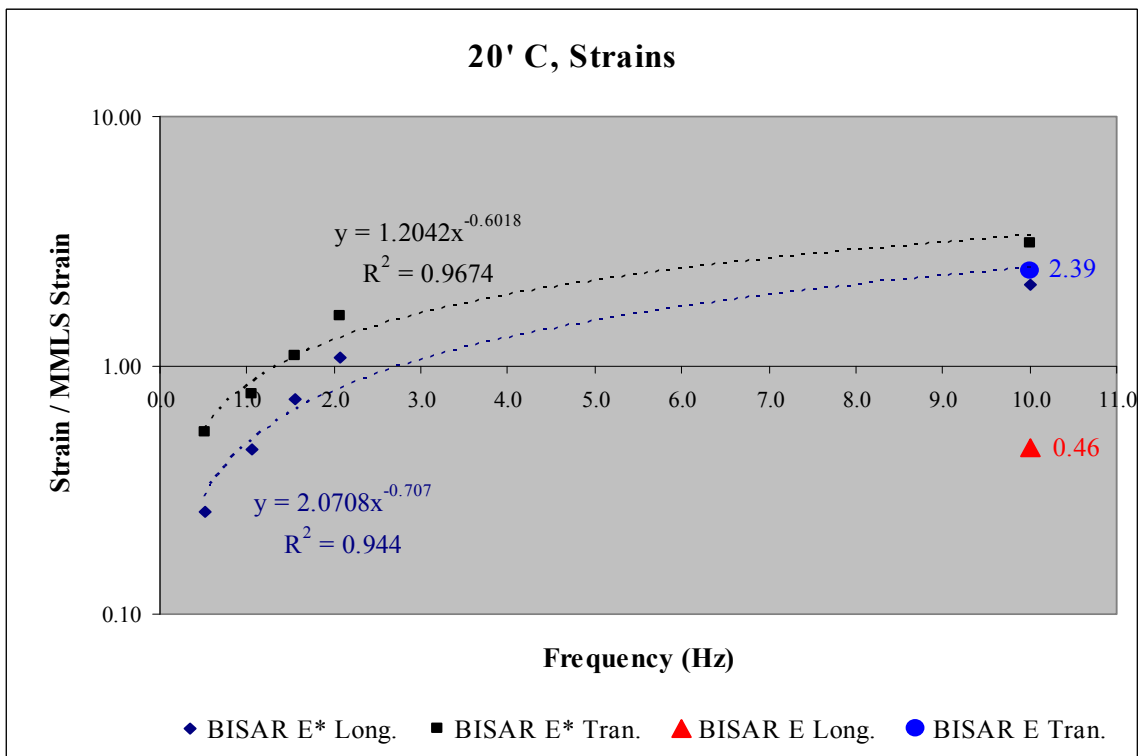


Figure 7.17 – Strain Correction Model for E and E* strains at 20 degrees Celsius

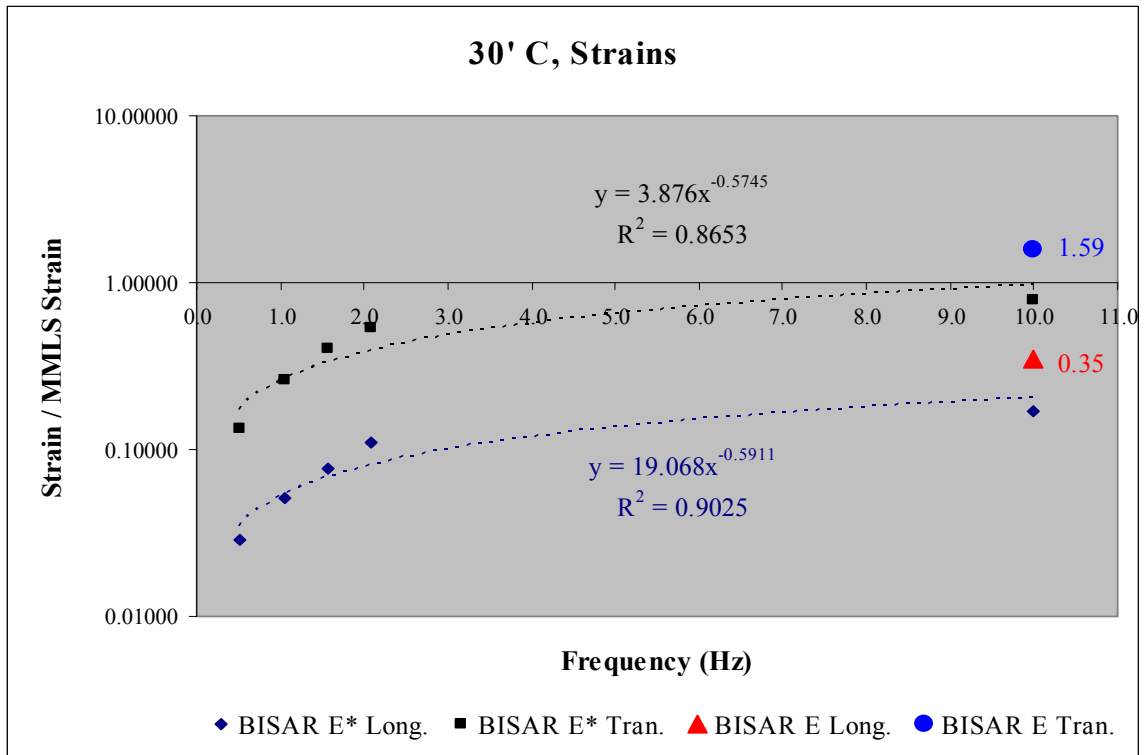


Figure 7.18 – Strain Correction Model for E and E* strains at 30 degrees Celsius

Table 7.6 – Correction Factors for the Indirect Test Method or Witzcak’s Dynamic Modulus Method

Indirect Tensile Testing (E)		
Temp	Strain Correction Factor	
°C	Longitudinal Strain	Transverse Strain
10	0.24	1.11
20	0.46	2.39
30	0.35	1.59

Witzcak's Dynamic Modulus (E*)		
Temp	Strain Correction Factor	
°C	Longitudinal Strain	Transverse Strain
10	$0.2509*f - 0.6913$	$0.2294*f - 0.5955$
20	$2.0708*f - 0.707$	$1.2042*f - 0.6018$
30	$19.068*f - 0.5911$	$3.876*f - 0.5745$

Note: f = frequency (Hz)

To understand the use of Table 7.6, consider the following example:

Suppose one has calculated from BISAR using E* a tensile strain value of 200 microstrain at 10°C and 5 Hz. The actual longitudinal tensile strain in the pavement at 10°C and 5 Hz can be calculated as:

$$\begin{aligned}\mu\varepsilon_{ACTUAL} &= \mu\varepsilon_{CALCULATED} * (.2509 * \text{frequency} - .6913) \\ \mu\varepsilon_{ACTUAL} &= 200 * (.2509 * 5 - .6913) \\ \mu\varepsilon_{ACTUAL} &= 200 * .56 \\ \mu\varepsilon_{ACTUAL} &= 112\end{aligned}$$

Equation 7.2 – Suggested method 2 example calculation

Since the E values were obtained from the 5-Pulse Indirect Tensile Strain Test only at the specified 10 Hz frequency no model relating correction factor to frequency could be developed. However, if one has calculated a strain using E at 10 Hz., it is possible to predict the actual strain at 10 Hz for varying temperatures using the correction factors give in the lower half of Table 7.6 above.

8 Conclusions

Based on the observations of several HMA pavement slabs, loading, testing and analysis of data, the following conclusions can be drawn:

1. Fabrication of a large scale pavement samples within a limited time frame to minimize differential aging is feasible. Furthermore, these pavement slabs can also be instrumented with everyday equipment in a reasonable time frame; Allowing for simulation of numerous testing scenarios to investigate everything from rutting and fatigue damage to the effect of temperature, frequency changes, and even the results of saturation.
2. It is not enough to estimate the strain at the bottom of a pavement layer in a single horizontal direction. Actual MMLS3 testing provided results which showed significant differences between the transverse and longitudinal directions when subjected to directional loading.
3. As the loading rate was reduced strain increased, and increased significantly under a frequency of 1.0 Hertz. This increase was not predicted in layered elastic models using either method of obtaining the resilient modulus input. The affect of frequency was most evident in the longitudinal strain where a change of 1.5 Hz could more than double the strain and at high temperatures result in longitudinal strain equal to the transverse strain.
4. Temperature changes also increase the strain in the pavement slab; however, changes were uniform across all frequency ranges. For example, the plot of transverse strain seen at 30 °C in Figure 7.5 is greater than at 25 °C, but is affected similarly at each frequency.
5. Although the combined effect of temperature and frequency influence strain values it was the frequency which impacted the strains most substantially. In fact, as the frequency approached zero, the longitudinal and transverse strains

became equal. This is actually the effect that would be anticipated for a repetitive point loading scenario (static traffic).

6. Linear elastic models did not predict the strains obtained through actual MMLS3 testing scenarios. There was a tendency to underestimate both longitudinal and transverse strains at very low frequencies. Longitudinal strains were substantially less than the model predicted which may be acceptable due to the transverse strains being more critical. The program only overestimated strains at higher frequencies at higher temperatures. This unveils the possibility of the over design of pavements in current methods of strain predictions using linear elastic modeling.
7. The effect of the difference in strains on fatigue life is significant. Good models can be developed relating strain to frequency at varying temperatures. The difference between the strains calculated between Indirect Tensile Testing (E) or Witczak's dynamic modulus equation (E*) and MMLS3 strains can be modeled with respect to frequency at different temperatures using correlation factors determined in this study.
8. The limitations of this study are acknowledged. Note that the loading was 1/3rd scale, the range of frequency and temperatures were relatively small, and that extrapolations were used to develop models.

9 Recommendations

It can be concluded from the results obtained in this study and in conjunction with past research, that accelerated loading using a 1/3 scale mobile model load has become an effective laboratory tool for material characterization. As such, proper specimen preparation guidelines, along with loading and testing protocols should be followed when using this equipment. Such protocols are currently being developed by researchers in the United States as well as in South Africa. Once these protocols are finalized and adopted by AASHTO, the MMLS3 should become a standard laboratory tool. It can be used to characterize a multitude of pavement behaviors, ranging from rutting and fatigue to stripping and delamination with particularly emphasis on the effects of material, traffic and the environment.

The use of accelerated testing with instrumentation is recommended as a means to better understand the effects of temperature and frequency on HMA pavements. The increased understanding of material responses will lead to the improvement of design procedures with the ultimate effect being a longer lasting, more durable pavement system.

The use of alternative methods for predicting strains, through the use of small-scale accelerated pavement testing or correction factors should be investigated further.

10 References

- 1 Guide for Mechanistic-Empirical Design of New and Rehabilitated Pavement Structures, NCHRP I-37A, March 2004
- 2 Yoder, E.J., and M.W. Witczak (1975). *Principles of Pavement Design*, Wiley, New York.
- 3 Burmister, D. M., "The Theory of Stresses and Displacements in Layered Systems and Application to the Design of Airport Runways," *Proceedings*, Highway Research Board, 1943
- 4 Burmister, D. M., "The General Theory of Stresses and Displacements in Layered Soils Systems," *Journal of Applied Physics*, Vol. 16, 1945
- 5 Burmister, D. M., "Evaluation of Pavement Systems of the WASHO Road Test by Layered System Methods," Highway Research Board Bulletin 177, 1958
- 6 Acum, W. E. A., and L. Fox, "Computation of Load Stresses in a Three-Layer Elastic System," *Geotechnique*, Vol. 2, pp. 293-300, 1951.
- 7 Jones, A., "Tables of Stresses in Three-Layer Elastic Systems," Highway Research Board Bulletin 342, 1962.
- 8 Peattie, K. R., "Stress and Strain Factors for Three-Layer Elastic Systems," Highway Research Board Bulletin 342, 1962.
- 9 Hibbeler, R.C. (2000), *Mechanics of Materials*, 4th ed. Upper Saddle River, New Jersey
- 10 Ksaibati, Khaled. "Pavement Design for Highways," University of Wyoming. Laramie, WY, 11 March 1996.
- 11 Garber, N.J., and Hoel L.A. (1996), *Traffic and Highway Engineering*, Revised 2nd Ed. Department of Civil Engineering University of Virginia
- 12 Macioce, P., Roush Industries, Inc. (2002)
http://www.roushind.com/news_downloads/white_papers/Insight.pdf
- 13 Huang, B., Mohammad, L., Wathugala, G. W., "Application of a Temperature Dependent Viscoplastic Hierarchical Single Surface Model for Asphalt Mixtures," *Journal of Materials in Civil Engineering* (ASCE), March/April 2004.
- 14 Muench, S.T., Mahoney, J.P., and Pierce, L.M., *Pavement Design Guide*, Washington State DOT,
http://training.ce.washington.edu/WSDOT/Modules/04_design_parameters/04-2_body.htm
- 15 Witczak, M. W., Kaloush, K. E., Pellinen, T., El-Basyouny, M., & Von Quintus, H., "Simple Performance Test for Superpave Mix Design," *NCHRP Report 465*, Transportation Research Board, National Research Council. 2002.
- 16 James C., Hall K., Williams C. (2005), "Development of Modulus-to-Temperature Relations for HMA Mixtures in Wisconsin,"
<http://wisconsindot.gov/library/research/docs/finalreports/03-14modtotemp-f.pdf>
- 17 Osvaldo A. Fonseca and Matthew W. Witczak, "A Prediction Methodology for the Dynamic Modulus of In-Place Aged Asphalt Mixtures," *Journal of the Association of Asphalt Paving Technologists*, 1996

-
- 18 Van-de-Ven M., Andre de-Fortier Smit, K Jenkins and F Hugo, "Scaled Down APT Considerations for Viscoelastic Materials," *Journal of the Association of Asphalt Paving Technologists*, 1998
 - 19 Westrack Program Website, Nevada Automotive Test Center, 1999
<http://www.westrack.com/>
 - 20 LinTrack Program Website, Technical University, Delft, Netherlands
<http://vbk.ct.tudelft.nl/LINTRACKhome/index.htm>
 - 21 Hugo F., Smit A. de F. and Epps A. "A Case Study Of Model APT In The Field," *Proceedings of the First International Conference on Accelerated Pavement Testing*, Reno, Nevada, 1999.
 - 22 Epps A. M., Ahmed T. and Little D. C. and Hugo F., "Performance Prediction with the MMLS3 at WesTrack," *Report No. 2134-1*, Texas A&M University, March, 2001.
 - 23 Smit A. dF., Walubita L., Jenkins K. and Hugo F. "The Model Mobile Load Simulator As a Tool for Evaluating Asphalt Performance Under Wet Condition." *Proceeding of the Ninth International Conference on Asphalt Pavements*, Copenhagen, August, 2002.
 - 24 Walubita, L.F., Hugo, F., Epps Martin, A. "Indirect Tensile Fatigue Performance of Asphalt After MMLS3 Trafficking Under Different Environmental Conditions," *Journal of the South African Institution of Civil Engineering*, Johannesburg, South Africa, 2002, Vol. 44, Number 3.
 - 25 MMLS3 Operator's Guide, Appendix B of this document.
 - 26 Sawangsurriya, A., and Edil, T. B., "Investigation of Soil Stiffness Gauge and Dynamic Cone Penetrometer for Earthwork Property Evaluation," Wisconsin DOT, 2005
<http://www.dot.wisconsin.gov/library/research/docs/finalreports/01-05final.pdf>
 - 27 Fiedler, S. A., Main, M., and DiMillio, A. F. (2000), "In-place Stiffness and Modulus Measurement," *Proceedings of Sessions of ASCE Specialty Conference on Performance Confirmation of Constructed Geotechnical Facilities*, Geotechnical Special Publication No. 94
 - 28 Kessler Soils Engineering Products, Inc. , "GeoGauge In-Place Soil Stiffness & Modulus Gauge for Compaction Evaluation," (2005)
http://www.kesslerdcp.com/geo_gauge.html
 - 29 ASTM D6758, "Standard Test Method for Measuring Stiffness and Apparent Modulus of Soil and Soil-Aggregate In-Place by an Electro-Mechanical Method", ASTM International
 - 30 TransTech Systems, Inc., "Pavement Quality Indicator™ Model 300 Operator's Handbook," 2000
<http://www.transtechsys.com/pdf/PQIManual041000.pdf>
 - 31 UTM 14P Operators Manual
 - 32 Omega Engineering, "Strain Gages - Extra-Long Grid Pattern for Inhomogeneous Materials,"
http://www.omega.com/Pressure/pdf/SGD_EXTRA-LONG.pdf
 - 33 Omega Engineering, "Ready-Made Insulated Thermocouples with Stripped Leads,"
<http://www.omega.com/Temperature/pdf/5TC.pdf>
 - 34 National Instruments®, "Data Acquisition Hardware,"
<http://www.ni.com/dataacquisition/>
 - 35 National Instruments®, "Labview® Software,"
<http://www.ni.com/labview/>
 - 36 Webster, S. L, R. H. Grau and T. P. Williams, "Description and Application of Dual Mass Dynamic Cone Penetrometer," USAE Waterways Experiment Station, Vicksburg, MS, 1992

-
- 37 Powell, W. D., J. F. Potter, H. C. Mayhew and M. E. Nunn, "The Structural Design of Bituminous Roads," *TRRL Report LR 1132*, 1984
- 38 Western Emulsions, "Emulsions." 2002
<http://www.westernemulsions.com/emulsions/>
- 39 Bhattacharjee, S., "Use of Accelerated Loading Equipment for Fatigue Characterization of Hot Mix Asphalt in the Laboratory," Thesis Dissertation, Worcester Polytechnic Institute, 2005
- 40 1/8 inch thrifty white tileboard with durable hardboard backing, Decorative Panels Intl, Home Depot Inc
- 41 Workzone Overhead Workshop Heater, W.B. Marvin Manufacturing Company, 211 Glenn Avenue, Urbana, Ohio, 43078.
- 42 Huang, Y. H. (2004), *Pavement Analysis and Design*, 2nd Ed. 2004, Prentice Hall, Englewood Cliffs, NJ, 07632

Appendix A – Data Tables

A.1 MMLS3 Strain Gauge Results

Table A.1.1 – MMLS3 Strain Gauge Results, 2.52 m/s

Setting	m/s	Hz		°C	$\mu\epsilon$					$\mu\epsilon$					Time
		Transverse			Strain Gauge					Longitudinal Strain Gauge					
		Speed	Frequency		Period	Temp	Max	Min	Mean	Mode	Resilient	Max	Min	Mean	
49.00	2.52	2.27	2.00	9.7	837	395	503	396	441	-96	-358	-168	-168	190	
49.00	2.52	2.27	2.00	10.3	851	369	486	407	444	-100	-370	-176	-175	194	
49.00	2.52	2.27	2.00	11.1	881	362	478	398	483	-115	-398	-194	-196	203	
49.00	2.52	2.27	2.00	11.8	902	360	484	399	503	-130	-423	-215	-214	209	
49.00	2.52	2.27	2.00	12.3	936	363	491	397	539	-146	-449	-229	-231	219	
49.00	2.52	2.27	2.00	12.7	950	366	498	402	548	-161	-476	-248	-247	229	
49.00	2.52	2.27	2.00	13.2	972	372	505	407	566	-169	-493	-261	-262	232	
49.00	2.52	2.27	2.00	13.6	1002	378	515	413	589	-183	-514	-274	-275	239	
49.00	2.52	2.27	2.00	13.9	1023	385	521	418	604	-191	-534	-286	-287	247	
49.00	2.52	2.27	2.00	14.2	1037	391	524	393	643	-200	-547	-299	-299	249	
49.00	2.52	2.27	2.00	14.3	1061	398	539	432	629	-205	-555	-306	-306	249	
49.00	2.52	2.27	2.00	14.7	1080	407	547	440	640	-209	-575	-315	-314	260	
49.00	2.52	2.27	2.00	14.9	1106	413	558	438	668	-211	-581	-319	-319	261	
49.00	2.52	2.27	2.00	15.1	1116	420	559	453	664	-215	-597	-326	-328	269	
49.00	2.52	2.27	2.00	15.3	1135	427	568	459	676	-219	-606	-330	-332	274	
49.00	2.52	2.27	2.00	15.5	1157	433	581	466	691	-218	-611	-334	-336	275	
49.00	2.52	2.27	2.00	15.7	1180	443	586	476	704	-222	-626	-340	-340	286	
49.00	2.52	2.27	2.00	15.8	1204	451	598	485	720	-225	-645	-345	-346	299	
49.00	2.52	2.27	2.00	15.9	1200	457	606	490	711	-226	-646	-349	-349	298	
49.00	2.52	2.27	2.00	16.0	1226	463	616	493	732	-228	-639	-352	-353	285	
49.00	2.52	2.27	2.00	16.3	1241	469	619	504	737	-229	-667	-354	-353	314	
49.00	2.52	2.27	2.00	16.4	1259	476	625	509	750	-230	-662	-360	-361	301	
49.00	2.52	2.27	2.00	16.5	1269	484	641	519	750	-232	-666	-363	-364	302	
49.00	2.52	2.27	2.00	16.5	1279	488	638	519	760	-235	-671	-368	-368	303	
49.00	2.52	2.27	2.00	16.7	1278	490	647	521	757	-237	-676	-371	-371	306	
49.00	2.52	2.27	2.00	16.8	1304	495	654	526	778	-236	-698	-372	-374	324	
49.00	2.52	2.27	2.00	16.9	1316	499	659	533	783	-237	-696	-379	-378	318	
49.00	2.52	2.27	2.00	17.0	1309	504	658	535	774	-239	-698	-378	-379	319	
49.00	2.52	2.27	2.00	17.1	1337	509	663	542	796	-238	-703	-381	-383	321	
49.00	2.52	2.27	2.00	17.2	1357	517	674	550	807	-240	-704	-382	-383	321	
49.00	2.52	2.27	2.00	17.2	1353	522	676	523	830	-242	-720	-384	-384	336	
49.00	2.52	2.27	2.00	17.3	1363	529	688	562	801	-240	-719	-388	-388	332	
49.00	2.52	2.27	2.00	17.3	1383	535	699	567	816	-242	-718	-388	-390	328	
49.00	2.52	2.27	2.00	17.5	1395	540	698	571	824	-241	-728	-391	-392	336	
49.00	2.52	2.27	2.00	17.5	1387	547	711	578	808	-243	-724	-394	-396	328	
49.00	2.52	2.27	2.00	17.5	1407	550	710	580	828	-244	-737	-394	-396	341	
49.00	2.52	2.27	2.00	17.6	1406	556	721	586	819	-245	-735	-396	-394	341	
49.00	2.52	2.27	2.00	17.7	1413	560	718	590	822	-248	-746	-400	-404	342	
49.00	2.52	2.27	2.00	17.8	1424	568	725	601	822	-247	-744	-402	-402	342	
49.00	2.52	2.27	2.00	17.9	1429	573	736	601	828	-249	-763	-401	-402	361	
49.00	2.52	2.27	2.00	17.9	1448	580	741	614	833	-248	-757	-404	-402	355	
49.00	2.52	2.27	2.00	17.9	1459	588	753	615	844	-247	-765	-403	-404	361	
49.00	2.52	2.27	2.00	18.3	1477	592	760	623	854	-246	-765	-408	-407	358	
49.00	2.52	2.27	2.00	18.7	1529	598	771	629	900	-241	-811	-417	-415	396	
49.00	2.52	2.27	2.00	19.1	1577	609	789	613	964	-231	-825	-423	-423	402	
49.00	2.52	2.27	2.00	19.7	1624	624	806	658	966	-235	-867	-434	-432	435	
49.00	2.52	2.27	2.00	20.5	1675	641	828	642	1033	-234	-865	-446	-451	413	
49.00	2.52	2.27	2.00	21.2	1742	664	856	707	1034	-237	-905	-458	-470	435	
49.00	2.52	2.27	2.00	22.0	1805	693	886	695	1110	-231	-945	-476	-483	462	
49.00	2.52	2.27	2.00	22.9	1899	726	936	728	1171	-226	-1000	-492	-503	497	
49.00	2.52	2.27	2.00	23.8	1992	765	984	817	1175	-217	-1044	-505	-520	525	
49.00	2.52	2.27	2.00	24.7	2086	799	1016	801	1285	-212	-1104	-523	-541	563	
49.00	2.52	2.27	2.00	25.6	2200	843	1071	845	1355	-199	-1153	-537	-558	595	
49.00	2.52	2.27	2.00	26.6	2308	883	1124	941	1366	-195	-1217	-555	-582	636	
49.00	2.52	2.27	2.00	27.5	2426	935	1192	997	1429	-172	-1264	-561	-569	695	
49.00	2.52	2.27	2.00	28.5	2507	966	1223	968	1539	-146	-1298	-567	-594	704	
49.00	2.52	2.27	2.00	29.3	2617	997	1278	1001	1616	-126	-1326	-578	-591	735	
49.00	2.52	2.27	2.00	30.1	2716	1017	1311	1020	1696	-95	-1368	-588	-595	773	

Table A.1.2 – MMLS3 Strain Gauge Results, 1.97 m/s

Setting	m/s	Hz		°C	µε					µε					Time
		Transverse			Transverse Strain Gauge					Longitudinal Strain Gauge					
		Speed	Frequency		Period	Temp	Max	Min	Mean	Mode	Resilient	Max	Min	Mean	
36.70	1.97	1.69	1.56	9.8	1012	354	501	394	618	-147	-549	-240	-237	312	9:25 PM
36.70	1.97	1.69	1.56	10.4	1047	347	493	382	665	-139	-548	-239	-237	310	9:30 PM
36.70	1.97	1.69	1.56	10.9	1083	355	503	386	697	-141	-561	-245	-244	317	9:35 PM
36.70	1.97	1.69	1.56	11.6	1107	362	509	393	714	-145	-582	-257	-253	329	9:40 PM
36.70	1.97	1.69	1.56	12.0	1128	375	523	405	722	-151	-604	-264	-263	342	9:45 PM
36.70	1.97	1.69	1.56	12.3	1141	385	534	413	728	-155	-640	-272	-268	372	9:50 PM
36.70	1.97	1.69	1.56	12.4	1160	393	534	424	737	-163	-630	-280	-276	354	9:55 PM
36.70	1.97	1.69	1.56	12.8	1184	400	549	424	760	-163	-646	-285	-282	365	10:00 PM
36.70	1.97	1.69	1.56	13.0	1194	408	558	439	755	-167	-660	-292	-291	368	10:05 PM
36.70	1.97	1.69	1.56	13.1	1199	415	564	445	754	-169	-658	-295	-292	367	10:10 PM
36.70	1.97	1.69	1.56	13.2	1208	418	569	448	760	-170	-683	-297	-294	389	10:15 PM
36.70	1.97	1.69	1.56	13.3	1218	424	568	454	764	-170	-660	-300	-295	365	10:20 PM
36.70	1.97	1.69	1.56	13.5	1228	431	575	457	771	-172	-684	-302	-302	382	10:25 PM
36.70	1.97	1.69	1.56	13.6	1234	440	589	469	765	-176	-686	-308	-305	381	10:35 PM
36.70	1.97	1.69	1.56	13.8	1252	448	594	479	773	-174	-699	-312	-309	390	10:45 PM
36.70	1.97	1.69	1.56	13.8	1258	458	606	489	769	-177	-710	-316	-313	397	11:00 PM
36.70	1.97	1.69	1.56	14.1	1267	471	614	500	767	-180	-719	-321	-317	402	11:20 PM
36.70	1.97	1.69	1.56	14.2	1279	481	624	515	764	-174	-714	-317	-313	401	11:40 PM
36.70	1.97	1.69	1.56	14.3	1287	492	636	521	766	-178	-740	-323	-317	422	12:00 AM
36.70	1.97	1.69	1.56	14.4	1290	502	646	528	762	-174	-736	-322	-319	417	12:20 AM
36.70	1.97	1.69	1.56	14.5	1300	510	653	539	762	-173	-745	-323	-319	426	12:40 AM
36.70	1.97	1.69	1.56	14.5	1294	517	658	547	748	-172	-759	-324	-322	437	1:00 AM
36.70	1.97	1.69	1.56	14.6	1303	530	663	559	744	-169	-752	-324	-322	430	1:20 AM
36.70	1.97	1.69	1.56	14.6	1298	529	666	556	742	-168	-741	-324	-321	420	1:40 AM
36.70	1.97	1.69	1.56	14.7	1286	531	666	565	721	-169	-760	-327	-323	437	2:00 AM
36.70	1.97	1.69	1.56	14.7	1280	536	672	564	715	-166	-762	-330	-323	438	2:20 AM
36.70	1.97	1.69	1.56	14.7	1280	543	677	573	707	-166	-778	-331	-326	452	2:40 AM
36.70	1.97	1.69	1.56	15.0	1293	543	680	575	718	-161	-784	-334	-332	452	2:45 AM
36.70	1.97	1.69	1.56	15.3	1317	544	678	573	745	-140	-817	-332	-327	490	2:50 AM
36.70	1.97	1.69	1.56	16.0	1367	549	697	583	784	-130	-855	-340	-339	517	2:55 AM
36.70	1.97	1.69	1.56	17.0	1423	566	718	567	856	-126	-896	-350	-350	546	3:00 AM
36.70	1.97	1.69	1.56	18.0	1504	588	748	622	883	-115	-958	-363	-360	598	3:05 AM
36.70	1.97	1.69	1.56	18.9	1568	610	776	610	958	-113	-996	-376	-378	618	3:10 AM
36.70	1.97	1.69	1.56	19.8	1642	639	811	679	963	-112	-1036	-393	-395	640	3:15 AM
36.70	1.97	1.69	1.56	20.7	1720	667	841	716	1004	-107	-1092	-409	-415	677	3:20 AM
36.70	1.97	1.69	1.56	21.6	1832	702	895	749	1084	-100	-1183	-430	-435	748	3:25 AM
36.70	1.97	1.69	1.56	22.6	1901	733	932	786	1115	-93	-1236	-445	-459	777	3:30 AM
36.70	1.97	1.69	1.56	23.6	2038	768	983	771	1267	-76	-1291	-461	-471	819	3:35 AM
36.70	1.97	1.69	1.56	24.6	2153	806	1022	812	1341	-63	-1386	-476	-500	886	3:40 AM
36.70	1.97	1.69	1.56	25.7	2261	843	1071	899	1362	-35	-1449	-494	-519	930	3:45 AM
36.70	1.97	1.69	1.56	26.6	2360	880	1119	884	1476	-19	-1539	-510	-530	1009	3:50 AM
36.70	1.97	1.69	1.56	27.6	2444	910	1156	911	1533	1	-1604	-522	-533	1071	3:55 AM
36.70	1.97	1.69	1.56	28.5	2562	935	1195	984	1578	28	-1712	-534	-555	1157	4:00 AM
36.70	1.97	1.69	1.56	29.3	2738	965	1243	966	1772	59	-1706	-549	-565	1142	4:05 AM
36.70	1.97	1.69	1.56	30.2	2771	987	1257	989	1782	82	-1810	-556	-576	1234	4:10 AM
36.70	1.97	1.69	1.56	31.0	2932	1011	1306	1013	1919	116	-1890	-574	-591	1299	4:15 AM

Table A.1.3 – MMLS3 Strain Gauge Results, 1.32 m/s

Setting	m/s	Hz		°C	$\mu\epsilon$					$\mu\epsilon$					Time
		Transverse			Transverse Strain Gauge					Longitudinal Strain Gauge					
Speed	Frequency	Period	Temp	Max	Min	Mean	Mode	Resilient	Max	Min	Mean	Mode	Resilient	File Name	
24.50	1.32	1.22	1.05	8.7	1036	354	506	398	638	-93	-603	-204	-203	400	9:45 AM
24.50	1.32	1.22	1.05	9.2	1062	317	463	355	707	-74	-594	-194	-194	399	9:50 AM
24.50	1.32	1.22	1.05	9.7	1082	315	464	349	734	-69	-633	-200	-198	435	9:55 AM
24.50	1.32	1.22	1.05	10.2	1091	315	479	344	747	-64	-639	-199	-195	444	10:00 AM
24.50	1.32	1.22	1.05	10.6	1101	318	471	348	753	-64	-646	-203	-200	446	10:05 AM
24.50	1.32	1.22	1.05	10.8	1108	322	470	351	757	-70	-683	-214	-208	475	10:10 AM
24.50	1.32	1.22	1.05	11.0	1112	328	474	357	755	-71	-693	-218	-216	477	10:15 AM
24.50	1.32	1.22	1.05	11.2	1120	334	480	364	756	-70	-697	-218	-214	483	10:20 AM
24.50	1.32	1.22	1.05	11.4	1122	340	483	369	753	-70	-709	-221	-217	492	10:25 AM
24.50	1.32	1.22	1.05	11.5	1133	343	484	373	760	-73	-720	-228	-223	498	10:30 AM
24.50	1.32	1.22	1.05	11.6	1128	347	487	377	751	-75	-723	-230	-226	497	10:35 AM
24.50	1.32	1.22	1.05	11.6	1133	354	490	384	750	-72	-731	-234	-228	503	10:40 AM
24.50	1.32	1.22	1.05	11.9	1136	357	493	388	748	-76	-763	-238	-236	527	10:45 AM
24.50	1.32	1.22	1.05	11.9	1137	363	500	391	746	-75	-758	-238	-233	525	10:50 AM
24.50	1.32	1.22	1.05	11.9	1132	367	504	393	740	-73	-757	-239	-235	522	10:55 AM
24.50	1.32	1.22	1.05	12.0	1133	372	510	400	733	-75	-766	-240	-238	527	11:00 AM
24.50	1.32	1.22	1.05	12.2	1118	385	520	414	704	-77	-781	-246	-240	540	11:20 AM
24.50	1.32	1.22	1.05	12.3	1111	400	531	429	682	-76	-791	-248	-244	547	11:40 AM
24.50	1.32	1.22	1.05	12.5	1101	411	539	441	660	-74	-839	-253	-249	590	12:00 PM
24.50	1.32	1.22	1.05	12.6	1093	420	546	450	643	-74	-817	-255	-254	564	12:20 PM
24.50	1.32	1.22	1.05	12.8	1094	428	555	459	635	-68	-815	-256	-251	564	12:40 PM
24.50	1.32	1.22	1.05	12.7	1090	436	559	467	623	-70	-832	-255	-251	580	1:00 PM
24.50	1.32	1.22	1.05	12.8	1082	439	561	470	612	-68	-839	-256	-254	584	1:20 PM
24.50	1.32	1.22	1.05	12.8	1073	440	562	457	616	-65	-838	-254	-253	585	1:40 PM
24.50	1.32	1.22	1.05	12.8	1072	441	567	468	604	-56	-828	-254	-250	577	2:00 PM
24.50	1.32	1.22	1.05	12.8	1071	443	573	474	596	-63	-842	-254	-251	591	2:20 PM
24.50	1.32	1.22	1.05	12.8	1062	444	570	475	587	-58	-878	-256	-248	630	2:40 PM
24.50	1.32	1.22	1.05	12.9	1063	444	563	475	587	-53	-829	-248	-246	583	3:00 PM
24.50	1.32	1.22	1.05	13.0	1061	444	560	472	589	-48	-819	-247	-244	574	3:20 PM
24.50	1.32	1.22	1.05	12.9	1062	445	561	475	587	-52	-861	-252	-253	608	3:40 PM
24.50	1.32	1.22	1.05	13.0	1052	444	560	462	590	-52	-845	-250	-246	599	4:00 PM
24.50	1.32	1.22	1.05	13.0	1049	447	563	479	570	-49	-845	-247	-245	601	4:20 PM
24.50	1.32	1.22	1.05	13.0	1059	447	563	477	581	-46	-856	-250	-246	610	4:40 PM
24.50	1.32	1.22	1.05	13.1	1058	447	563	480	578	-46	-853	-249	-244	609	5:00 PM
24.50	1.32	1.22	1.05	13.1	1061	449	564	479	582	-45	-847	-248	-250	597	5:20 PM
24.50	1.32	1.22	1.05	13.0	1062	450	565	480	583	-44	-846	-251	-247	599	5:25 PM
24.50	1.32	1.22	1.05	13.3	1078	450	568	482	596	-41	-894	-255	-252	641	5:30 PM
24.50	1.32	1.22	1.05	13.7	1102	453	572	485	617	-28	-905	-254	-254	651	5:35 PM
24.50	1.32	1.22	1.05	14.1	1136	455	590	486	649	-19	-957	-263	-260	697	5:40 PM
24.50	1.32	1.22	1.05	14.9	1190	464	597	498	691	-4	-968	-266	-268	700	5:45 PM
24.50	1.32	1.22	1.05	15.7	1257	476	614	519	738	4	-1039	-279	-280	759	5:50 PM
24.50	1.32	1.22	1.05	16.7	1327	498	641	539	788	14	-1087	-290	-296	791	5:55 PM
24.50	1.32	1.22	1.05	17.5	1406	521	672	545	861	18	-1146	-303	-310	836	6:00 PM
24.50	1.32	1.22	1.05	18.3	1470	543	687	587	883	22	-1219	-320	-323	896	6:05 PM
24.50	1.32	1.22	1.05	19.2	1542	565	723	611	931	28	-1262	-333	-339	924	6:10 PM
24.50	1.32	1.22	1.05	20.0	1644	592	779	644	1000	37	-1354	-351	-363	991	6:15 PM
24.50	1.32	1.22	1.05	20.9	1735	618	801	669	1065	44	-1439	-372	-378	1060	6:20 PM
24.50	1.32	1.22	1.05	21.8	1830	649	835	651	1179	63	-1525	-385	-399	1126	6:25 PM
24.50	1.32	1.22	1.05	22.6	1946	683	879	684	1261	82	-1592	-402	-420	1173	6:30 PM
24.50	1.32	1.22	1.05	23.5	2055	714	928	770	1285	92	-1705	-424	-445	1260	6:35 PM
24.50	1.32	1.22	1.05	24.4	2152	748	947	751	1401	122	-1723	-437	-452	1271	6:40 PM
24.50	1.32	1.22	1.05	25.3	2275	775	986	780	1495	130	-1918	-451	-478	1440	6:45 PM
24.50	1.32	1.22	1.05	26.1	2408	804	1059	805	1604	172	-1893	-465	-492	1401	6:50 PM
24.50	1.32	1.22	1.05	26.8	2490	830	1079	831	1658	169	-2051	-486	-500	1551	6:55 PM
24.50	1.32	1.22	1.05	27.6	2558	852	1100	853	1705	198	-2118	-505	-523	1595	7:00 PM
24.50	1.32	1.22	1.05	28.3	2725	877	1145	881	1844	222	-2218	-515	-553	1664	7:05 PM
24.50	1.32	1.22	1.05	29.0	2827	902	1181	904	1923	249	-2314	-529	-552	1762	7:10 PM
24.50	1.32	1.22	1.05	29.7	2939	924	1211	925	2014	279	-2422	-549	-565	1858	7:15 PM
24.50	1.32	1.22	1.05	30.5	3032	939	1241	940	2092	308	-2462	-560	-589	1873	7:20 PM
24.50	1.32	1.22	1.05	31.0	3146	953	1280	958	2188	334	-2520	-569	-619	1902	7:25 PM

Table A.1.4 – MMLS3 Strain Gauge Results, 0.54 m/s

Setting	m/s	Hz		°C	µε					µε					Time
		Transverse			Temp	Transverse Strain Gauge					Longitudinal Strain Gauge				
Speed	Frequency	Period	Temp	Max		Min	Mean	Mode	Resilient	Max	Min	Mean	Mode	Resilient	File Name
12.25	0.64	0.60	0.51	9.5	1069	209	374	251	819	33	-681	-140	-136	544	10:01 AM
12.25	0.64	0.60	0.51	9.8	1077	204	373	242	835	42	-703	-137	-137	566	10:06 AM
12.25	0.64	0.60	0.51	10.1	1076	205	372	240	836	41	-772	-150	-149	623	10:11 AM
12.25	0.64	0.60	0.51	10.4	1083	211	371	244	839	35	-799	-165	-155	645	10:16 AM
12.25	0.64	0.60	0.51	10.6	1083	216	376	248	834	36	-802	-168	-166	636	10:21 AM
12.25	0.64	0.60	0.51	10.8	1099	225	388	257	842	37	-844	-169	-168	676	10:26 AM
12.25	0.64	0.60	0.51	11.0	1103	232	365	265	839	40	-846	-172	-173	674	10:31 AM
12.25	0.64	0.60	0.51	11.1	1101	239	399	273	828	42	-841	-175	-177	664	10:36 AM
12.25	0.64	0.60	0.51	11.2	1108	247	403	280	828	39	-886	-178	-176	710	10:41 AM
12.25	0.64	0.60	0.51	11.4	1120	254	392	291	830	44	-890	-186	-180	710	10:46 AM
12.25	0.64	0.60	0.51	11.5	1109	262	418	297	812	44	-911	-187	-186	726	10:51 AM
12.25	0.64	0.60	0.51	11.6	1106	268	391	302	804	47	-910	-185	-183	727	10:56 AM
12.25	0.64	0.60	0.51	11.6	1115	271	432	307	808	44	-934	-200	-191	743	11:01 AM
12.25	0.64	0.60	0.51	12.0	1143	277	430	299	843	60	-942	-194	-192	750	11:06 AM
12.25	0.64	0.60	0.51	12.6	1194	285	419	324	871	77	-993	-198	-203	789	11:11 AM
12.25	0.64	0.60	0.51	13.8	1265	294	465	336	929	96	-1106	-213	-217	889	11:16 AM
12.25	0.64	0.60	0.51	15.1	1387	323	503	324	1063	120	-1240	-235	-239	1001	11:21 AM
12.25	0.64	0.60	0.51	16.3	1459	354	533	356	1104	127	-1277	-253	-255	1023	11:26 AM
12.25	0.64	0.60	0.51	17.1	1556	386	570	386	1170	143	-1370	-278	-278	1093	11:31 AM
12.25	0.64	0.60	0.51	17.9	1605	416	612	463	1141	137	-1419	-284	-290	1129	11:36 AM
12.25	0.64	0.60	0.51	18.4	1675	439	633	480	1195	135	-1501	-301	-311	1191	11:41 AM
12.25	0.64	0.60	0.51	18.9	1713	463	632	464	1249	149	-1551	-308	-318	1233	11:46 AM
12.25	0.64	0.60	0.51	19.3	1783	-911	701	490	1294	1048	-1642	-315	-333	1309	11:51 AM
12.25	0.64	0.60	0.51	19.7	1817	509	715	509	1308	173	-1630	-323	-341	1289	11:56 AM
12.25	0.64	0.60	0.51	20.1	1850	529	706	530	1320	183	-1678	-336	-345	1333	12:01 PM
12.25	0.64	0.60	0.51	20.6	1962	554	776	555	1407	198	-1803	-344	-352	1452	12:06 PM
12.25	0.64	0.60	0.51	21.3	2034	578	795	579	1456	219	-1898	-366	-389	1509	12:11 PM
12.25	0.64	0.60	0.51	22.0	2084	604	791	605	1479	245	-1925	-384	-389	1536	12:16 PM
12.25	0.64	0.60	0.51	22.7	2189	632	878	633	1556	262	-2047	-397	-396	1651	12:21 PM
12.25	0.64	0.60	0.51	23.2	2266	657	903	696	1570	278	-2108	-393	-409	1699	12:26 PM
12.25	0.64	0.60	0.51	23.6	2290	679	872	681	1610	286	-2127	-416	-426	1701	12:31 PM
12.25	0.64	0.60	0.51	24.0	2357	699	947	701	1656	306	-2195	-418	-440	1755	12:36 PM
12.25	0.64	0.60	0.51	24.3	2422	718	974	720	1703	313	-2302	-430	-457	1845	12:41 PM
12.25	0.64	0.60	0.51	24.5	2471	738	973	740	1731	323	-2320	-438	-459	1861	12:46 PM
12.25	0.64	0.60	0.51	24.8	2528	757	1019	759	1768	338	-2371	-446	-459	1912	12:51 PM
12.25	0.64	0.60	0.51	25.1	2608	779	1047	780	1827	353	-2427	-460	-500	1928	12:56 PM
12.25	0.64	0.60	0.51	25.3	2649	793	1054	796	1853	354	-2434	-470	-480	1954	1:01 PM
12.25	0.64	0.60	0.51	25.5	2638	808	1081	810	1828	370	-2437	-471	-489	1948	1:06 PM
12.25	0.64	0.60	0.51	25.8	2670	818	1093	820	1850	382	-2500	-484	-506	1994	1:11 PM
12.25	0.64	0.60	0.51	26.0	2715	831	1098	836	1879	388	-2533	-500	-518	2016	1:16 PM
12.25	0.64	0.60	0.51	26.3	2798	839	1076	842	1956	401	-2613	-513	-530	2083	1:21 PM
12.25	0.64	0.60	0.51	26.5	2817	850	1144	853	1964	396	-2721	-527	-575	2146	1:26 PM
12.25	0.64	0.60	0.51	26.7	2859	859	1184	862	1997	403	-2773	-530	-565	2208	1:31 PM
12.25	0.64	0.60	0.51	26.9	2927	868	1111	872	2056	400	-2712	-550	-574	2138	1:36 PM
12.25	0.64	0.60	0.51	27.2	2954	876	1174	879	2075	395	-2755	-562	-584	2171	1:41 PM
12.25	0.64	0.60	0.51	27.4	2971	885	1187	888	2083	402	-2835	-577	-634	2201	1:46 PM
12.25	0.64	0.60	0.51	27.6	3002	894	1192	897	2105	414	-2863	-593	-614	2249	1:51 PM
12.25	0.64	0.60	0.51	27.7	3126	905	1176	909	2217	435	-2892	-605	-631	2261	1:56 PM
12.25	0.64	0.60	0.51	27.9	3131	909	1267	913	2218	426	-2980	-615	-673	2306	2:01 PM
12.25	0.64	0.60	0.51	28.2	3142	916	1228	919	2223	422	-3037	-631	-658	2379	2:06 PM
12.25	0.64	0.60	0.51	28.4	3166	924	1178	928	2238	440	-3215	-670	-671	2544	2:11 PM
12.25	0.64	0.60	0.51	28.6	3194	927	1251	930	2263	443	-3201	-672	-690	2511	2:16 PM
12.25	0.64	0.60	0.51	28.7	3293	940	1275	944	2349	455	-3843	-717	-703	3140	2:21 PM
12.25	0.64	0.60	0.51	28.9	3324	949	1270	953	2371	457	-3975	-742	-720	3255	2:26 PM
12.25	0.64	0.60	0.51	29.1	3363	947	1289	950	2413	455	-4173	-754	-746	3427	2:31 PM
12.25	0.64	0.60	0.51	29.3	3377	953	1295	956	2420	458	-4396	-792	-770	3626	2:36 PM
12.25	0.64	0.60	0.51	29.4	3361	951	1285	958	2403	425	-4742	-842	-825	3917	2:41 PM
12.25	0.64	0.60	0.51	29.7	3442	963	1249	969	2473	435	-7817	-981	-851	6966	2:46 PM

A.2 BISAR (E) Model Results

BISAR MODEL						
Temperature (°C)	10			DATE: 4/ 9/2005 TIME: 11: 9: 3. 6		
SYSTEM NUMBER 1						
Layer Number	Calculation Method (0-1000)	Young's Modulus (E)	Poisson's Ration (ν)	Layer Thickness (in)		
1	Smooth	767395	0.35	1.57		
2	Smooth	6345	0.45	3.00		
3	Smooth	29007550	0.26	0.63		
4		5091	0.40			
0=Smooth (complete adhesion), 1000=(frictionless slip)						
Load Number	Normal Load (lb-f)	Shear Stress (σ)	Radius of Loaded Area (in)	Load-Position X Y (lb-in)		Shear Direction
1	607	0.00	1.3	0.00	0.00	0.00
Position Number:	1			X-Coordinate (in):	0.00	
Layer Number:	1			Y-Coordinate (in):	0.00	
				Z-Coordinate (in):	1.56	
TOTAL STRESSES, STRAINS AND DISPLACEMENTS						
	Horizontal in X	Horizontal in Y	Vertical in Z	Shear YZ	Shear XZ	Shear XY
Stress (σ)	2.440E+02	2.440E+02	-8.720E+00	0.000E+00	0.000E+00	0.000E+00
Strain (ϵ)	2.100E-04	2.100E-04	-2.340E-04	0.000E+00	0.000E+00	0.000E+00
Displacement (in)	0.000E+00	0.000E+00	6.040E-03			

Figure A.2.1 – BISAR MODEL, 10 Degrees Celsius

BISAR MODEL							
Temperature (°C)	15					DATE:	4/ 9/2005
						TIME:	11:12:48. 4
SYSTEM NUMBER 1							
Layer Number	Calculation Method (0-1000)	Young's Modulus (E)	Poisson's Ration (ν)	Layer Thickness (in)			
1	Smooth	576090	0.35	1.57			
2	Smooth	6345	0.45	3.00			
3	Smooth	29007550	0.26	0.63			
4		5091	0.40				
0=Smooth (complete adhesion), 1000=(frictionless slip)							
Load Number	Normal Load (lbf)	Shear Stress (σ)	Radius of Loaded Area (in)	Load-Position X Y (lb-in)		Shear Direction	
1	607	0.00	1.3	0.00	0.00	0.00	
Position Number:	1			X-Coordinate (in):	0.00		
Layer Number:	1			Y-Coordinate (in):	0.00		
				Z-Coordinate (in):	1.56		
TOTAL STRESSES, STRAINS AND DISPLACEMENTS							
	Horizontal in X	Horizontal in Y	Vertical in Z	Shear YZ	Shear XZ	Shear XY	
Stress (σ)	2.280E+02	2.280E+02	-1.020E+01	0.000E+00	0.000E+00	0.000E+00	
Strain (ε)	2.640E-04	2.640E-04	-2.950E-04	0.000E+00	0.000E+00	0.000E+00	
Displacement (in)	0.000E+00	0.000E+00	6.470E-03				

Figure A.2.2 – BISAR MODEL, 15 Degrees Celsius

BISAR MODEL							
Temperature (°C)	20					DATE:	4/ 9/2005
						TIME:	11: 9:17.45
SYSTEM NUMBER 1							
Layer Number	Calculation Method (0-1000)	Young's Modulus (E)	Poisson's Ration (ν)	Layer Thickness (in)			
1	Smooth	559701	0.35	1.57			
2	Smooth	6345	0.45	3.00			
3	Smooth	29007550	0.26	0.63			
4		5091	0.40				
0=Smooth (complete adhesion), 1000=(frictionless slip)							
Load Number	Normal Load (lbf)	Shear Stress (σ)	Radius of Loaded Area (in)	Load-Position X Y (lb-in)		Shear Direction	
1	607	0.00	1.3	0.00	0.00	0.00	
Position Number:	1			X-Coordinate (in):	0.00		
Layer Number:	1			Y-Coordinate (in):	0.00		
				Z-Coordinate (in):	1.56		
TOTAL STRESSES, STRAINS AND DISPLACEMENTS							
	Horizontal in X	Horizontal in Y	Vertical in Z	Shear YZ	Shear XZ	Shear XY	
Stress (σ)	2.260E+02	2.260E+02	-1.040E+01	0.000E+00	0.000E+00	0.000E+00	
Strain (ε)	2.690E-04	2.690E-04	-3.020E-04	0.000E+00	0.000E+00	0.000E+00	
Displacement (in)	0.000E+00	0.000E+00	6.520E-03				

Figure A.2.3 – BISAR MODEL, 20 Degrees Celsius

BISAR MODEL							
Temperature (°C)	25					DATE:	4/ 9/2005
						TIME:	11: 9:47.61
SYSTEM NUMBER 1							
Layer Number	Calculation Method (0-1000)	Young's Modulus (E)	Poisson's Ration (ν)	Layer Thickness (in)			
1	Smooth	280938	0.35	1.57			
2	Smooth	6345	0.45	3.00			
3	Smooth	29007550	0.26	0.63			
4		5091	0.40				
0=Smooth (complete adhesion), 1000=(frictionless slip)							
Load Number	Normal Load (lbf)	Shear Stress (σ)	Radius of Loaded Area (in)	Load-Position X Y (lb-in)		Shear Direction	
1	607	0.00	1.3	0.00 0.00		0.00	
Position Number:	1			X-Coordinate (in):		0.00	
Layer Number:	1			Y-Coordinate (in):		0.00	
				Z-Coordinate (in):		1.56	
TOTAL STRESSES, STRAINS AND DISPLACEMENTS							
	Horizontal in X	Horizontal in Y	Vertical in Z	Shear YZ	Shear XZ	Shear XY	
Stress (σ)	1.900E+02	1.900E+02	-1.490E+01	0.000E+00	0.000E+00	0.000E+00	
Strain (ε)	4.570E-04	4.570E-04	-5.260E-04	0.000E+00	0.000E+00	0.000E+00	
Displacement (in)	0.000E+00	0.000E+00	7.770E-03				

Figure A.2.4 – BISAR MODEL, 25 Degrees Celsius

BISAR MODEL							
Temperature (°C)	30					DATE:	4/ 9/2005
						TIME:	11:10:04.96
SYSTEM NUMBER 1							
Layer Number	Calculation Method (0-1000)	Young's Modulus (E)	Poisson's Ration (ν)	Layer Thickness (in)			
1	Smooth	177091	0.35	1.57			
2	Smooth	6345	0.45	3.00			
3	Smooth	29007550	0.26	0.63			
4		5091	0.40				
0=Smooth (complete adhesion), 1000=(frictionless slip)							
Load Number	Normal Load (lbf)	Shear Stress (σ)	Radius of Loaded Area (in)	Load-Position X Y (lb-in)		Shear Direction	
1	607	0.00	1.3	0.00 0.00		0.00	
Position Number:	1			X-Coordinate (in):		0.00	
Layer Number:	1			Y-Coordinate (in):		0.00	
				Z-Coordinate (in):		1.56	
TOTAL STRESSES, STRAINS AND DISPLACEMENTS							
	Horizontal in X	Horizontal in Y	Vertical in Z	Shear YZ	Shear XZ	Shear XY	
Stress (σ)	1.650E+02	1.650E+02	-1.890E+01	0.000E+00	0.000E+00	0.000E+00	
Strain (ε)	6.450E-04	6.450E-04	-7.610E-04	0.000E+00	0.000E+00	0.000E+00	
Displacement (in)	0.000E+00	0.000E+00	8.770E-03				

Figure A.2.5 – BISAR MODEL, 30 Degrees Celsius